THE MERGING OF FLOW FROM A SLUICE GATE WITH A PARALLEL STREAM

by

Luis Ernesto Macias de Melo Magalhaes

Thesis submitted to the University of London for the Degree of Doctor of Philosophy in the Faculty of Engineering, and to the Imperial College of Science and Technology for the Diploma of Membership.

January, 1974.

ABSTRACT

Experimental work has been carried out to investigate the flow of a supercritical stream of water merging with a deeper and subcritical stream flowing in the same direction. The characteristics of the supercritical stream were controlled by a sluice gate. A dividing wall inserted inside a rectangular flume separated the two parallel streams and the flow depth of the sub-critical stream was controlled by a downstream discharge-weir. Two particular properties of the flow were studied in detail, the formation of the hydraulic jump between the supercritical and subcritical flows, and the diffusion of the resulting jet.

Three basic forms of the hydraulic jump were observed: oblique, normal and submerged. The properties of the jumps were measured, and the effects on the jumps of the subcritical flow were investigated down to the limit of zero flow. The results were compared with two-dimensional theory of hydraulic jumps and the available information on jumps forming at abrupt expansions in rectangular channels. The effect of the uniform stream on the formation of the jump was found to be small. A survey of the literature revealed a surprising lack of information on three-dimensional (spatial) forms of the hydraulic jump. The present experiments would appear to be the first in which the effect of the uniform stream on a hydraulic jump has been considered.

The rate of growth of the sluice jet and the decay of its maximum velocity were calculated from velocity profiles measured across the flow. Dynamic similarity conditions were specifically investigated and three distinct regions of flow were found: (a) a wall region close to the flume wall; (b) a free-mixing region of turbulent flow; (c) an outer region of uniform flow. The experimental results were compared with other work on two-dimensional turbulent jets of incompressible fluid and found to agree well with measurements of wall-jets diffusing in a uniform stream.

TABLE OF CONTENTS i

LIST OF FIGURES iv

LIST OF TABLES vi

LIST OF SYMBOLS vii

ACKNOWLEDGEMENTS xii

I INTRODUCTION 1

II LABORATORY EQUIPMENT AND TEST PROCEDURE 7

2.1 LABORATORY ARRANGEMENTS 7

.1 Metal Flume 7

.2 Wood Structure 9

2.2 WATER SUPPLY 11

2.3 FLOW MEASUREMENTS 12

.1 Water Levels 12

.2 Discharge Calibration Tests 13

.3 Mean Velocities 16

2.4 TEST PROCEDURE 18

.1 Jump Classification Tests 19

.2 The Effect of a Uniform Stream on the Jumps 21

.3 Scale Effects in the Depth of the Fast Stream 21

.4 Diffusion of the Jet 24

2.5 FLOW VISUALIZATION 29

.1 Ahlborn Tank 30

.2 Photographic Tests 32

III HYDRAULIC JUMPS IN PARALLEL CO-FLOWING STREAMS 35

3.1 HYDRAULIC JUMPS - A REVIEW OF THE LITERATURE 35

3.2 JUMP CLASSIFICATION TESTS 39

.1 Experimental Results 45

.2 Normal Hydraulic Jump at an Abrupt Expansion 48

.3 Oblique Jumps. 51

3.3 THE EFFECT OF A UNIFORM STREAM ON THE HYDRAULIC JUMPS 54

3.4 THE HYDRAULIC ANALOGY TO SUPERSONIC FLOW 60

IV THE DIFFUSION OF THE JET IN A UNIFORM STREAM 65

4.0 INTRODUCTION 65

4.1 IMPULSE-MOMENTUM ANALYSIS 69

.1 The Impulse-Momentum Balance 69

.2 Experimental Results 74

4.2 THEORETICAL ANALYSIS OF TURBULENT SHEAR FLOWS 76

.1 General Considerations of Submerged Jets 76

.2 Turbulent Flow Equations of a Jet of Incompressible Fluid 82

.3 Dimensional Analysis on Two-dimensional Jets 90

4.3 MEASURED MEAN FLOW PATTERN 97

.1 Growth of the Jet 98

.2 Decay of the Maximum Jet Velocity 104

.3 Geometrical Similarity in the Mean Velocity Profiles 108

.4 An Engineering Solution 117

V SUMMARY OF RESULTS AND CONCLUSIONS SUGGESTIONS FOR FUTURE RESEARCH WORK 121

APPENDICES

A DISCHARGE CALIBRATION CURVES 127

A.1 Orifice Plate 127

A.2 Check in the Venturi Calibration Curve 127

B SCALE EFFECTS IN THE DEPTH OF THE FAST STREAM 132

C VELOCITY MEASUREMENTS TAKEN WITH A PITOT-STATIC TUBE 134

C.1 The Diffusion of the Jet 134

C.2 Vertical Velocity Profiles 136

D VELOCITY MEASUREMENTS MADE WITH A MINI-CURRENT METER 139

D.1 Current Meter Tests 139

D.2 Check on the Measurements of the Pitot-static Tube 140

D.3 Velocity Measurements at the Control Sections 141

E CRITICAL ANALYSIS ON R-JUMPS 142

F CALCULATION OF THE MOMENTUM COEFFICIENT IN THE DOWNSTREAM CONTROL SECTION 144

G EVALUATION OF THE ENERGY DISSIPATED INSIDE THE CONTROL VOLUME 149

H SIMILARITY IN THE VELOCITY PROFILES OF THE DIFFUSING JET 151

BIBLIOGRAPHY 155

LIST OF FIGURES

2.1-1	Schematic Representation of the two Channels inside the Metal Flume and Tapping Points (P_i)	8
2.1-2	Experimental Equipment	10
2.3-1	Calibration Curves	15
2.4-1	Free Surface Profiles of the Flow	20
2.4-2	Scale Effects in the Depth of the Fast Stream	22
2.4-3	Vertical Velocity Profiles	28
2.5-1	Glass-Sided Flume and Photographic Positions	28
2.5-2	Travelling Waves	31
2.5-3	Transverse Waves	33
2.5-4	Normal Hydraulic Jump	33
3.2-1	Oblique Jump	40
3.2-2	Flow Patterns	42
3.2-3	Hydraulic Jump at an Abrupt Expansion	44
3.2-4	Hydraulic Jump Forms	46
3.2-5	Normal Jumps at an abrupt expansion	50
3.2-6	Oblique Standing Waves	53
3.3-1	Hydraulic Jumps in a Uniform Stream	55

3.3-2	Normal Jumps in a Coflowing Stream	58
3.3-3	Jump Depth in a Coflowing Stream	61
3.3-4	Jump Depth at an Abrupt Expansion	61
4.1-1	Two-Dimensional Diffusion of the Sluice Jet	70
4.1-2	The Control Volume	70
4.2-1	The Diffusion of a Turbulent Jet	77
4.2-2	Typical Velocity Profile of a Wall-Jet Diffusing in a Uniform Stream	77
4.3-1	The Diffusion of the Jet	99
4.3-2	Jet Diffusion in a Medium at Rest	101
4.3-3	Jet Diffusion in a Uniform Stream	101
4.3-4	Decay of the Maximum Jet Velocity	106
4.3-5	Linear Velocity Decay	106
4.3-6	Jet Velocity Profiles	110
4.3-7	Analytical Velocity Profiles	110
4.3-8	Excess Velocity Profiles	114
4.3-9	Wall-Jet Velocity Profiles	116
4.3-10	Sluice Jet Flow	119
4.3-11	Excess Velocity Profile	120
A-1	Orifice Plate Calibration Curves	128
A-2	Rods Weir Depth-Discharge Curve	128

LIST OF TABLES

2.4-1	Corrected Manometer Heads and Velocities of the Pitot-static Tube	26
3.2-1	Hydraulic Jumps at an Abrupt Expansion	47
3.3-1	Hydraulic Jumps at an Abrupt Expansion in a Uniform Stream	56
3.3-2	Normal Hydraulic Jumps in a Coflowing Stream	59
3.3-3	Normal Hydraulic Jump Depth Ratio at an Abrupt Expansion	62
4.3-1	The Growth of the Jet	103
4.3-2	Maximum Velocity Decay	107
A - 1	Results of Orifice Calibration Tests	129
A - 2	Weir Depth-Discharge Curve	130
A - 3	Venturi Meter Calibration Check	130
B - 1	Scale Effects in the Depth of the Fast Stream	133
C - 1	Calculation of the Flow Rates from the Velocity Profiles	137
F - 1	Calculation of the Momentum and Energy Coefficients in the Downstream Control Section (S_3)	146

LIST OF SYMBOLS

Symbol	Definition	Dimensions
A	General dependent variable	
A_o	Area of the exit cross-section of the jet	L^2
A_3	Cross-section area of the flow	L^2
$\Delta A, A_y$	Elemental area	L^2
a	Speed of a sound wave	LT^{-1}
B, b	Width of the channel after and before the expansion	L
b	Semi-thickness of a plane jet	L
b_o	Semi-thickness at the exit section	L
b_1, b_2, b_3	Width of channels 1, 2 and 3	L
C, c	Empirical constants (used with subscripts)	
c	Speed of small gravity wave	LT^{-1}
D	Diameter of the orifice plate	L
d	Mean depth of the flow	L
d_1, d_2, d_3	Mean depth of streams 1, 2 and 3	L
$\bar{d}_1$	Conjugate depth of stream 1	L
d_{23}	Downstream characteristic depth of the jump	L
d_{SL}	Aperture of the sluice gate	L
E	Energy flux of the jet	ML^2T^{-3}
E_o	Energy flux at the exit section	ML^2T^{-3}
E_3	Specific energy at control section S_3	L
F_1, F_2, F_3	Momentum forces	MLT^{-2}
Fr_1	Froude number of the fast stream	

Fr'_j	Characteristic Froude number	
$f(\ )$	Similarity functions (used with subscripts)	
g	Acceleration of gravity	LT^{-2}
$g_1(\ ), g_2(\ ), g_{12}(\ )$	Self-preserving functions	
H	Head of water over the crest of the rods weir	L
h_{SL}	Depth of water upstream of the sluice gate	L
Δh	Manometer head	L
Δh_{HG}	Mercury manometer head (orifice plate)	L
Δh_{H_2O}	Water manometer head (orifice plate)	L
Δh_{VE}	Manometer head of the Venturi meter	L
i	Index	
i,j	Tensor subscripts	
k	Empirical constant of turbulence	
K_1, K_2	Empirical coefficient	
ΔL	Depth of water in the volumetric tank	L
l	Mixing length	L
M	Momentum flux of the jet	$ML^{\cancel{2}}T^{-2}$
M_o	Momentum flux at the exit section	$ML^{\cancel{2}}T^{-2}$
m	Rate of growth of the jet	
Ma	Mach number	
n	Depth ratio	
P	Static pressure	$ML^{-1}T^{-2}$
P_s	Stagnation pressure	$ML^{-1}T^{-2}$
P_i	Pressure tapping number i (i=1,2,....,9)	
p_1, p_2, p_3	Pressure	$ML^{-1}T^{-2}$

Q	Flowmeter discharge	L^3T^{-1}
Q_1, Q_2, Q_3	Flow rate of streams 1, 2 and 3	L^3T^{-1}
Q_x	Elemental flow rate	L^3T^{-1}
Q_{OR}	Discharge of the orifice plate	L^3T^{-1}
Q_{VE}	Discharge of the Venturi meter	L^3T^{-1}
Q_{WR}	Discharge over the rods weir	L^3T^{-1}
q	Flow rate per unit width	L^2T^{-1}
q_1, q_3	Flow rate per unit width of streams 1 and 3	L^2T^{-1}
r'	Characteristic length of an outlet	L
Re	Reynolds number	
S_1, S_2, S_3	Control sections in streams 1, 2 and 3	
T	Interval of time	T
t	Variable time	T
T_1, T_3	Temperature	
U	Mean uniform velocity	LT^{-1}
U_o	Uniform velocity at the exit section	LT^{-1}
$U_o, \bar{U}_o$	Scale velocities	LT^{-1}
U_1, U_2	Mean uniform velocity of streams 1 and 2	LT^{-1}
U_H	Uniform velocity of the co-flowing stream	LT^{-1}
U_m	Maximum velocity in the direction of flow (x)	LT^{-1}
u, v, w	Velocity components	LT^{-1}
V	Velocity at a point	LT^{-1}
V_3	Velocity at a point of stream 3	LT^{-1}
V_m	Maximum velocity at a cross-section	LT^{-1}
V_{max}	Maximum velocity of the velocity profile	LT^{-1}
V_{min}	Minimum velocity at a cross-section	LT^{-1}

X,Y,Z	Components of body force	LT^{-2}
x	Distance to the pole of the jet	L
x_o	Distance to the edge of the dividing wall	L
x_s	Distance between the pole and the exit section of the jet	L
x,y,z	Cartesian co-ordinates	L
Δx	Elemental distance	L
y	Distance to the right wall of the flume	L
Δy	Elemental distance	L
W_1,W_2,W_3	Hydraulic energy	ML^2T^{-3}
ΔW	Hydraulic energy dissipated inside the control volume	ML^2T^{-3}
w	Specific weight	$ML^{-2}T^{-2}$
z	Vertical distance to the bed of the flume	L
α	Energy coefficient	
β	Momentum coefficient	
β_a,β_b,β_c	Momentum coefficient calculated from different velocity profiles	
β^o	Wave angle	
γ	Ratio of specific heats	
δ	Boundary layer thickness	L
δ_o	Distance from the wall to the point of maximum velocity in a wall-jet	L
δ_1	Characteristic width of a wall-jet	L
ϵ	Eddy viscosity	$ML^{-1}T^{-1}$
η	Dimensionless coordinate (y/b)	
θ	Empirical constant	
θ^o	Angle of deflection of the wall	
μ	Dynamic viscosity	$ML^{-1}T^{-1}$

ν	Kinematic viscosity	L^2T^{-1}
ρ, ρ_1, ρ_3	Mass density	ML^{-3}
σ	Standard deviation	L
τ_{xy}	Total shear stress	$ML^{-1}T^{-2}$
τ'_{xy}	Turbulent shear stress	$ML^{-1}T^{-2}$
$\varkappa$	Coefficient of turbulent viscosity	

Notes: (1) - Overbar indicates a time averaged mean (Equation 4.2-3)

(2) - Apostrophe indicates a deviation from the mean

(3) - Asterisk indicates an empirical value found in the present research

(4) - Subscripts 1, 2 and 3 for the flow variables corresponds to:

(1) - supercritical stream

(2) - uniform stream

(3) - merged flow

ACKNOWLEDGEMENTS

The topic of this research was suggested by Professor J.R.D. Francis, to whom I am grateful for the facilities he made available in the Department and also for his stimulating comments and assistance. This research was directly supervised by Mr. Paul Minton. Special mention is due to his active supervision and constant encouragement throughout all the stages of this work. His friendship was a very important factor in making my wife's and my experience in England so positive.

I am extremely grateful to the Calouste Gulbenkian Foundation, Portugal, and to the University of Lourenco Marques, Mozambique, not only for their financial support but also for the opportunity of doing this research work in England. I would also like to mention Professor Barreiros Martins who, as the Head of the Civil Engineering Department at Lourenco Marques University, encouraged me, from the beginning, to achieve higher academic qualifications.

From most of the academic and the technical staff in the Hydraulics Section and Laboratory I received much sympathy and practical advice in carrying out this research work. I wish to record my appreciation for their individual and effective help. In particular, credit for the photographic work belongs to Miss Joyce Gurr, and for the excellent typing to Mrs. Rosemary Mudie.

The opportunity of meeting people from so many different countries and varied cultural and social backgrounds was one of the most interesting experiences of my stay in London. The friendship of some of the post-graduate students in the Hydraulics and Hydrology Sections was very much appreciated.

Finally, I cannot forget my wife, Constanca, for her continuous encouragement and precious help in improving and typing drafts, and drawing graphs. During the writing of the thesis there were many other "little helps" and, among them, the birth of our first daughter, Ana Teresa, was a sweet stimulus for my work which was also increased for the same reason.

I - INTRODUCTION

The initial aim of the present research work in the field of Civil Engineering Hydraulics was to investigate the flow characteristics of a fast stream merging with a slow stream at different angles and to attempt a general analysis of the flow conditions in an open-channel junction. The flow through a channel junction is a phenomenon that involves numerous variables, such as the number of adjoining channels, the angles of intersection, the shape and slope of the channels, the directions and discharges of flow, the rounding of corners at the intersecting channels, etc. (4,70,71). Owing to the complexities of the boundary geometry and the presence of a free surface, the behaviour of the flow at the junction is not, in general, amenable to a completely theoretical analysis. In engineering practice most of the problems concerning channel junctions are studied in reduced scale models.

Taylor (70) investigated the specific cases of combining and dividing flow when the flow conditions in each channel were subcritical. The analysis of dividing flow is considerably more difficult than that of combining flow because the flow depth in the tributary channels at the junction is controlled by the tailwater levels in the combined channel (69,70). When one (or more) of the adjoining streams in a combining flow situation is supercritical, the flow conditions become more complicated and a hydraulic jump may form at the junction depending upon the characteristics of the junction design, the discharge and depth of flow in the adjoining channels (4,68). If the flow conditions are supercritical throughout

the whole junction a complex pattern of cross waves will be propagated for a considerable distance downstream before being damped by the channel friction (4,26).

Preliminary visualization tests in the flow characteristics of a fast stream of water merging with a uniform stream flowing in the same direction or in an opposite direction were carried out in an Ahlborn tank (Section 2.5-1). The tests revealed the existence of several forms of hydraulic jumps and, for certain conditions, important undulation in the free surface of the downstream merged flow. The characteristics of the turbulent jet (supercritical stream) diffusing into the deeper flow of the surrounding medium varied with the flow conditions. The flow pattern with both streams flowing in the same direction was the most stable, and for that reason the tests in the laboratory flume (Section 2.4) were started with that simple situation.

Three basic forms of the hydraulic jump were observed, being identified as oblique, normal and submerged jumps. The oblique and normal forms of the jump appeared at the end of the wall separating the two parts of the channel. For higher tail-water levels, normal or submerged hydraulic jumps would form well inside the channel. The laboratory arrangements described in Chapter II (with the test procedure), could have been employed to study the two limiting cases of a channel junction flow in which a supercritical stream intersected a subcritical stream at an angle of 0° or 180°. The complexities in the different forms of the hydraulic jump observed and the limited amount of time available made it impossible to investigate the characteristics of the counter-flowing streams.

The hydraulic jump is not only an effective mean of reducing the mean flow energy of a supercritical stream, but also a very efficient mechanism of increasing (abruptly) the depth of the flow and restoring its conditions of uniformity (4,12,36). Depending on the position and direction of the front, the hydraulic jumps observed were called oblique, normal or submerged jumps. The hydraulic jump with a front normal to the direction of the flow is the most common form of the jump found or designed in Civil Engineering practice. If the position of a normal jump in a channel is at an abrupt expansion of its cross-section, then a hydraulic jump under spatial conditions will occur (24). The results of previous investigations in normal hydraulic jumps forming at an abrupt expansion (33,38) were compared with the present results. A new aspect of the problem, the effect of a uniform stream on the formation of the jump, was investigated: It was confirmed that the spatial hydraulic jump requires a smaller tail-water level than the classical two-dimensional jump with the same inflow conditions (25,38). The effect of the uniform stream is to cause slight increase in the tail-water levels.

The tests on normal and submerged hydraulic jumps were carried out with a supercritical stream 3.0 cm deep and a range of Froude numbers for the fast and slow streams varying between 2.3 to 4.6, and 0.0 to 0.65. Only a qualitative analysis was possible on the flow through oblique jumps. These were produced by a difference in depth between the fast stream and the subcritical flow, and in this sense they differ from the oblique jumps analysed by Ippen (26,27) which were produced by the deflection of a wall into a supercritical stream.

The characteristics of the flow further downstream in the (combined) channel and, in particular, the diffusion of the fast sluice discharge in the uniform stream were also analysed in the present research. A review of the theoretical background on turbulent shear flow (8,13,16) was made. The motion of a turbulent jet is defined by the Navier-Stokes equations but, due to the non-linearity of these equations, there is no general solution to the problem. The similarity solution approach is often applied in the analysis of turbulent jet flow and is based on the fact that the diffusion characteristics of turbulent jets are dynamically similar when the jet Reynolds number is not too low. It pre-supposes that the turbulent structure of the flow is self-preserved in the diffusing jet. This simplified solution is valid for incompressible fluids in which the effects of temperature, viscosity and surface tension are neglected.

In the laboratory, half-depth velocity profiles were measured at seven cross-sections of the flow with a mini-current meter and a Pitot-static tube. The quality of the measurements was checked through an impulse-momentum analysis and an evaluation of the energy dissipated in a normal hydraulic jump was performed. The velocity measurements were used to investigate the similarity of the velocity profiles at each section of the flow and to calculate the growth of the jet and the decay of maximum velocity of the jet. Three regions of flow were observed in the diffusion of the jet: (a) a wall-~~jet~~ region controlled by the growth of the boundary layer along the flume wall; (b) a free mixing region where the velocity profile could be represented by an exponential curve of Gaussian type; (c) an outer region of uniform

flow. The experimental results were successfully compared with two-dimensional turbulent free jets and wall-jets spreading throughout a uniform stream or a medium at rest.

The free surface of the merging streams was found to be disturbed by waves, standing or travelling in the flume, which were of considerable amplitude in the flows involving an oblique hydraulic jump. Progressive waves are known to occur downstream of a hydraulic jump and they are undesirable because of the damage they can produce to the earth embankment and their interference with the measurements and operation of gauging stations. These waves are irregular in height, and period and their statistical distribution depends on the Froude number of the supercritical flow (61). One of the characteristics of a flow pattern with oblique jumps was the system of standing waves crossing the diffusing jet and being reflected, successivelly, from the wall of the flume and the shear boundary separating the jet from the surrounding medium. This pattern of waves resembled the shock waves found in the discharge of a free supersonic jet. Large waves travelling downstream in the flume, and waves parallel to the shear boundary of the jet were observed and have been photographed. Unfortunately, no time was available to investigate further the characteristics of these waves.

The basic equipment used to carry out the present experimental work consisted of a wooden partition set inside a metal flume in the Hydraulics Laboratory. The two channels so formed had independent supplies of water and the depth of the supercritical stream was controlled by a sluice gate. The depth of the uniform subcritical stream was controlled by a weir at the downstream end of the flume. The flow rates of the streams were

measured by an orifice plate (supercritical stream) and a Venturi-meter (subcritical stream) in the pipes supplying each channel. Water levels and depths of flow were measured either by point gauges or by pressure tappings. Flow velocities were measured with a Pitot-static tube and a mini-current meter.

In brief, the hydraulic jump tests were conducted in the following way: (a) the characteristics of the supercritical stream (d_1,Fr_1) were controlled by the aperture of the sluice gate (d_{SU}), and the discharge of the orifice plate (Q_{OR}); (b) the form of the hydraulic jump to be studied was set in the flow by a convenient control of the tail-water levels in the flume (d_{23}); the Froude number of the uniform flow (Fr_2) was determined by the Venturi-meter discharge (Q_{VE}) and the depth of the flow in the downstream channel ($d_2 = d_{23}$). The characteristics of the jet diffusing in a uniform stream were investigated in the following particular conditions: (a) normal hydraulic jump forming inside the sluice channel; (b) supercritical stream: $d_1 = 3.0$ cm and $Fr_1 = 2.3$; (c) uniform stream: $d_2 = 7.8$ cm and $U_2 = 22.8$ cm/s. All the tests were carried out with the bed of the flume in a horizontal position.

Through the text 65 references are mentioned. The references were grouped under the following four headings: (a) Basic references: which include 17 textbooks; (b) Hydraulic jumps: which include 19 papers and theses; (c) Turbulent jets: with 18 papers and theses; (d) Other references: including 11 papers or theses in subjects only generally related to the subject investigated.

II - LABORATORY EQUIPMENT AND TEST PROCEDURE

2.1 - LABORATORY ARRANGEMENTS

The basic equipment used in the experimental work carried out in this study consisted of two parallel channels, with separate supplies of water and independent control of the water levels inside each. A schematic representation of the two channels is given in Fig. 2.1-1.

2.1.1 - Metal Flume

The 11.70 m long steel flume of the Civil Engineering Hydraulics Laboratory at Imperial College was used to investigate the flow characteristics of a fast stream of water merging with a slow and deeper uniform stream flowing in the same direction. In Fig. 2.1-2 a general view of the metal flume is presented.

The flume, of rectangular cross-section, was 0.76 m wide and 0.46 m deep. It had a wedge mechanism which allowed adjustments in the slope of the channel, but all the experiments were carried out with the bottom of the channel in a horizontal position. Every day, at the end of the tests, the channel was sloped to help the drying of the metal flume and avoid corrosion. The water was supplied to the flume through a 0.20 m diameter pipe which discharged vertically into a small inlet chamber 0.76 m long, 0.76 m wide and 0.56 m deep. At the entrance of the channel was fixed a honeycomb baffle, 0.24 m thick. The tail water level was controlled, at the end of the flume, by a combined arrangement of a Tainter gate and a simple weir structure. The weir, which was made of two wood plates and nine cylindrical rods of 1.3 cm diameter, was used for a coarse control of the flow depths inside the flume.

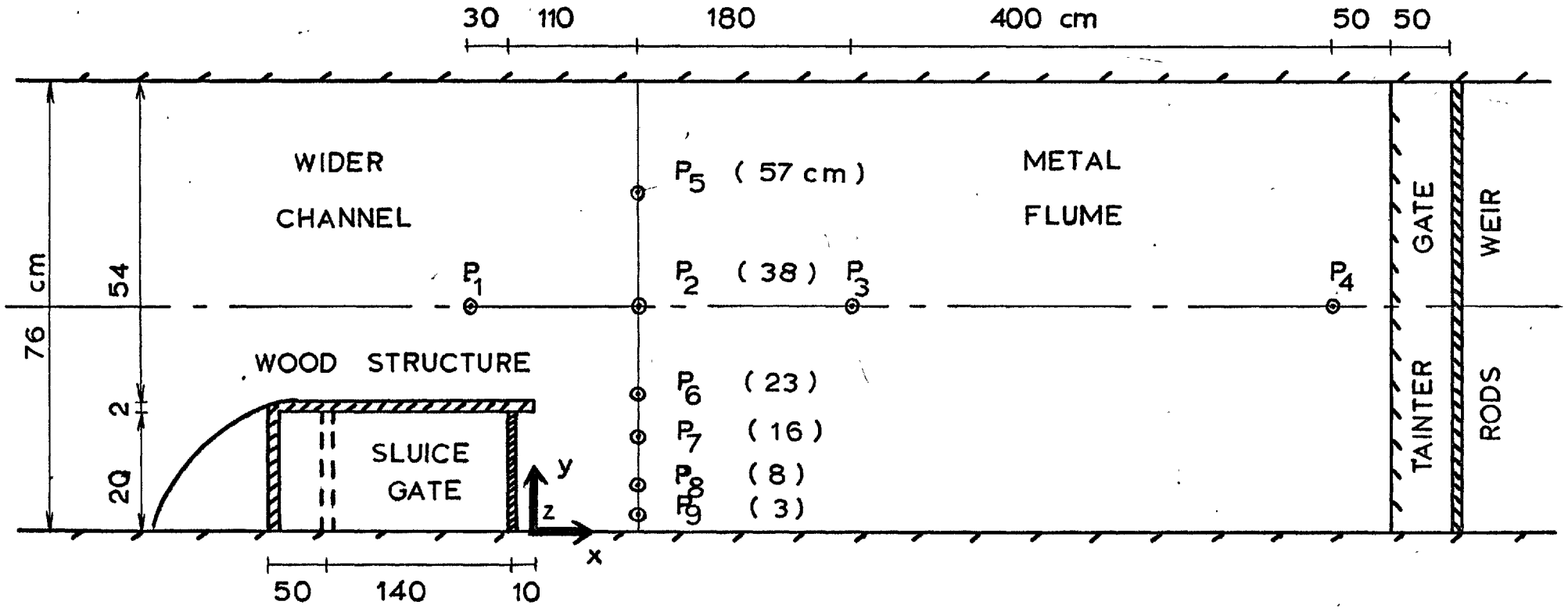


FIG. 2.1-1 SCHEMATIC REPRESENTATION OF THE TWO CHANNELS INSIDE THE METAL FLUME AND TAPPING POINTS (P_i).

The Tainter gate provided a finer control of the same water levels. At the end of the flume an outlet chamber, 0.67 m long, 0.87 m wide and 0.67 m deep, discharged into the sump of the laboratory through a 0.30 m pipe. The adjustable weir was located at the entrance of the outlet chamber. On top of the side walls of the flume a set of rails allowed an instrument carriage to be moved along the flume.

2.1.2 - Wood Structure

A simple and economic structure of wood was fitted inside the metal flume to divide the flume into two smaller channels, 0.20 m and 0.54 m wide, respectively. A sheet of wood 20 mm thick, 2.00 m long and 0.45 m high, with a sluice gate was fixed to the right wall of the metal flume (looking in the direction of the flow), and the joints were carefully sealed with plasticine. The sluice gate controlled the water depth in the smaller channel.

The water was supplied to the 0.20 m channel by a 0.10 m diameter vertical pipe. This pipe discharged in a small inlet chamber 0.35 m long, confined by three perforated manifold sheets. In the other end of the channel a sluice gate controlled the supercritical velocity and depth of the fast discharge into the wider channel, so that the range of Froude number tested varied between 2.0 and 6.0. The discharge under the sluice gate was faster and shallower than the uniform stream of the wider channel. The edge of the wood sluice gate was protected with a sheet of metal. The fast stream was separated from the deeper water of the other channel by a dividing wall 0.10 m long and 0.02 m thick. The tests revealed that this length of wall was not long enough for the higher discharges from the sluice when normal hydraulic jumps were formed inside this channel. The jump did not remain in the same position in the channel, and usually caused an early submergence of the sluice gate.

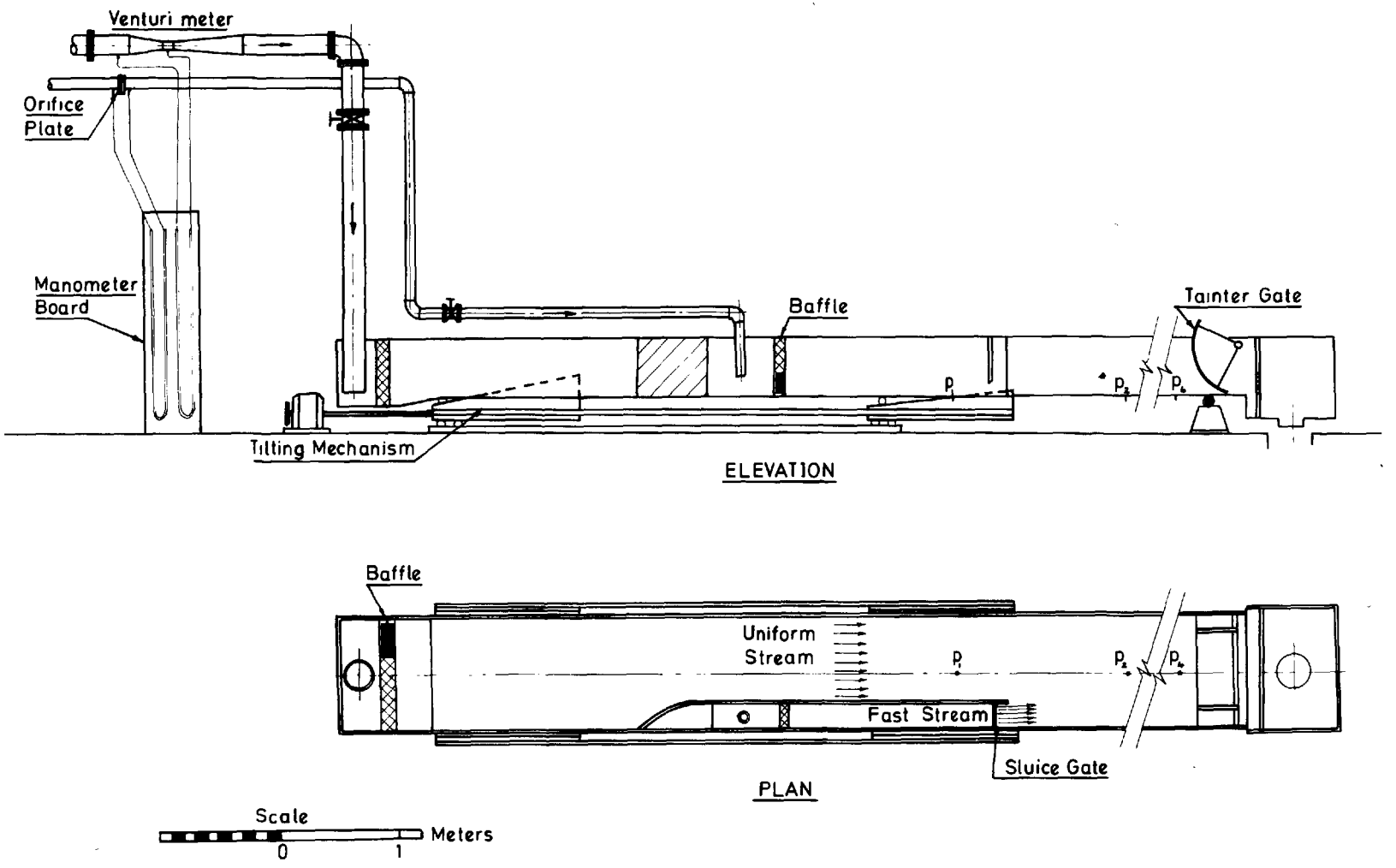


Fig. 2.1-2

EXPERIMENTAL EQUIPMENT

A transition profile 0.60 m long was used at the entrance of the wider channel in order to reduce the 0.76 m wide cross section of the metal flume to a width of 0.54 m.

2.2 - WATER SUPPLY

The main supply of water in the Hydraulics Laboratory consisted of a self-contained circuit in which the water of the sumps was pumped up into several head tanks and then distributed, at constant pressure, to the flumes and equipment of the laboratory. The two channels inside the metal flume were supplied independently from the low head tank of the laboratory which had a capacity of 88.5 m^3 and was supplied by a single low head pump (13.5 m head of water, and 24.3 Kw).

The water was supplied to the flume through a 0.20 m diameter pipe and was measured by a standard Venturi-meter tube with a throat ratio of 1-5.25. The Venturi-meter was connected to a differential manometer filled with mercury. The calibration curve of this instrument was previously made by Gill (65) and the results were checked in this study against the depth-discharge curve of the downstream weir of the flume. Discharges up to 60 l/s were controlled by a gate valve. Important vibrations in the flume were observed at the beginning of the tests due to the impact on the flume of the jet which issued under the gate of the valve. The valve was moved back 2.0 m from its position at the exit section of the vertical supply pipe and a manifold plate (which dissipated part of the energy of the jet) was placed immediately downstream from the valve. This arrangement proved to be satisfactory.

The small channel was supplied through a 0.10 m diameter pipe, the volumetric discharge being controlled by a gate valve and measured through

an orifice plate of 4 cm diameter (D). The orifice plate with D and D/2 tappings was designed according to B.S. 3680 to measure discharges up to 30 l/s. The pressure tappings were connected to a differential mercury manometer.

2.3 - FLOW MEASUREMENTS

Efficient and accurate measurements are absolutely essential for correct conclusions in the various fields of Fluid Mechanics research. In the present experimental work, water levels and flow depths, flow rate discharges, and local velocities were the flow variables measured throughout the tests. The details of the installation and operation of the various measuring devices used are described in this section.

2.3.1 - Water Levels

The water levels and the depth of the flow at different points in the flume were measured either by point gauges or by pressure tappings connected to piezometric tubes. The locations of the nine tapping points (P_1,P_2..., P_9) drilled in the bottom of the flume are given in Fig. 2.1-1. The pressure tappings were connected to the tubes of a piezometric board by plastic tubes, and were calibrated in still water against a point gauge which could read accurately up to 0.005 cm.

The mean depth of the stream in the wider channel was measured at point P_1 (Fig. 2.1-1) and was always controlled by a point gauge. The free surface of the merged streams was highly disturbed by progressive waves which were reflected at both walls of the flume. For certain conditions a set of standing waves was observed over the jet of the sluice discharge diffusing downstream in the main channel as well. The readings of a point gauge in

these conditions would be inaccurate, and instead pressure tappings were used, to measure the mean depth of the flow. The estimated accuracy of the pressure measurements was 0.1 cm.

A direct measurement of depth in a supercritical stream is always inaccurate due both to standing waves in the free surface (generated at the boundaries of the flow), and to its shallowness. A tapping pressure measurement is inadequate because of the fast characteristic of the flow. Alternatively, the depth of the fast stream was calculated from the energy equation applied to the flow of the sluice gate, for which the approaching velocity and the energy dissipated at the gate were neglected. The corresponding depth was measured in a scale and the discharge by the orifice plate. The depth of the fast stream was calculated with an accuracy of 0.05 cm. This depth could be evaluated by a coefficient of discharge for the sluice gate of 0.60.

2.3-2 - Discharge Calibration Tests

Orifice Plate

An orifice plate of 4 cm diameter was designed to measure the volumetric discharge in the fast channel. The orifice plate was connected to a differential manometer and was calibrated in a volumetric tank with a cross-section area of 23.6 m^2. Inside the tank, the water levels were measured with a magic eye point gauge, which could read precisely up to 0.01 cm (maximum depth measured - 0.82 m). The volume of water in the tank was measured within 1%. The time of the discharge was controlled by a stop-watch with an accuracy of 0.1 of a second. Linear scales, with intervals of 0.2 cm, were used to measure the water levels in the manometer tubes. Manometer heads were measured within 1.5%. For

discharges smaller than 8 l/s a water manometer (H_2O) was calibrated and, for greater discharges up to 30 l/s, a manometer filled with mercury (Hg) was used. The calibration curve of the mercury manometer is shown in Fig. 2.3-1.

Two simple expressions for the discharge of the orifice plate have been calculated, and appear in Appendix A,

$$Q_{OR} = 3.43\ (\Delta h_{Hg})^{\frac{1}{2}} \qquad (8 < Q_{OR} < 30\ (l/s))$$

$$Q_{OR} = 0.98\ (\Delta h_{H_2O})^{\frac{1}{2}} \qquad (Q_{OR} < 8\ (l/s))$$

(l/s) (cm)

in which the discharge of the orifice (Q_{OR}) is expressed in (l/s), and the mercury (Δh_{Hg}) and the water (Δh_{H_2O}) manometer heads are expressed in (cm).

Venturi-meter

The existing calibration curve of the Venturi-meter (65) was checked. The results of the orifice calibration were used to calculate a depth-discharge curve for the downstream weir of the flume. Good agreement was found between the discharges of Gill's Venturi rating curve (65), which was a straight line fitting a logarithmic plot, and the corresponding values measured from the depth-discharge curve of the weir. A maximum difference of 2.7% was observed. All the results are presented in Appendix A.

From Gill's experimental points, an empirical expression was calculated for the Venturi calibration curve

$$Q_{VE} = 9.6\ (\Delta h_{Hg})^{\frac{1}{2}}$$

where the discharge (Q_{VE}) is expressed in (l/s), and the mercury manometer head (Δh_{Hg}) in (cm).

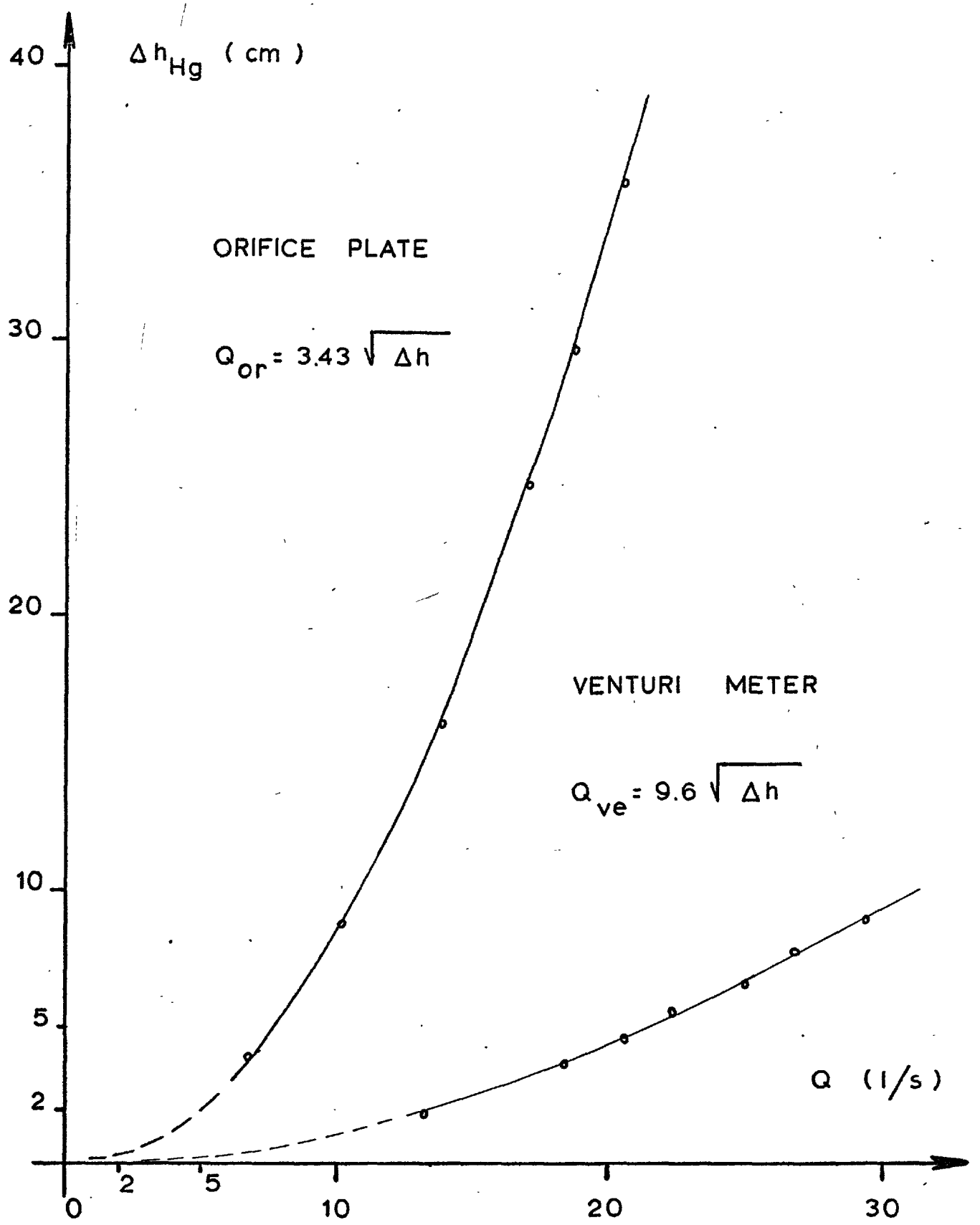


FIG. 2.3-1 CALIBRATION CURVES.

2.3.3 - Mean Velocities

Both a Pitot-static tube and a mini-current meter were used to measure local velocities at different points of the flume so that velocity profiles could be drawn for different sections in the merged flows. The simultaneous use of both measuring devices doubled the number of measurements made during tests and allowed comparison of the particular velocity measurements of each instrument. The current meter proved to be a more sensitive instrument in the range of conditions tested. The maximum velocity measured was 74.8 cm/s.

Pitot-static Tube

The general equation for a Pitot-static Tube, when it is used to measure velocity (V), is

$$V = C\sqrt{2g}\left(\frac{P_s - P}{w}\right)^{\frac{1}{2}}$$

where (P_s) is the stagnation pressure, (P) the static pressure, (w) the specific weight of the water, (g) the gravitational acceleration, and C an instrument coefficient, which is nearly equal to unity for most instruments. The differential pressure head $\left(\frac{P_s - P}{w}\right)$ can be read direct in a differential pressure-manometer (Δh). The expression used to calculate the approximate velocity was

$$V = 44.3(\Delta h)^{\frac{1}{2}}$$

(cm/s) (cm)

The Pitot tube was fixed to an adjustable point gauge installed on a trolley support which could be moved along the flume, and was connected

to a differential-manometer of water. The water levels in the manometer tubes were measured with a travelling microscope reading accurately up to 0.01 cm. A systematic error in the manometer zero reading was detected, for when the two tubes of the manometer were connected, a zero head value was not read, but an average reading of 0.15 cm was always found, which was subtracted from all manometer heads. Two possible explanations for the residual zero reading are capillarity effects inside the small diameter manometric tubes, and an error in the levelling of the microscope itself.

The calibration of the Pitot-static tube was not carried out during the tests. However, the velocity measurements of the Pitot-tube were compared with the measurements of a calibrated mini-current meter, and correlation was found to be satisfactory. The range of manometer heads varied between 0.20 cm and 2.90 cm. The smaller heads were difficult to measure with accuracy, and therefore the velocities calculated from them were not very reliable. It was observed that the values of velocity smaller than 20 cm/s were not consistent, which implied that the Pitot-tube method was not adequate for such a range of velocities. Consequently, it was decided to repeat the same measurements with a current-meter.

Mini-current Meter

A miniature current flowmeter provided with an electronic unit to count the revolutions of the propeller was also used in the measurement of local velocities in the confluent streams. The electronic unit could count automatically the revolutions in a period of 10 seconds, stop for 30 seconds, begin a new count for 10 seconds, and stop again, and can continue this process for as long as required. Testing the current meter it was found

that the value of successive readings of the propeller revolutions could vary by more than 10%, probably due to unstable conditions in the local flow around the propeller. Consequently, the mean value of the velocity had to be averaged from several readings. A small variation with time was also observed in the averaged value of the velocity (4.3% in an interval of 3 hours and 45 minutes). Therefore, a simple method to carry out the measurements which could correct both of the effects mentioned before was required. It was found necessary to run the current meter equipment for half an hour before taking any reading. At each point, five readings of the propeller meter (number of revolutions in 10 seconds) were taken and, after five minutes, a second series of readings was made. The ten readings were averaged and the flow velocity was calculated from the calibration curve of the instrument. The accuracy of this simple method to measure the velocity of the flow was estimated to be within 1%.

The current meter proved to be a more sensitive instrument for measuring velocities in the range of 10 cm/s to 80 cm/s than the Pitot-static tube. In general, the current meter velocities were found to be smaller (7%) than the corresponding values of the Pitot-static tube. Variations of 50% in the values of the propeller readings for velocities smaller than 10 cm/s suggested this method also to be unreliable, for that range of velocity.

2.4 - TEST PROCEDURE

The experimental apparatus and the measuring equipment used to carry out the present work have been briefly described in the previous sections. The test procedures employed to conduct the experiments are detailed now. The research was initially concentrated in the hydraulic jump formed close

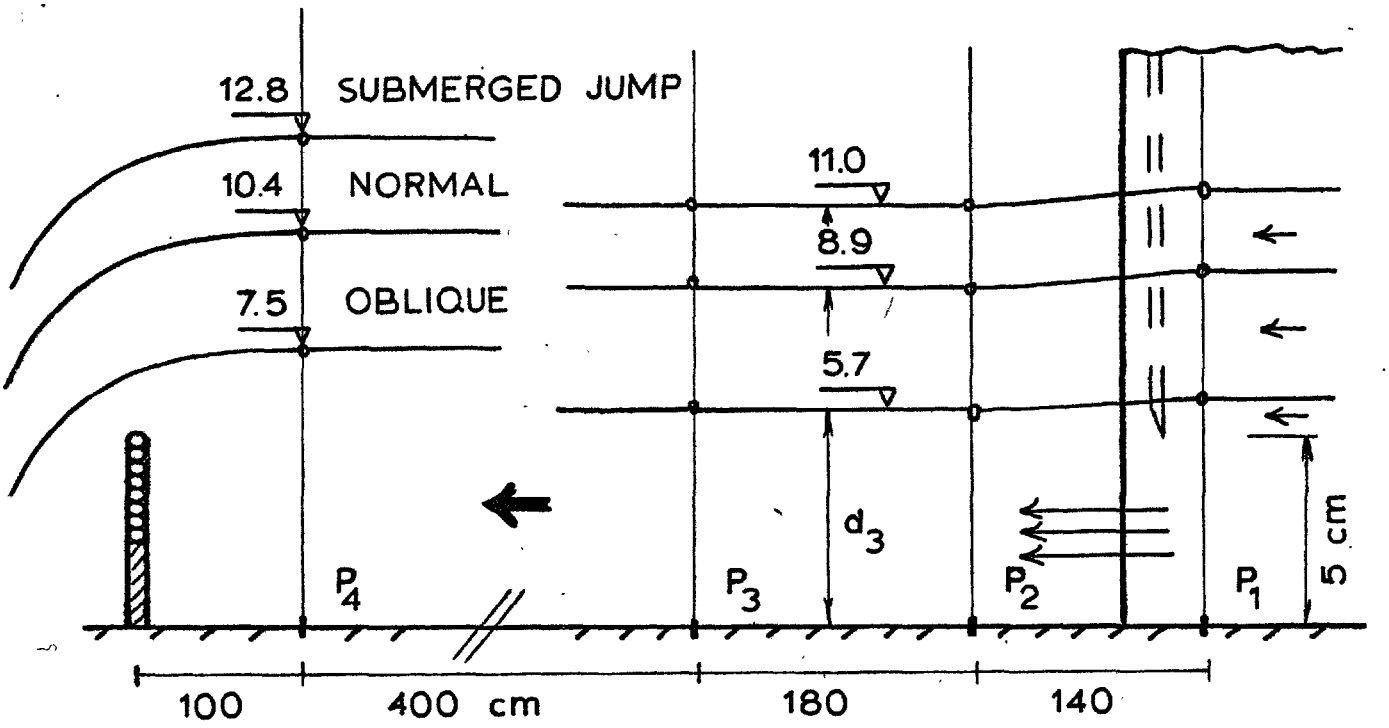
to the exit section of the fast channel, and later in the characteristics of the sluice jet diffusing downstream in the flume.

2.4.1 - Jump Classification Tests

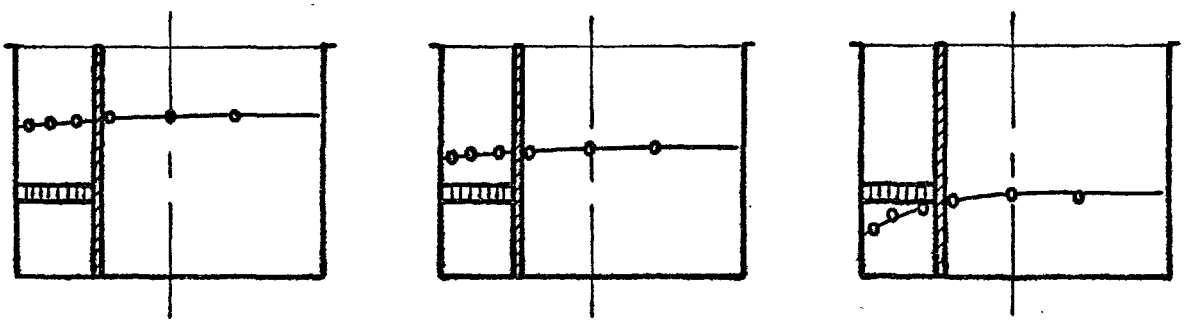
In this series of tests a constant aperture of the sluice gate of 5.0 cm was used, which corresponds to an approximate depth of 3.0 cm for the fast stream. The water levels in the downstream end of the flume were controlled by a combined operation of the Tainter gate and the weir structure. For each discharge of the sluice gate the tail water depth of the flume was adjusted, in order to reproduce the three basic forms of the jumps (which were found to be oblique, normal and submerged hydraulic jumps, and are described in Chapter 3). Eight different discharges were used in the tests corresponding to a range of Froude numbers for the fast (supercritical) stream of 2.1 to 4.9. For the higher Froude numbers it was observed that the deeper water in the main channel circulated around the edge of the dividing wall and spilled over the thin jet producing an early submergence of the sluice gate. This effect could have been avoided completely if the dividing wall had been longer. The actual length of the wall (10 cm), in spite of not being long enough, proved to be satisfactory for most of the conditions investigated. No water was supplied to the wider channel in these tests, but it was confirmed later that the effect of the slow stream on the jump formation is small.

The discharge of the fast stream (Q_1) was measured at the orifice plate. The mean velocity (U_1), which was assumed to be uniform, was calculated from the orifice discharge and the dimensions of the cross-section of the flow (d_1 = 3.0 cm; b_1 = 20 cm). The flow depths downstream of the jump were measured at tapping points (P_2 and P_3), which were placed in the middle of the flume at 1.00 m and 2.80 m from the edge of the dividing wall. The mean

MAIN FLOW PROFILE ON FLUME CENTER LINE



CROSS SECTION AT (P_2) LOOKING UPSTREAM



SUBMERGED JUMP NORMAL JUMP OBLIQUE JUMP

FIG. 2.4-1 FREE SURFACE PROFILES OF THE FLOW

averaged value of these two depths was taken as the characteristic depth of the downstream flow (d_{23}). Typical water surface profiles are sketched in Fig. 2.4-1.

2.4.2 - The Effect of a Uniform Stream on the Jumps

In these tests the same depth for the fast flow (d_1 = 3.0 cm) was used, and well defined forms of the hydraulic jump occurred at a Froude number (Fr_1) of 2.3. Different values of depth and velocity of the uniform stream were used to investigate the effect of this stream on the three basic forms of the jump.

The depth of the uniform stream (d_2) was measured by a pressure tapping at point (P_1) in the flume. This measurement was always checked with a point gauge, and it was used to calibrate the measurements of the tapping points connected to a piezometric board. The depth (d_2) was controlled by the tail water level in the flume. The discharge (Q_2) was measured by the Venturi-meter in the pipe supplying the flume. The Froude numbers (Fr_2) of the slow stream flow varied between 0.0 and 0.7.

2.4.3 - Scale Effects in the Depth of the Fast Stream

Hydraulic Engineers very often use small scale models to investigate solutions for the practical problems encountered in their work. In modelling the physical conditions of a specific situation, it is very convenient to know how small the model may be made. The scale effects will be greatest in the fast flow and will depend on its depth. The measurements of depth made in the fast stream collapse on to one single curve for a depth of flow (d_1) greater than 3.0 cm. The marked discrepancies of the experimental results for the streams 2.0 and 2.6 cm deep are explained in terms of boundary layer growth. It was calculated that the boundary layer thickness at the edge

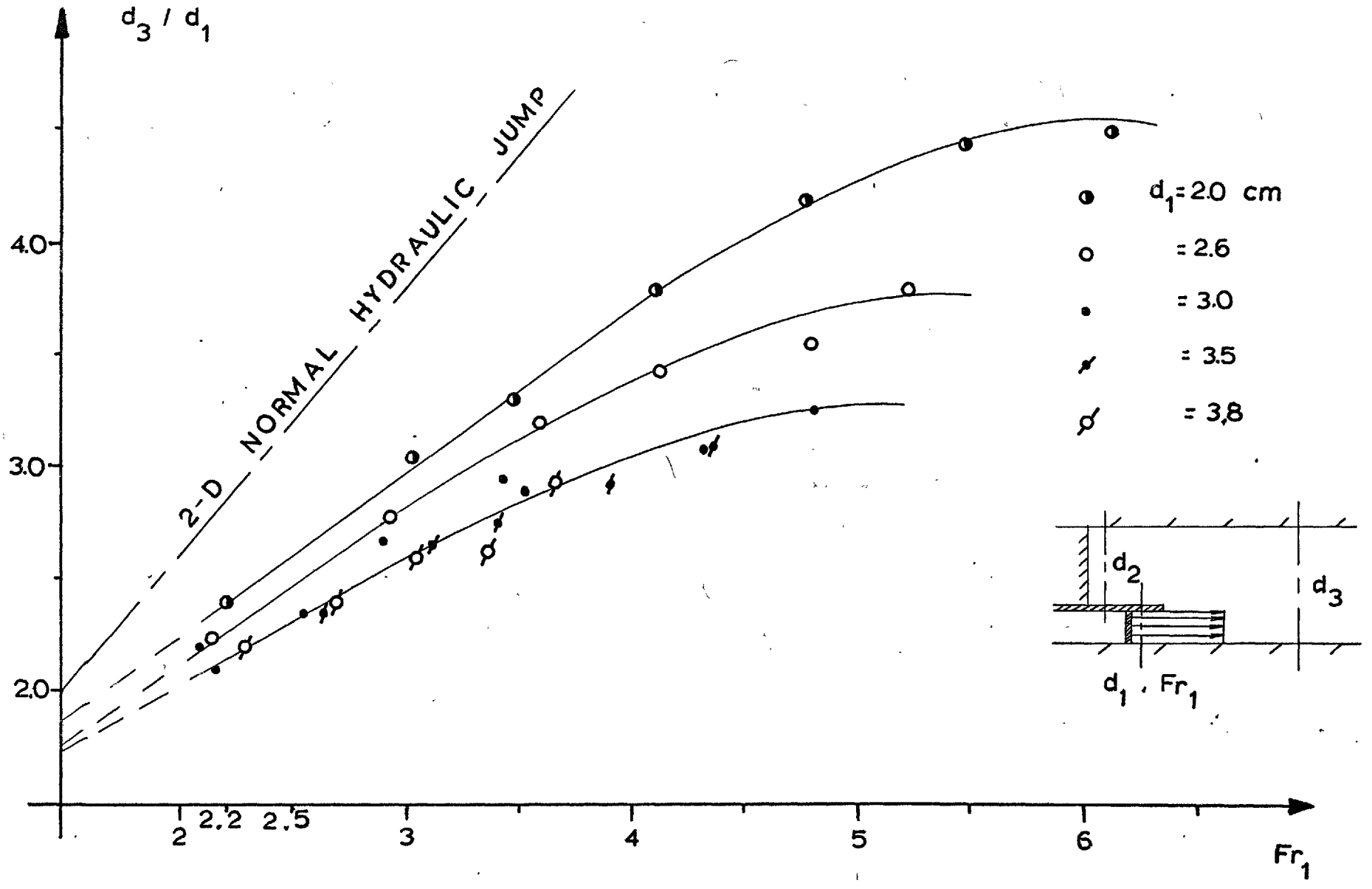


FIG. 24-2 SCALE EFFECTS IN THE DEPTH OF THE FAST STREAM

of the dividing wall was of the order of 0.3-0.4 cm, representing 15 to 20% of the depth of the fast stream. Results of the tests are given in Appendix B, and plotted in Fig. 2.4-2. They show that the Reynolds number of the fast flow (based on the depth of the flow) varies between 20,000 and 85,000.

The tests were carried out with five different apertures of the sluice gate corresponding to depths of (d_1 = 2.0; 2.6; 3.0; 3.5; and 3.8 cm) for the sluice stream. The tail water depth in the flume was adjusted by the Tainter gate and well-defined normal hydraulic jumps were set inside the fast channel. No discharge was supplied to the slow channel. Froude numbers (Fr_1) ranging from 2.1 to 6.1 were tested. In flows with higher Froude numbers (unstable location of the jump), the classification of the form of jump (whether it was an intermediate normal-oblique jump, a normal hydraulic jump, or a normal-submerged jump) was difficult. In these cases the length of the dividing wall of the channels was extended with a thin plate of metal 20 cm long, which helped in defining the form of the jump. On the other hand, the situations in which an early submergence of the sluice gate was observed (due to the big depth of water in the parallel channel), the characteristic depth (d_{23}) of the normal hydraulic jump, were estimated in the following way:

(1) the characteristic depths of the intermediate forms of a submerged-normal and a normal-oblique jump were measured;

(2) the downstream depth required for the formation of a normal jump should be somewhere between these two values of depth;

(3) the mean was taken as the characteristic depth of the normal hydraulic jump.

2.4.4 - Diffusion of the Jet

The characteristics of the jet issuing from the sluice gate and diffusing in a deeper stream of water, flowing in the same direction, were also investigated. A mini-current flowmeter and a Pitot-static tube were used to measure velocities at different points of the cross-sections of the flow. The corresponding velocity profiles were used in calculating the rate of growth of the jet, the decay of maximum velocity, and the similarity form of the velocity profile.

A particular case of the flow conditions in the flume was analysed which involved the formation of a stable normal hydraulic jump inside the fast channel. The uniform stream in the parallel channel prevented the formation of reverse currents at any point in the flume. The specific characteristics of the two parallel streams with different depths and velocities were:

a) A slow stream, 7.8 cm deep and 54 cm wide, with a mean velocity of 22.8 cm/s (a discharge of 9.6 l/s).

b) A fast stream, 3.0 cm deep and 20 cm wide, with a mean velocity of 1.40 m/s (discharge of 8.4 l/s).

c) The walls and bed of the flume confined the diffusion of the jet.

The tests were carried out with the bottom of the flume in a horizontal position. After switching on the low head pump of the laboratory, the valves of the pipes supplying the two channels had to be regulated for discharges of 9.6 l/s and 8.4 l/s, respectively. Three cylindrical rods were fitted on the downstream weir to produce a mean depth of flow of 7.8 cm in the flume. At the tapping points, the flow depths were measured on a piezometric board. A constant aperture of 5 cm in the sluice gate was kept during these tests.

The flow conditions in the flume were checked, from time to time, by a simple reading of the water level (h_{SL}) upstream of the sluice gate (fast stream) and of the depth of flow at tapping point number 1 (uniform stream).

Before beginning the measurements in the flume a check on the conditions of the measuring equipment was done. The propeller meter had to be run for half an hour before reliable readings could be expected. All the bubbles of air in the plastic tubes connecting the Pitot-static tube to the manometer had to be eliminated. The exact position of each velocity measurement was recorded by the distance (x_o) to the edge of the dividing wall, the distance (y) to the right wall of the flume, and the distance (z) to the bottom of the flume (see Fig. 2.1-1).

Pitot-static tube

The Pitot tube was used to measure velocity profiles at seven cross-sections (x_o = 50; 100; 190; 280; 390; 530; and 680 cm) of the diffusing jet. The measurements were taken at approximately half the depth of the flow (z = 3.8 cm), and in each cross-section the velocity was measured at seven points (y = 3; 8; 16; 23; 38; 57; and 72 cm).

A single measurement of velocity was taken in most of the points in the flow. The Pitot tube was placed at a point in the cross-section where the measurement was required and only after ten minutes the manometric head of the Pitot was read. In the measurement of the first manometric heads, the water levels in the manometer tube connected to the Pitot were estimated to 0.05 cm. Using a telescope, it was possible to measure more accurately (up to 0.01 cm) the manometer heads, and the previous measurements were repeated. Because the tests were carried out for several weeks, some of the points in the sections were measured more than once in order to control or check the flow conditions. In all the points in which

TABLE 2.4-1 CORRECTED MANOMETER HEADS AND VELOCITIES OF THE PITOT-STATIC TUBE

x_o (cm) \ y (cm)	3	8	16	16 (check)	23	38	57	72	$(\frac{V_{16}}{V_{check}})$
50	2.46 69.50	2.85 74.80	1.47 53.60	(1.27) (50.00)	0.24 21.70	0.21 20.30	0.21 20.30	0.12 15.30	1.157 (1.072)
100	2.43 69.10	2.47 69.60	1.56 55.40	(1.48) (53.90)	0.51 31.60	0.20 19.80	0.14 16.50	0.11 14.70	1.054 (1.028)
190	2.10 64.20	1.97 62.10	1.07 45.80	(1.25) (49.60)	0.76 38.50	0.33 25.50	0.12 15.30	0.10 14.00	0.856 (0.923)
280	1.85 60.20	1.85 60.20	1.40 52.40	(1.20) (48.60)	0.83 40.30	0.33 25.50	0.15 17.10	0.05 9.90	1.167 (1.078)
390	1.11 46.60	1.12 46.90	1.07 45.80	(1.06) (45.60)	0.82 40.10	0.34 25.80	0.15 17.10	0.06 10.80	1.009 (1.004)
530	0.79 39.30	0.85 40.80	0.79 39.30	(0.91) (42.30)	0.66 35.90	0.38 27.30	0.18 18.80	0.11 14.70	(0.868) (0.929)
680	0.70 37.00	0.80 39.40	0.95 43.20	(0.80) (39.40)	0.70 37.00	0.65 35.70	0.32 25.00	0.17 18.30	1.187 (1.096)

Notes: (1) first value is the corrected manometer head (Δh - 0.15) in (cm);

(2) second value is the velocity (V) in (cm/s);

(3) V (cm/s) = 44.3 $(\Delta h \text{ (cm)})^{\frac{1}{2}}$.

there was available more than one reading of the Pitot head the mean value was calculated. When all the measurements were completed, a last control test was carried out in which the velocity at a point (y = 16; z = 3.8 cm) in each section was measured again. Differences up to + 18.7% were found. The residual zero reading (0.15 cm) found during the tests was subtracted from all the manometric heads, and a complete list of the results of the Pitot-static tube measurements is presented in Table 2.4-1. To satisfy continuity it was found necessary to correct by a constant factor (up to 9.2%) some of the velocity profiles.

The velocity profiles at sections (x_o = 190; and 280 cm) were measured, as well, with a calibrated mini-current meter. These tests were carried out to check the measurements of the Pitot-tube and to compare the characteristics of both instruments. In general, the velocities measured by the Pitot were higher than the velocities of the current meter. Both velocity profiles were used to calculate the flow rate of the corresponding sections. The ratio of the discharge calculated from the Pitot profile to the discharge of the current meter was 1.084 and 1.089 at sections (x_o = 190 cm) and (x_o = 280 cm), respectively.

One of the simplifications made in the analysis of the flow conditions in the flume was to assume that flow pattern was two-dimensional (the same at each depth of the flow). Velocity measurements were carried out with the Pitot-tube at different depths of the flow (z = 1.0; 2.5; 3.8; 5.0; 6.0; and 7.0 cm) at points (x_o = 110; y = 8 cm), (x_o = 290; y = 12 cm), and (x_o = 290; y = 45 cm). These measurements confirmed the previous assumption and suggested that the velocity measured at the mean depth of the flow is approximately the mean value of the vertical velocity profile (see Fig. 2.4-3).

All the results of the velocity measurements made with the Pitot-static tube are presented in Appendix C-1, and the calculations of the flow rates from the velocity profiles in Table C-1.

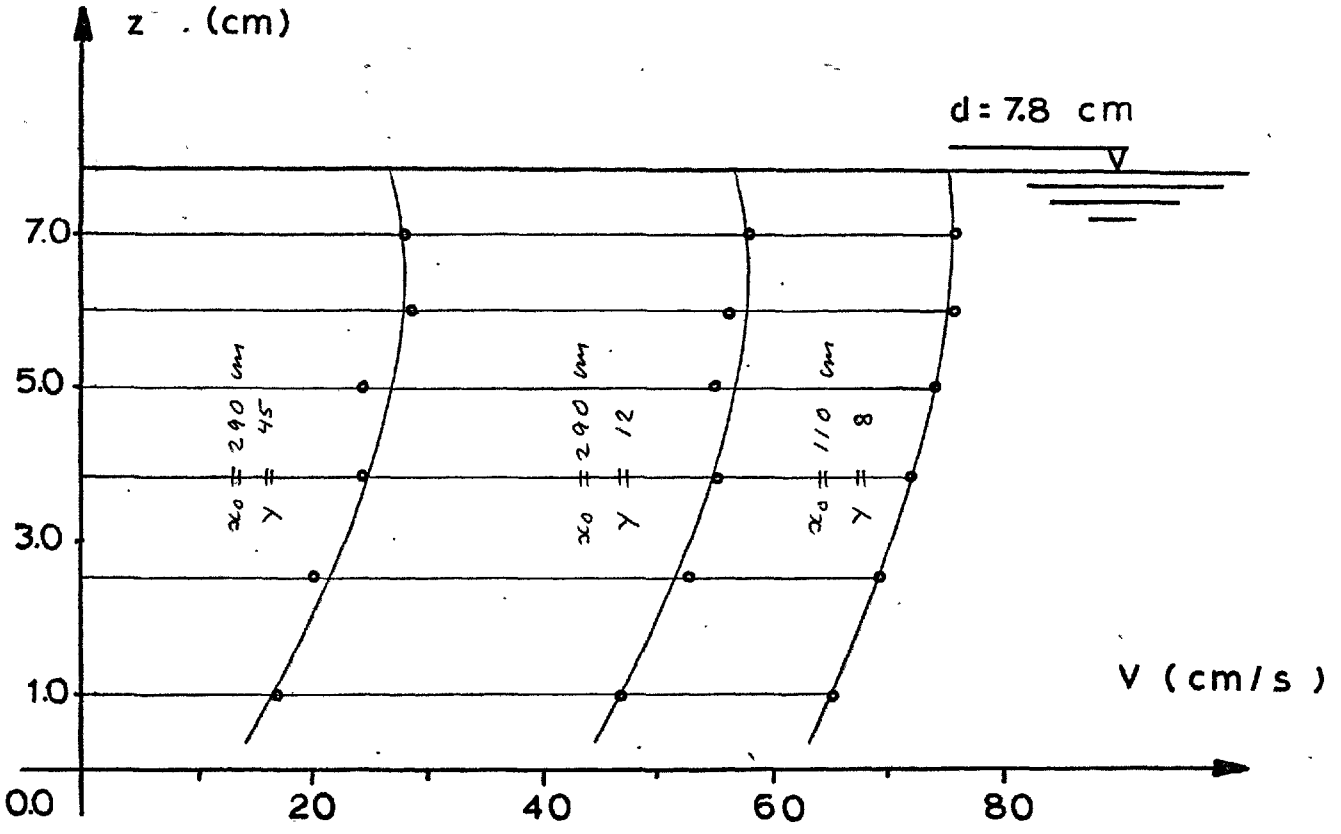


FIG. 2.4-3 VERTICAL VELOCITY PROFILES

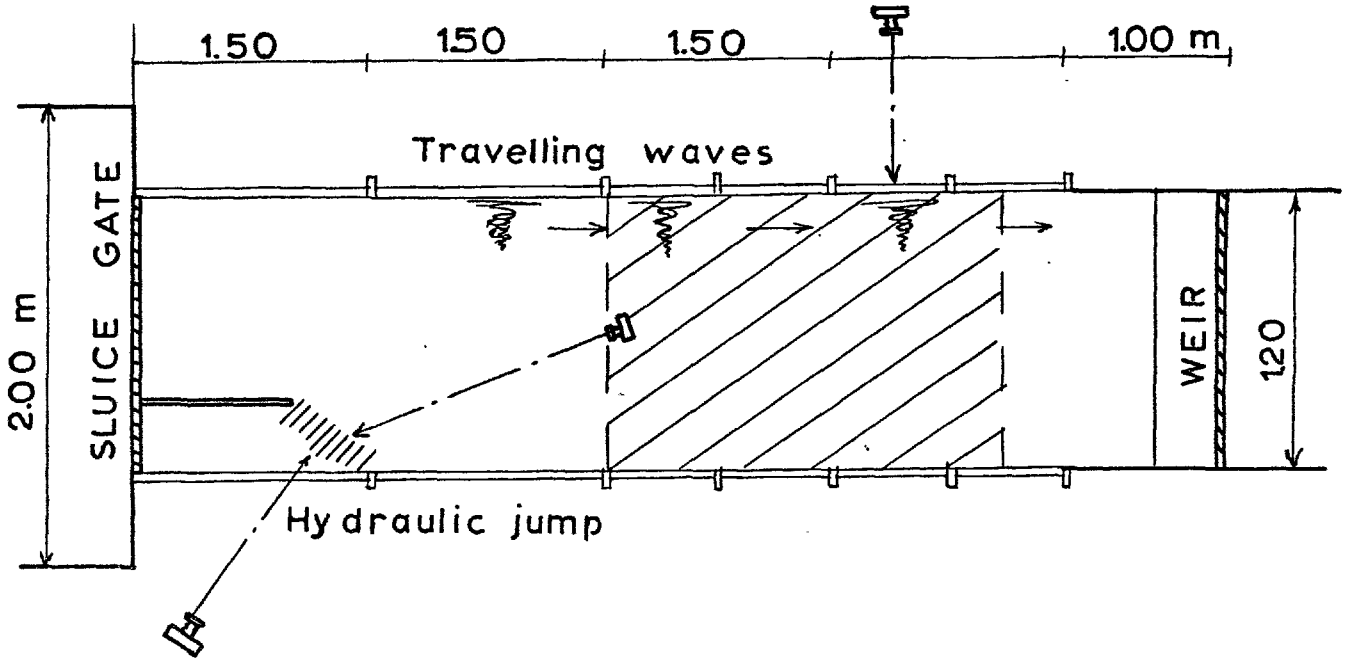


FIG. 2.5-1 GLASS SIDED FLUME AND PHOTOGRAPHIC POSITIONS

Mini-current meter

A balance of momentum and energy was investigated using a control volume in the flow of the two mixing streams. The section in the flume ~~with six tapping points~~ (x_o = 190 cm) was selected to be the downstream section of the control volume, and the section of tapping point (P_1) was the upstream control section (x_o = -40 cm). The length of the control volume (230 cm) had to be short, so that significant energy of the flow would not be dissipated in the boundaries of the flume. A mini-current meter was used to measure the velocities at the control sections.

Flow velocities were measured at seven points (y = 3; 8; 16; 23; 38; 57; and 72 cm) and at three different depths (z = 1.0; 3.8; and 6.0 cm) in the downstream section of the control volume. Large variations in the readings of the propeller meter (up to 90%) were observed for small velocities (less than 10 cm/s) of the flow measured near the right wall of the flume (y = 72 cm). These velocities were not consistent among themselves because the current meter was inadequate for that range of velocities. In the upstream control section the velocities were measured at points (y = 36; and 62 cm) and at depths (z = 1.0; 3.8; and 6.0 cm). The averaged velocity was 25.0 cm/s (the uniform velocity of the stream calculated from the Venturi discharge and cross-section area was 22.8 cm/s), and differences up to 10% were found among the measured values. All the results of the tests with the current meter are presented in Appendix (D).

2.5 - FLOW VISUALIZATION

The experimental work done for this thesis was initiated and completed with visualization tests. The first analysis in the flow conditions of a fast (supercritical) stream merging with a deeper and uniform stream was carried out in an Ahlborn tank. The peculiar flow characteristics observed in these tests were the form of the hydraulic jump and the diffusion of the fast jet. The

second series of visualization tests were carried out in a larger flume (1.20 m wide), with the objective of taking photographs of the hydraulic jumps and the large travelling waves observed in the test flume.

2.5.1 - Ahlborn Tank

A box of galvanized iron, 0.27 m long and 0.20 m wide, with a sluice gate in one of the ends, was fixed inside the Ahlborn tank (1.20 m long and 0.60 m wide). The box, with a supply of water independent from the supply of the tank, was used as the fast channel, the characteristics of the supercritical stream being controlled by the sluice gate. This simple arrangement used in the visualization tests was similar to the apparatus used for the full scale tests described in Section 2.1.

Two series of visualization tests were carried out in the Ahlborn tank. Initially, the fast stream was merged with a uniform stream flowing in the same direction (co-flowing streams). In the second series of tests the uniform stream flowed in the opposite direction of the fast stream (counter-flowing streams). In both tests the three basic forms of the hydraulic jump were observed. The diffusion patterns of the fast jet issued from the sluice gate were different in the two situations. The flow conditions of the counter-flow streams were more unstable than the co-flowing conditions, and consequently the measurements were more difficult. At that stage it was decided to analyse the simpler flow conditions first. Finally, it was also found, from these tests, that a small length of wall (a dividing wall) separating the fast stream from the uniform stream avoided the interference of the deeper flow with the discharge of the sluice gate and more stable conditions were obtained.

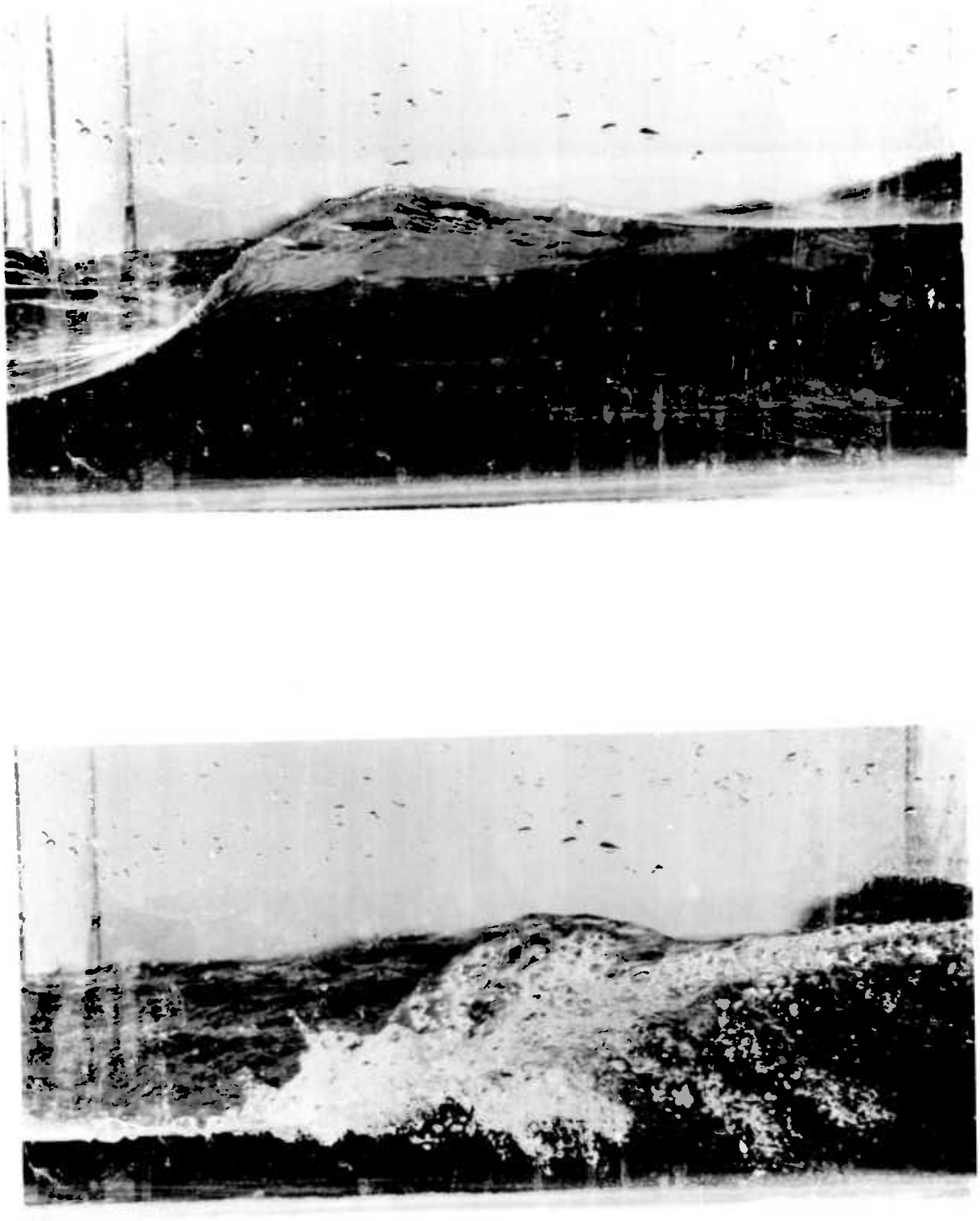


Fig. 2.5-2 TRAVELLING WAVES

2.5.2 - Photographic Tests

Oblique and normal forms of the hydraulic jump were photographed in a glass-sided flume in the Hydraulics Laboratory. At the entrance of the 1.20 m wide flume a sluice gate controlled the velocity and depth of the supercritical flow. The sluice gate flow section was reduced to a gap 30 cm wide and 7.5 cm high. A sheet of metal, 90 cm long, was used as a dividing wall. This arrangement is similar to the conditions tested in Section (3.2) and a sketch of the glass-sided flume arrangement is given in Fig. 2.5-1. The upstream water level at the sluice gate was measured with a piezometric tube (h_{SL} = 37 cm), and the approximate depth of the fast stream (d_1 = 4.5 cm) was calculated from the aperture of the gate ($d_1 \cong 0.60 \times 7.5$ cm). The Froude number of the fast stream was $F_1 = 3.9$. Side views and plan views of the jumps were photographed.

During the experiments, it was noticed that the free surface of the merging streams was always disturbed by waves standing and travelling in the flume. A particular characteristic of the flow pattern with an oblique jump was a set of standing waves on top of the diffusing jet. The oblique front of the jump was reflected at the right wall of the metal flume, crossed over the fast jet to be reflected, again, at the shear boundary (separating the fast and slow streams) towards the flume wall. Very large waves, which eventually would break, were observed travelling downstream in the flume for the particular conditions with an oblique jump and no uniform stream. During the photographic tests a maximum amplitude of 12 cm was measured in the travelling waves (the mean depth of the flow was 8.5 cm). These large waves were observed in the tests on the metal flume, the Ahlborn tank and the glass-sided flume. Two photographs of travelling waves, one of them a breaking wave, are given in Fig. 2.5-2. The origin of these

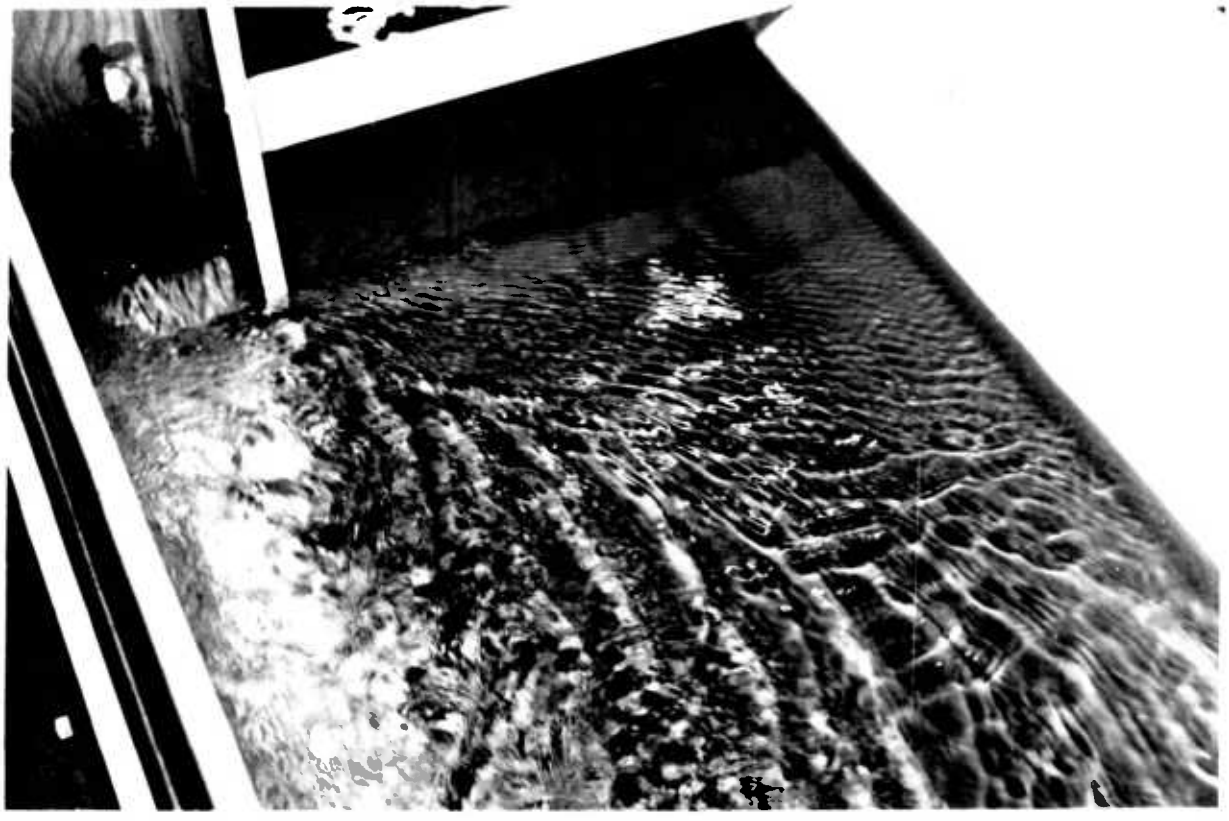


Fig. 2.5-3 TRANSVERSE WAVES

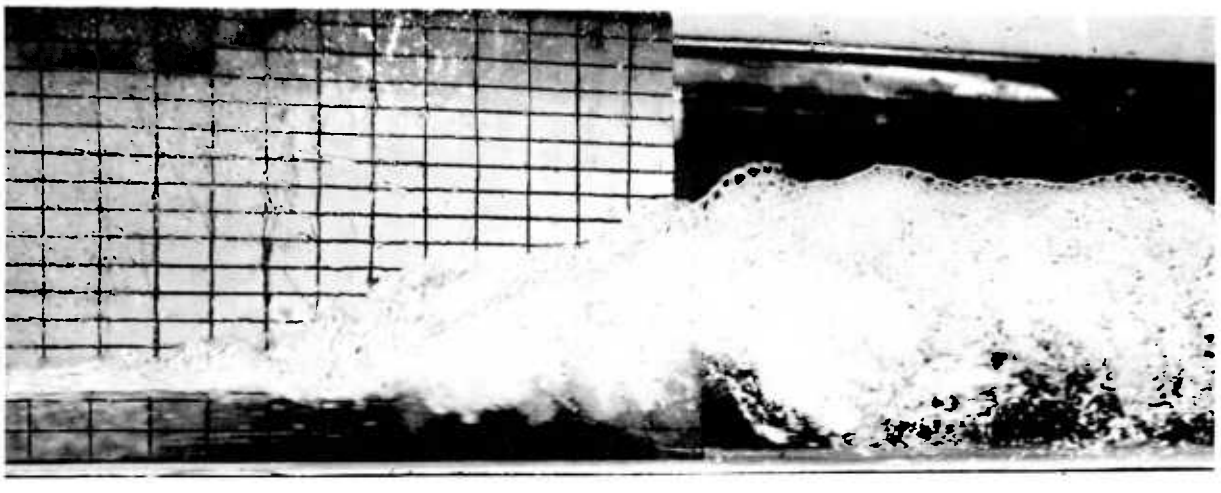


Fig 2.5-4. NORMAL HYDRAULIC JUMP

travelling waves seemed to be the shear boundary of the two parallel streams. In Fig. 2.5-3, a pattern of waves parallel to the shear boundary can be seen. This particular photograph was taken in the metal flume with a normal hydraulic jump, and a small flow in the wider channel. Permanganate of potassio was added to the water of the slow stream to improve the contrast in the photograph. Unfortunately, no time was available to do more work on the waves.

III - HYDRAULIC JUMPS IN PARALLEL COFLOWING STREAMS

3.1 - HYDRAULIC JUMPS - A REVIEW OF THE LITERATURE

When a change from supercritical to subcritical flow occurs in open channel flow a hydraulic jump appears through which the depth increases abruptly in the direction of the flow. In Civil Engineering practice the hydraulic jump is made to form just downstream of a hydraulic structure, such as a spillway or a sluice gate where velocities are high and it is necessary to dissipate part of the kinetic energy of the flow, or to raise the water level on the downstream side of a measuring flume. The turbulent characteristics of the jump can be used either to mix chemicals or to aerate the water used in city water supplies or recovered in sewage plant treatment. The hydraulic jump is not only an effective mean of reducing mean flow energy, but a very efficient mechanism for restoring conditions of uniformity to the flow.

The phenomenon of the hydraulic jump has been a subject of interest to engineers for many years and its characteristics (conjugate depth ratio and energy dissipation), geometry (length and shape of the surface profile), and location have been the object of much experimental work. Ven Te Chow (4) gives a good summary of the results of some of the most important investigations. Rouse et al (36) investigated the turbulence characteristics of the hydraulic jump in an air-flow model using a hot-wire anemometer. They found that except for Froude numbers well below 2 the hydraulic jump presents a breaking front (the roller) which is responsible for the formation of the turbulence and hence the dissipation of energy. At the juncture between the oncoming stream and the return flow of the roller of the jump there is a pronounced velocity gradient, and the resulting shear gives rise to the

rapid generation of turbulence (22,36). For Froude numbers below 2 an undular hydraulic jump occurs, characterised by a succession of water surface undulations involving a negligible loss of energy in the jump (4,36).

In spite of the complex appearance of a hydraulic jump, which can be accompanied by violent turbulence, eddying, surface undulations, and air entrainment with consequential head loss, it may be successfully analysed by application of the impulse-momentum principle. The analysis of a two-dimensional normal hydraulic jump in a horizontal smooth channel is usually made with the following assumptions: (a) all boundary friction losses are neglected; (b) the hydraulic jump is assumed to take place instantaneously; (c) hydrostatic pressure and uniform velocity distributions exist immediately before and after the jump. With these assumptions and from the momentum equation the conjugate depth ratio of the hydraulic jump in a rectangular channel can be derived (4),

$$\frac{\bar{d}_1}{d_1} = \tfrac{1}{2}\left((1 + 8Fr_1^2)^{\frac{1}{2}} - 1\right) \qquad \ldots (3.1\text{-}1)$$

where $\bar{d}_1$ is the conjugate depth, d_1 the depth of the supercritical stream and Fr_1 its corresponding Froude number. This equation is known as Belanger equation (12).

The location of the hydraulic jump is known to be sensitive to changes of tail-water level and boundary shear. Wilson et al (39) found that the jump becomes less sensitive to tail-water changes if the Froude number or the channel slope are increased due to the effects of the boundary layer growth in the flume. Several definitions of the jump length have been proposed.

Two of the most commonly used are: (a) the distance from the toe of the jump to the end of the roller; (b) the distance from the toe of the jump to the point where the tail-water depth is reached. Naas (30) found that the length of the jump in a rock sausage basin is much shorter (nearly half) than the length on a smooth horizontal basin.

The control of a hydraulic jump so that the supercritical flow will not travel outside the limit of a stilling basin and scour the natural channel floor can be achieved by different methods. The use of sills or baffle piers is recommended when the downstream depth is smaller than the conjugate depth of the normal jump. The function of the sill or piers is to ensure the formation of the jump and to control its position under all probable operating conditions. If the downstream depth is larger than the conjugate depth of the jump, then a drop in the channel floor must be used in order to ensure the jump. The effective control of a hydraulic jump may be achieved, by a submerged cross-jet (37). A gradual (21) or an abrupt (33) expansion in the channel cross-section is also an efficient method of controlling the formation of a jump.

Rajaratnam and Subramanya (33) investigated the characteristics of hydraulic jumps forming below abrupt symmetrical expansions in a rectangular cross-section channel. Inside the wider channel a repelled jump (R-jump) with a normal front and a strong surface roller formed for certain tail-water levels. For higher tail-water depths the hydraulic jump appeared at the exit section of the narrow channel and resembled a normal jump with small submergence. They called this jump a spatial jump (S-jump). The characteristics of hydraulic jumps in gradually expanding channels were analysed by Arbhabhirama and Abella (21). They

treated the jump as a section of a circular hydraulic jump and assuming a quarter elliptical shape for the jump profile they derived the length and the conjugate depth of these jumps.

A hydraulic jump under spatial conditions occurs when a supercritical stream confined by parallel boundaries meets a wider and deeper tail-water level. Examples of spatial jumps are found when the water flows through only a portion of the adjoining gate openings in a barrage or in the flow over part of the weir crest of a reservoir spillway. Such jumps, which are strongly influenced by the formation of side eddies, were studied by Unny (38) and Herbrand (24). Both of them found that the spatial jump requires a smaller tail-water depth for its formation than the classical two-dimensional hydraulic jump with the same inflow conditions.

In engineering practice the hydraulic jumps can appear under three basic forms: oblique, normal and submerged jumps. Normal hydraulic jump forms have been described previously. Changes in section or alignment of open channels flowing at super-critical velocities produce depth changes in the flow that may be abrupt or gradual depending on the type of wave produced. A series of experiments were undertaken by Ippen and Harleman (27) to verify the hydrodynamic theory of oblique hydraulic jumps. In this work they also found that the transition between undular and roller-type jumps occurs at a depth ratio of 2. Submerged hydraulic jumps were studied by Rao and Rajaratnam (34) in 1963, and later, in 1965, Rajaratnam (31) treated this jump as a particular case of a plane turbulent wall-jet under an adverse pressure gradient.

3.2 - JUMP CLASSIFICATION TESTS

The visualisation tests carried out in the Ahlborn Tank (Section 2.5-1) showed three basic forms of the hydraulic jump forming within the expanding section of the fast stream. According to the position of the jump front wave, these hydraulic jumps were called oblique, normal and submerged jumps, respectively. When the tail-water depth was small, the supercritical stream expanded freely until it occupied the full width of the channel and created a system of diagonal surface waves due to successive reflections at the walls of the flume. As the tail-water depth was increased a hydraulic jump with an oblique front formed attached to the edge of the dividing wall. Raising the tail-water level the oblique front attached to the edge of the wall gradually became normal to the direction of the flow. With a slight increase in the tail-water depth the normal jump with its front wave of rolling water moved back inside the sluice channel, and a further increase of the water levels would gradually drown the outlet of the sluice gate.

The details of the tests on the different forms of the jumps were given in Section 2.4-1. The approximate depth of the supercritical stream was 3.0 cm with a range of Froude numbers varying from 2.1 to 4.9, and no flow was supplied to the wider channel. The threebasic forms of the jumps and the characteristics of some intermediate forms of jump observed in the laboratory flume are now described.

Oblique Jump

With a small tail-water depth in the flume the deeper water of the main channel spilled over the shallower stream forming an oblique front standing across the supercritical stream and attached to the edge of the dividing wall. Plan and side views of this oblique jump can be





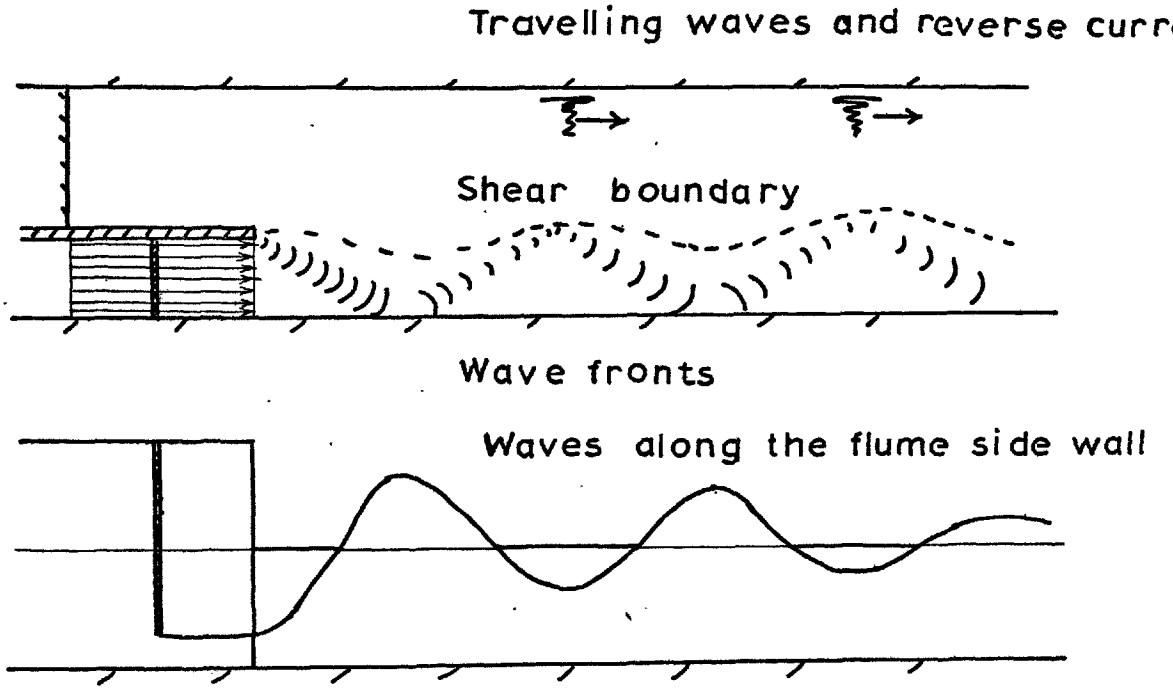
Fig. 3.2-1. OBLIQUE JUMP

seen in Fig. 3.2-1. This oblique standing wave was reflected at the wall of the flume towards the shear boundary (separating the jet from the still water), where it was reflected, again. The shear boundary had a meandering shape. This flow pattern of standing waves crossing the diffusing jet resembled the pattern of shock waves (the wall being a plane of symmetry) found in the discharge of a two-dimensional supersonic jet (of gas) into a free space where the pressure is greater than the pressure in the jet. The oblique water waves were similar to the oblique shock waves of compression generated at both edges of the orifice, crossing one another, and being reflected from the opposite boundaries of the jet as waves of rarefaction (11). The flow pattern of an oblique jump is sketched in Fig. 3.2-2. Large waves travelling downstream in the flume along the left wall of the flume were observed only when there was no flow in the wider channel, as were the reverse currents outside the jet region of the flow.

Normal Hydraulic Jump (at an abrupt expanding section)

As the tail-water depth was increased the oblique front of the hydraulic jump gradually became normal to the direction of the flow, and eventually a normal hydraulic jump formed at the abrupt expanding section of the narrow channel (see Fig. 3.2-3). Around the edge of the dividing wall, water from the main channel (with a bigger depth of flow) spilled over the fast stream of the narrow channel and a front wave with a surface roller formed in the other side of the expanding section, but without filling it completely. Along the right wall of the flume the standing waves observed were smaller than in the case of an oblique jump. The position of this jump was stable at the abrupt expansion. An intermediate

OBLIQUE JUMPS



NORMAL JUMPS

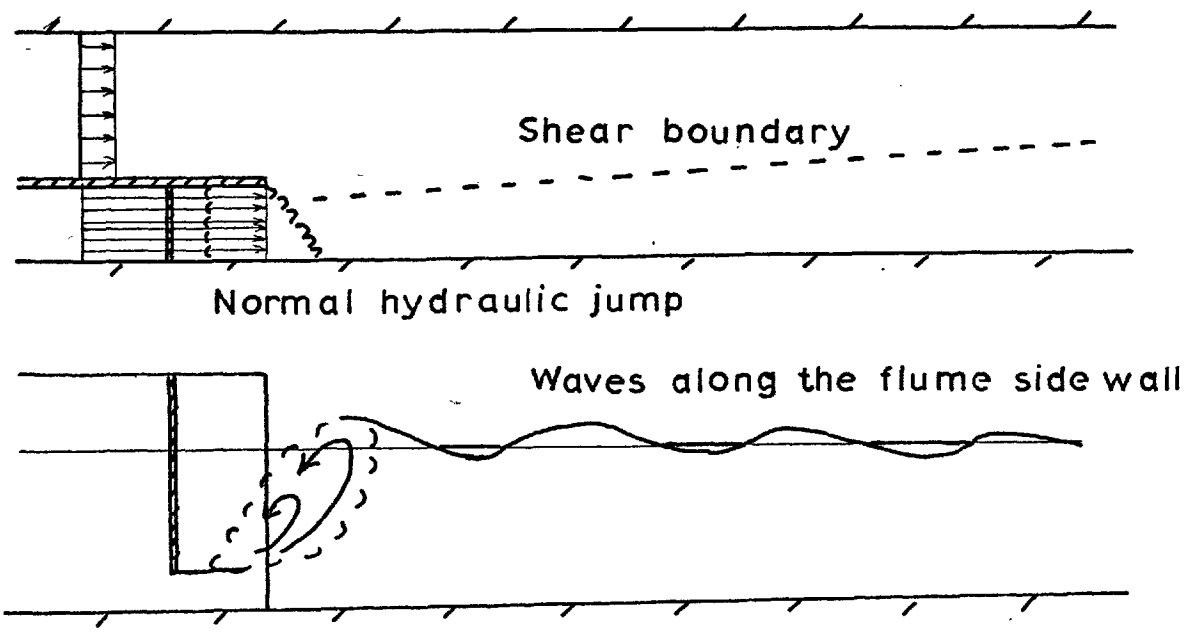


FIG. 3.2-2 FLOW PATTERNS

form of the hydraulic jump with an oblique front and a small amount of air-entrained water rolling at the intersection zone of the oblique front and the wall of the flume was also observed.

Normal Hydraulic Jump (inside the narrow channel)

For higher tail-water levels a normal jump formed inside the narrow channel (Fig. 2.5-4), which had the characteristic of a two-dimensional normal hydraulic jump. Its description coincides with the one given by Rajaratnam (12): "The water surface starts to raise abruptly at the beginning or toe, of the jump, and continues to raise up to a section beyond which it is essentially level". "The change from super-critical to subcritical conditions in the flow is always accompanied by considerable turbulence and energy loss, and for certain types of jumps a surface roller entrains in the flow an important amount of air". In the free surface of the downstream flow, no pattern of standing waves was observed. The length of the sluice channel was small (10 cm), and because the normal jump oscillated up and down in the channel, the equipment used was not adequate to investigate normal hydraulic jumps in streams with Froude numbers greater than 3.5.

Submerged Jump

When the depth in the main channel was greater than the conjugate depth required for the formation of a normal hydraulic jump, then the sluice gate outlet became drowned and the jet of water issuing from beneath the gate was overlaid by a mass of water. The flow patterns of submerged jumps were stable and the free surface smooth. At the corner of the sluice gate with the dividing wall a strong vortex rotating with a clockwise movement

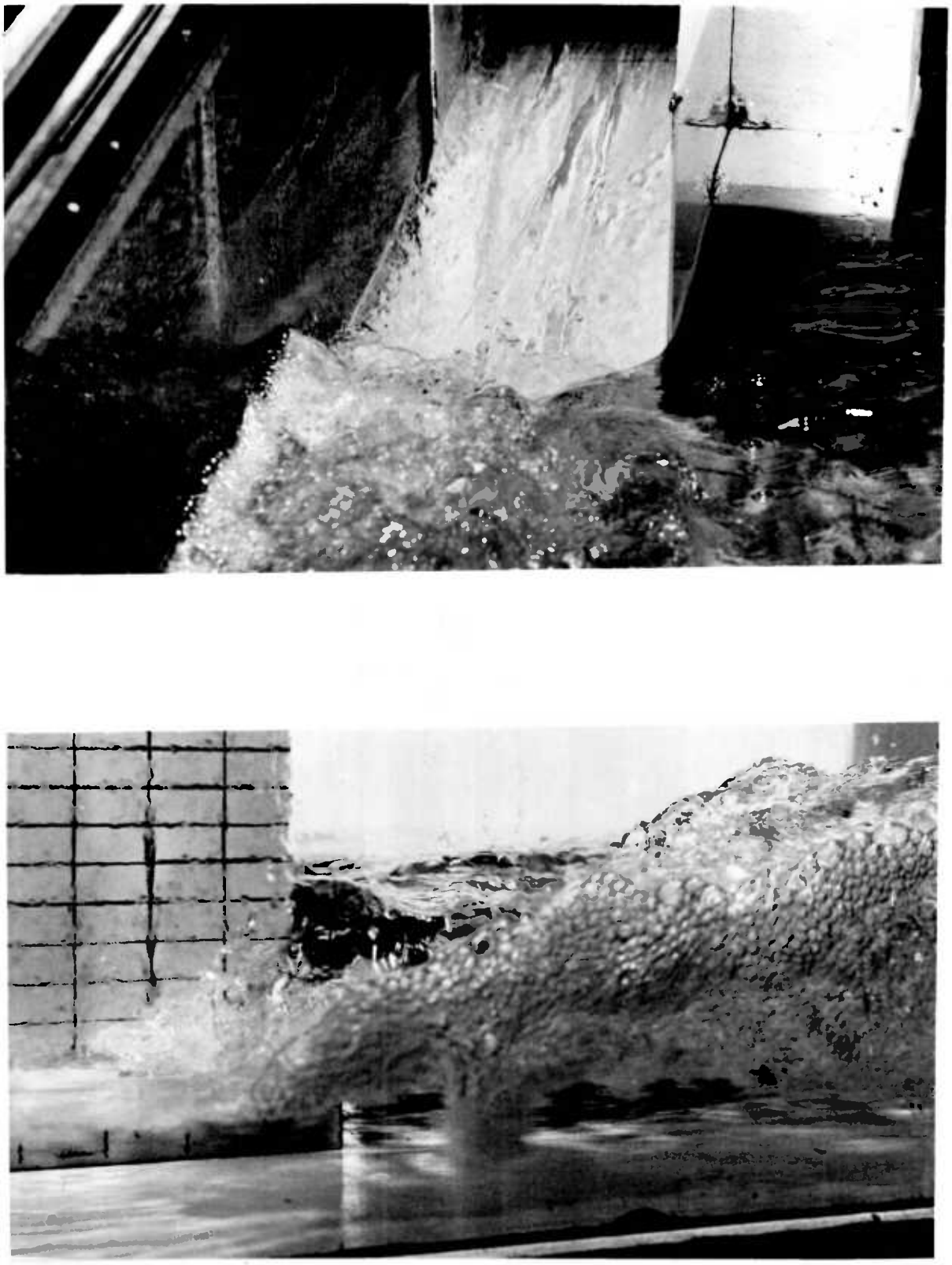


Fig. 3.2-3. HYDRAULIC JUMP AT AN ABRUPT EXPANSION

was always observed. An intermediate form of submerged-normal jump occurred for smaller tail-water levels. This jump was characterised by the strong oscillation of its normal front up and down in the channel. The jump periodically moved towards the gate and submerged the gate outlet, but the roller surface in its movement downstream in the channel detached from the sluice gate.

3.2-1 - Experimental Results

The details of the tests and procedures were given in Section 2.4-1. Briefly, a constant aperture of the sluice gate (5.0 cm) was kept during the tests and the tail-water levels and the discharges of the orifice plate were adjusted to set up in the flume the different forms of the hydraulic jump.

The results of the jump classification tests (given in Table 3.2-1) are plotted in Fig. 3.2-4. A family of characteristic curves can be fitted to the form of jumps which are classified in the following way: oblique (OBL); oblique jump with rolling water (No-Ob); normal jump at the expanding section (Nor); normal hydraulic jump inside the sluice channel (NOR); normal jump oscillating at the sluice gate section (Su-No); submerged (SUB). Two curves were drawn to separate the conditions required in the formation of the three basic forms of the jump: oblique, normal and submerged hydraulic jumps. The characteristic curve of a two-dimensional jump was also drawn. The results confirm the observation of Rajaratnam (33), Herbrand (25), Unny (38) and other authors, that the spatial hydraulic jump requires a smaller tail-water depth than the classical two-dimensional jump with the same initial conditions (d_1,Fr_1).

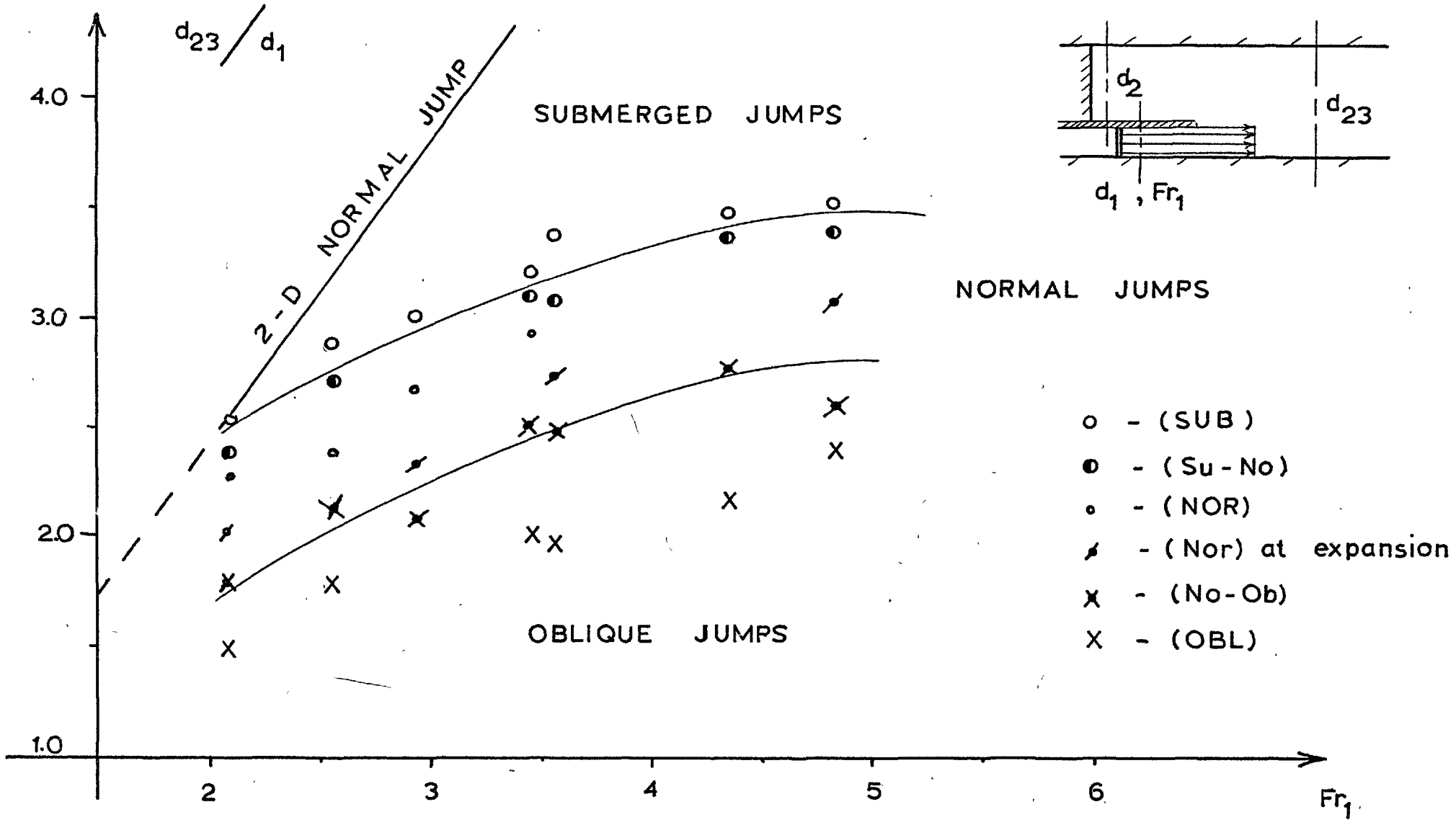


FIG. 3.2-4 HYDRAULIC JUMP FORMS

TABLE 3.2-1 HYDRAULIC JUMPS AT AN ABRUPT EXPANSION

Jump	Q_1	d_1	d_2	d_{23}	U_1	F_1	$\frac{d_{23}}{d_1}$	Date
form	l/s	cm	cm	cm	m/s	-	-	
OBL	11.6	3.0	6.1	5.9	1.93	3.56	1.97	30/3/73
No-Ob			7.7	7.4		3.56	2.47	
Su-No			9.4	9.2		3.56	3.07	
SUB			10.4	10.1		3.56	3.37	
Nor			8.4	8.2		3.56	2.73	
NOR	6.8	3.0	6.8	6.8	1.13	2.08	2.27	5/4/73
Su-No			7.2	7.1		2.08	2.37	
SUB			7.7	7.6		2.08	2.53	
Nor			6.0	6.0		2.08	2.00	
No-Ob			5.3	5.3		2.08	1.77	
OBL			4.4	4.4		2.08	1.47	
No-Ob	15.7	3.0	8.3	7.8	2.62	4.83	2.60	6/4/73
Nor			10.0	9.2		4.83	3.07	
SUB			11.6	10.6		4.83	3.53	
Su-No			11.1	10.2		4.83	3.40	
OBL			7.3	7.2		4.83	2.40	
No-Ob	14.1	3.0	8.8	8.3	2.35	4.34	2.77	11/4/73
Su-No			10.4	10.1		4.34	3.37	
SUB			11.0	10.4		4.34	3.47	
OBL			7.0	6.5		4.34	2.17	
No-Ob	11.3	3.0	7.8	7.5	1.88	3.46	2.50	11/4/73
Su-No			9.5	9.3		3.46	3.10	
SUB			9.8	9.6		3.46	3.20	
OBL			6.1	6.0		3.46	2.00	
NOR			9.0	8.8		3.46	2.93	17/5/73
No-Ob	9.5	3.0	6.4	6.2	1.58	2.92	2.07	12/4/73
NOR			8.1	8.0		2.92	2.67	
SUB			9.2	9.0		2.92	3.00	
Nor			7.2	7.0		2.92	2.33	
OBL			5.4	5.3		2.92	1.77	
No-Ob	8.3	3.0	6.5	6.4	1.38	2.55	2.13	2/5/73
Su-No			8.1	8.1		2.55	2.70	
OBL			5.3	5.3		2.55	1.77	
NOR			7.2	7.1		2.55	2.37	
SUB			8.6	8.6		2.55	2.87	

3.2-2 - Normal Hydraulic Jump at an Abrupt Expansion

When a hydraulic jump takes place in a channel expansion, it is strongly influenced by the formation of side eddies, and could be defined as a "spatial" hydraulic jump (24,38). The existing equations for the conjugate depth ratio of a spatial jump are empirical. The formula developed by Kuznetzow for an expansion ratio varying from (0.01) to (1.00) and Froude numbers from (1.00) to (7.25) is quoted by Unny (38) as:-

$$\frac{\bar{d}_1}{d_1} = 0.5\,\frac{b}{B}\,(0.8 - 0.15\,(0.9 - \frac{b}{B}))\,.\,(\,(1 + \frac{8Fr_1^2}{b/B})^{\frac{1}{2}} - 1)$$

... (3.2-1)

where $(\bar{d}_1)$ is the conjugate depth of the supercritical stream $(d_1;Fr_1)$ and b/B is the expansion ratio of the channel, (b) and (B) being the width of the channel before and after the expansion.

Unny (38) showed the inconsistencies of Equation 3.2-1. First, for a two-dimensional jump (b/B=1), Equation 3.2-1 cannot be reduced to Equation 3.1-1; secondly, the formula does not take into account the geometrical ratio of the supercritical stream (d_1/b), which also affects the jump. Unny also investigated another semi-empirical formula with a structure similar to the formula for a two-dimensional hydraulic jump, given as

$$\frac{\bar{d}_1}{d_1} = \tfrac{1}{2}(1 + K_1.\,\frac{d_1}{b}.\,Fr_1^2)\,.\,(\,(1 + \frac{8Fr_1^2}{(1 + K_1.\,\frac{d_1}{b}.Fr_1^2)^2})^{\frac{1}{2}} - 1)$$

... (3.2-2)

where K_1 is a coefficient which he found to be (K_1=2.2) for the conditions of his experiments in which the expansion ratio of the channels was 0.50.

Equations 3.2-1 and 3.2-2 are both plotted in Fig. 3.2-5. Unny's equation (3.2-2) fits the results of the present research better than that due to Kuznetzow (3.2-1), and predicts the shape of the experimental curve, but the disagreement is still important.

Rajaratnam and Subramanya (33) quoted Abramov's empirical formula from the Russian hydraulic literature,

$$\frac{\bar{d}_1}{d_1} = \frac{K_2 + 14}{10(K_2+2)} \cdot \left((1 + 600 \cdot \frac{K_2 + 2}{(K_2 + 14)^2} \cdot Fr_1^2\right)^{\frac{1}{2}} - 1) \qquad \ldots (3.2\text{-}3)$$

where K_2 is an empirical factor which could be taken as three to four for b/B greater than 0.10. In Fig. 3.2-5 a value of (K_2=4) was used. The results of this equation are not very different from the results of Equation 3.2-2 in the range of Froude numbers tested in the laboratory (Fr_1 = 2.0-5.0).

The same authors (33) analysed two forms of the hydraulic jump taking place below abrupt symmetrical expansions: a repelled jump (R-jump) formed in the wider channel and a spatial jump (S-jump) with a small submergence formed at the expanding section. For the R-jump the following empirical equation was developed,

$$\frac{\bar{d}_1}{d_1} = (\frac{b}{B} + 0.30) \cdot (Fr_1 - 0.85) + 0.75 \qquad \ldots (3.2\text{-}4)$$

The calculations in Appendix (E) show that this equation is not essentially

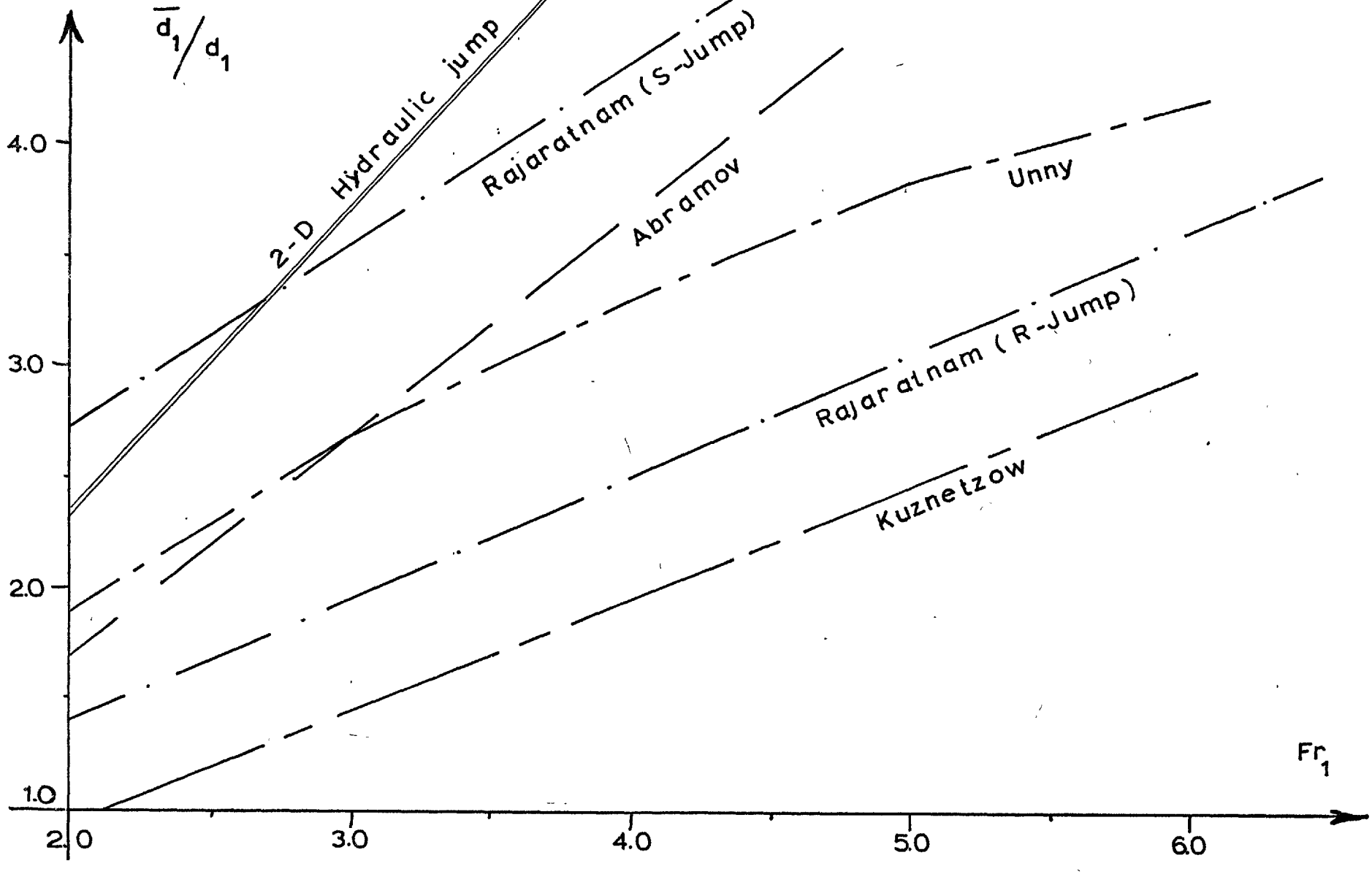


FIG. 3.2-5 NORMAL JUMPS AT AN ABRUPT EXPANSION

different from the equation of a two-dimensional hydraulic jump forming in the wider channel. This result implies that the characteristics of the R-jump do not depend on the geometry of the expanding channel. The equation developed in (33) for the S-jump was,

$$\frac{\bar{d}_1}{r'} = 1.08\ Fr'_1 + 1.40 \qquad \ldots (3.2\text{-}5)$$

where r' is a characteristic length of the outlet and Fr'_1 the corresponding Froude number described as,

$$r' = \frac{b.d_1}{b + 2d_1} \quad ; \qquad Fr'_1 = \frac{U_1}{(gr')^{\frac{1}{2}}}$$

An empirical equation derived from the results of the present investigation (Fig. 3.2-4) on normal hydraulic jumps at an abrupt expansion, and valid for Froude numbers varying from 2 to 6, is,

$$\frac{\bar{d}_1}{d_1} = 0.65(1 + 0.67\ Fr_1^2)\left(\left(1 + \frac{8Fr_1^2}{(1 + 0.67\ Fr_1^2)^2}\right)^{\frac{1}{2}} - 1\right) \qquad \ldots (3.2\text{-}6)$$

This equation is similar to Equation 3.2-2, which was developed by Unny (38), and corresponds to an approximate value of ($K_1 = 4.4$).

3.2-3 - Oblique Jumps

If a boundary wall is deflected into a supercritical stream through

an angle θ^o, a hydraulic jump (also called the oblique shock wave by analogy to the supersonic case) will occur at an angle β^o with respect to the original flow direction (see Fig. 3.2-6). The wave crosses the channel to the opposite wall, where it is reflected, and in this fashion it continues almost undiminished in the downstream direction (26,27). For small disturbances (d_3/d_1 less than 3), the depth of the jump before and after the wave front are related to the Froude number of the oncoming flow (Fr_1), and the wave angle (β^o) in the following way (4,26):

$$\frac{d_3}{d_1} = \frac{1}{2}\left((1 + 8Fr_1^2 \sin^2\beta^o)^{\frac{1}{2}} - 1\right) \qquad \ldots (3.2\text{-}7)$$

The limiting case of the oblique standing wave is the normal hydraulic jump in which the front is normal to the direction of the flow (β^o=90). This equation is only valid when the flow conditions before and after the wave front are supercritical and the head losses are small and may be neglected (26).

In a normal hydraulic jump, much of the hydraulic energy transported in the fast (supercritical) stream is dissipated and the downstream flow is subcritical. The oblique hydraulic jump analysed by Ippen (and described above) is controlled by the deflection of a wall and not by the downstream conditions of the flow. As the energy dissipated in these oblique front waves is negligible and the downstream flow conditions are supercritical it is more appropriate to describe them as oblique standing waves.

Exploratory tests were carried out with the oblique jumps observed in the laboratory flume. These oblique jumps were produced by a difference

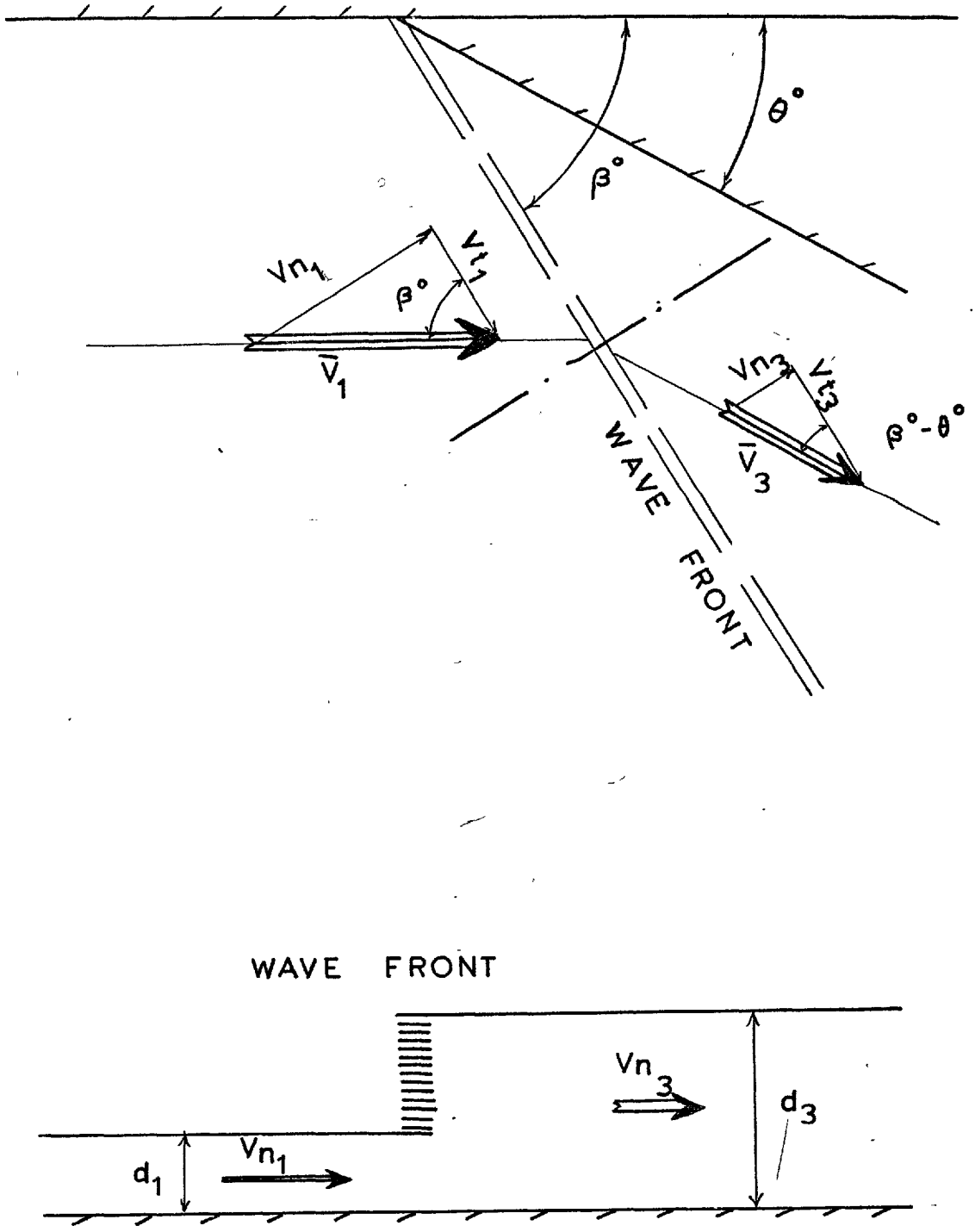


FIG. 3.2-6 OBLIQUE STANDING WAVES

in depth between the fast and slow streams. It was observed that for a fixed Froude number of the sluice discharge (Fr_1), the angle of the standing wave (β^o) increased when the tail-water levels were raised, and eventually a normal hydraulic jump formed inside the narrow channel. To obtain a fixed value of the angle (β^o), the tail-water levels had to be raised when the (Fr_1) was increased. Unfortunately, it was not possible to establish a physical relation among the flow variables (d_1, d_3, Fr_1, β^o) or check Equation 3.2-7, because it was difficult to measure the wave angle, due to the reflection of the oblique standing wave in the right wall of the flume and the three-dimensional characteristics of the flow across the front of the oblique jump.

3.3 - THE EFFECT OF A UNIFORM STREAM ON THE HYDRAULIC JUMPS

The arrangements of the two-channels inside the flume were adequate to investigate the effect of a co-flowing stream in the flow pattern of the sluice discharge. A survey of the literature in hydraulic jumps revealed that the effect of a uniform stream on a jump forming at an abrupt expansion of a channel has not been investigated before. The experiments revealed that while the co-flowing stream has little effect on the formation of the jump, it makes a large difference to the diffusion of the jet (see Chapter 4) and to the waves travelling downstream in the flume. A small uniform stream is enough to eliminate travelling waves and to avoid reverse currents in the region of the flow outside the diffusing jet.

Fig. 3.3-1 shows the results of the tests carried out to investigate the effects of a uniform stream in the three basic forms of the jump

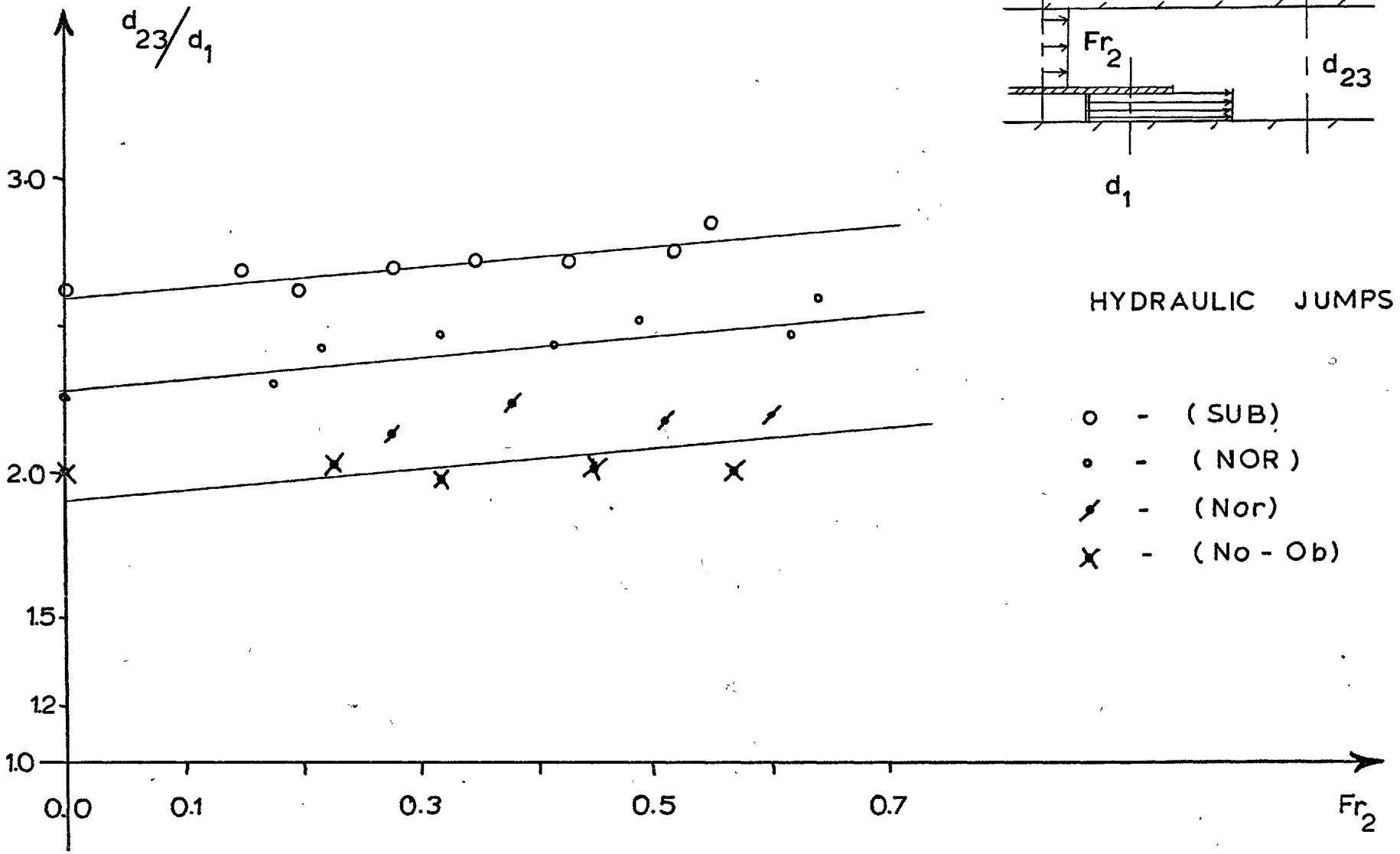


FIG. 3.3-1 HYDRAULIC JUMPS IN A UNIFORM STREAM

TABLE 3.3-1 HYDRAULIC JUMPS AT AN ABRUPT EXPANSION IN A UNIFORM STREAM.

Jump	Q_2	d_1	d_2	d_{23}	U_2	F_{r_2}	$\frac{d_{23}}{d_1}$	DATE
form	l/s	cm	cm	cm	cm/s	-	-	
NOR	0.0	3.0	6.8	6.8	-	-	2.27	4/5/73
SUB			7.8	7.9			2.63	
No-Ob			5.9	6.0			2.00	
NOR	22.5	3.0	7.6	7.8	55	0.64	2.60	4/5/73
SUB			8.3	8.6	50	0.55	2.87	
NOR	20.1	3.0	7.2	7.4	52	0.62	2.47	4/5/73
SUB			8.1	8.3	46	0.52	2.77	
Nor	16.6	3.0	6.4	6.6	48	0.60	2.20	4/5/73
SUB			8.0	8.2	38	0.43	2.73	
NOR			7.4	7.6	42	0.49	2.53	
No-Ob	13.6	3.0	5.8	6.0	43	0.57	2.00	4/5/73
Nor			6.3	6.5	40	0.51	2.17	
NOR			7.2	7.3	35	0.42	2.43	
SUB			8.0	8.2	31	0.35	2.73	
Nor	10.5	3.0	6.5	6.7	30	0.38	2.23	7/5/73
SUB			7.9	8.1	25	0.28	2.70	
NOR			7.3	7.4	27	0.32	2.47	
No-Ob			5.8	6.0	34	0.45	2.00	
No-Ob	7.4	3.0	5.8	5.9	24	0.32	1.97	7/5/73
NOR			7.3	7.3	19	0.22	2.43	
SUB			7.9	7.9	17	0.20	2.63	
Nor			6.3	6.4	22	0.28	2.13	
NOR	5.7	3.0	6.9	6.9	15	0.18	2.30	7/5/73
Su-No			7.3	7.3	14	0.17	2.43	
SUB			8.1	8.1	13	0.15	2.70	
No-Ob			6.0	6.1	18	0.23	2.03	

Notes: (1) The aperture of the sluice gate was 5.0 cm (d_1 = 3.0 cm)

(2) The constant discharge of the orifice plate was (Q_{OR} = 7.4 l/s)

(3) The Froude number (F_{r_1}) of the sluice stream was 2.27 (U_1 = 1.23 m/s).

(Table 3.3-1). The depth and the Froude number of the sluice discharge were kept constant during these tests (d_1 = 3.0 cm; Fr_1= 2.3) and the flow rate (Q_2) and the depth (d_2) of the uniform stream varied. The ratio of depths before (d_1) and after each jump (d_{23}) are plotted against the Froude number of the uniform stream (Fr_2). A family of straight lines can be drawn to separate the characteristics of oblique, normal and submerged hydraulic jumps. The depth ratio of the jump increases by approximately 10% when the Froude number of the uniform stream varies from zero to 0.6

A second series of tests was carried out to investigate the effect of a uniform stream on the normal hydraulic jump formed inside the narrow channel. A constant aperture of the sluice gate was used (d_1= 3.0 cm) and the Froude number of its discharge was increased from 2.3 to 4.6 (Fr_1 = 2.3; 2.8; 3.1; 3.8; 4.1; and 4.6). To the wider channel four different discharges were supplied (Q_2 = 5.7; 10.5; 16.6; and 21.9 l/s). The results of these tests are plotted in Fig. 3.3-2 where a family of straight lines (one for each Fr_1) was fitted to the experimental points, and a second family of curves of constant flow rate discharge (Q_2) was drawn.

An empirical equation can be produced (Table 3.3-3) to calculate the downstream depth of the normal hydraulic jump formed inside the sluice channel, and may be expressed as

$$\frac{d_{23}}{d_1} = Fr_1(0.56 + 0.20\ Fr_2) + 1 \qquad \ldots (3.3\text{-}1)$$

The family of straight lines drawn in Fig. 3.3-2 were reduced to a single curve by a convenient rearrangement of the flow variables shown in Fig. 3.3-3.

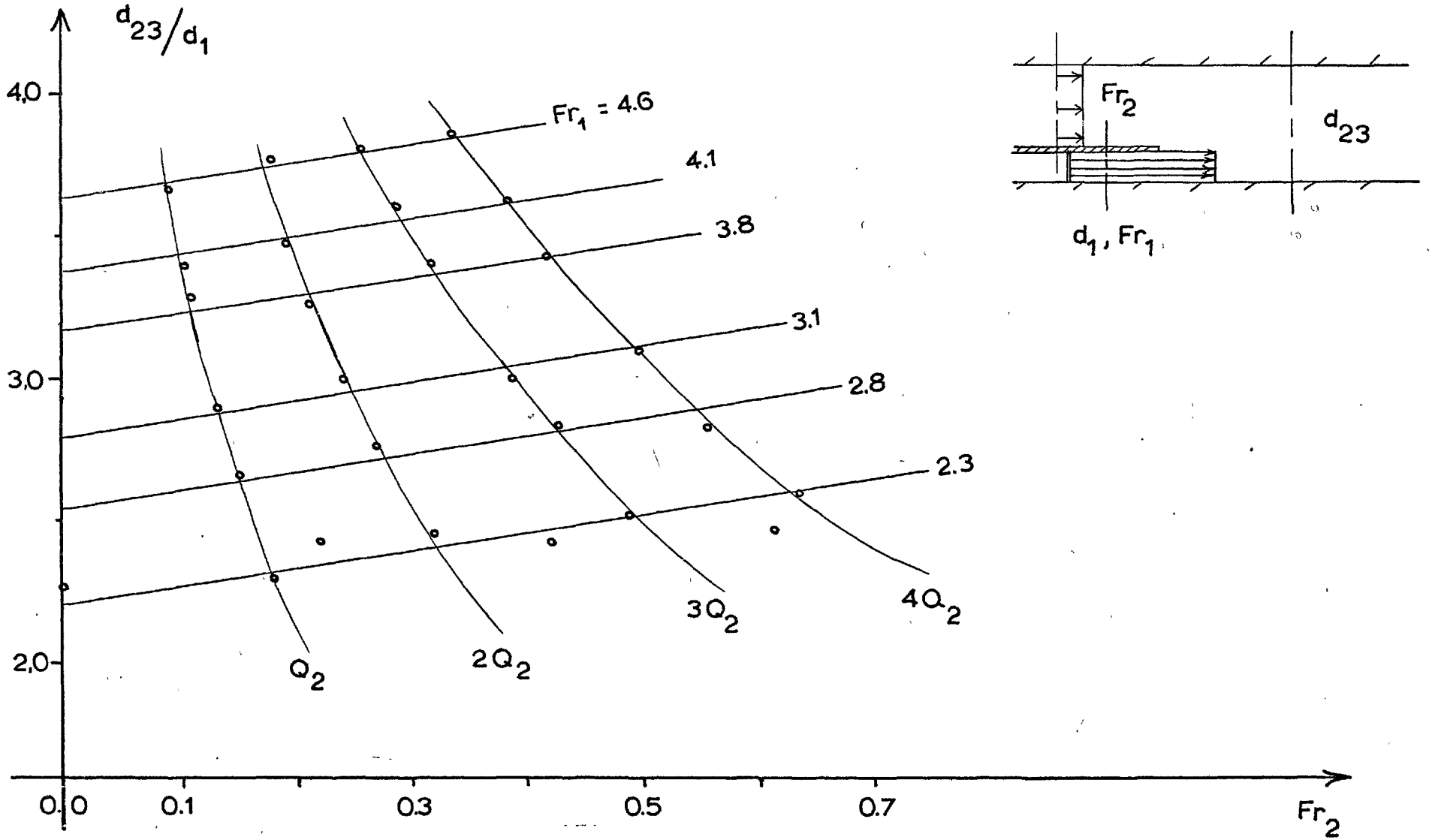


FIG 3 3 2 NORMAL JUMPS IN A COFLOWING STREAM

TABLE 3.3-2 NORMAL HYDRAULIC JUMPS IN A COFLOWING STREAM.

Q_1	Q_2	d_1	d_2	d_{23}	U_1	F_{r_1}	U_2	F_{r_2}	$\frac{d_{23}}{d_1}$	DATE
l/s	l/s	cm	cm	cm	m/s	-	cm/s	-	-	
9.0	5.7	3.0	8.0	8.0	1.50	2.77	13.2	0.15	2.67	7/5/73
10.2			8.7	8.7	1.70	3.14	12.1	0.13	2.90	7/5/73
14.8			11.0	11.0	2.47	4.56	9.6	0.09	3.67	8/5/73
13.4			10.2	10.2	2.23	4.11	10.3	0.10	3.40	8/5/73
12.3			9.9	9.9	2.05	3.78	10.7	0.11	3.30	8/5/73
12.3	16.6	3.0	9.9	10.2	2.05	3.78	31.1	0.32	3.40	8/5/73
9.1			8.1	8.5	1.52	2.80	38.0	0.43	2.83	8/5/73
14.8			11.3	11.4	2.47	4.56	27.2	0.26	3.80	9/5/73
13.4			10.4	10.8	2.23	4.11	29.6	0.29	3.60	9/5/73
10.1			8.6	9.0	1.68	3.10	35.8	0.39	3.00	9/5/73
10.1	21.9	3.0	8.7	9.3	1.68	3.10	46.6	0.50	3.10	9/5/73
14.8			11.2	11.6	2.47	4.56	36.2	0.34	3.97	9/5/73
13.4			10.4	10.9	2.23	4.11	39.0	0.39	3.63	15/5/73
12.4			9.8	10.3	2.07	3.82	41.4	0.42	3.43	15/5/73
9.0			8.1	8.5	1.50	2.77	50.1	0.56	2.83	15/5/73
9.0	10.5	3.0	8.1	8.3	1.50	2.77	24.0	0.27	2.77	15/5/73
12.3			9.7	9.8	2.05	3.78	20.0	0.21	3.27	15/5/73
14.8			10.8	11.0	2.47	4.56	18.0	0.17	3.67	15/5/73
13.4			10.1	10.4	2.23	4.11	19.3	0.19	3.47	17/5/73
10.1			8.7	9.0	1.68	3.10	22.3	0.24	3.00	17/5/73

Equation 3.3-1 shows that:

1. Higher water levels (d_{23}) in the downstream channel are required in the formation of a normal hydraulic jump when the Froude number of the uniform stream (Fr_2) is increased.

2. The jump depth ratio (d_{23}/d_1) is proportional to the Froude number of the supercritical stream (Fr_1).

The ratio of the jump downstream depth (d_{23}) to the conjugate depth ($\bar{d}_1$) of a two-dimensional hydraulic jump with the same initial characteristics (d_1,Fr_1) are plotted against the Froude number (Fr_1) in Fig. 3.3-4, which shows:

3. d_{23} is smaller than $\bar{d}_1$ (12,24) and their ratio decreases with Fr_1. The ratio varied between 85% and 63% for Froude number of 2.3 and 4.6, respectively.

4. The variation of ($d_{23}/\bar{d}_1$) with Fr_1 is linear.

Equation 3.3-1 is only valid for the particular flow conditions investigated here and for the flume and geometry of the channels used which had a width ratio of 0.264. However, the general remarks set above, specifically 1, 2 and 3, are believed to stand in any other flume conditions or in a full-scale model, and can be used as a guide line in the design of hydraulic structures.

3.4 - THE HYDRAULIC ANALOGY TO SUPERSONIC FLOW

The flow of a liquid with a free surface is analogous to the isentropic flow of a compressible gas having a ratio of specific heats equal

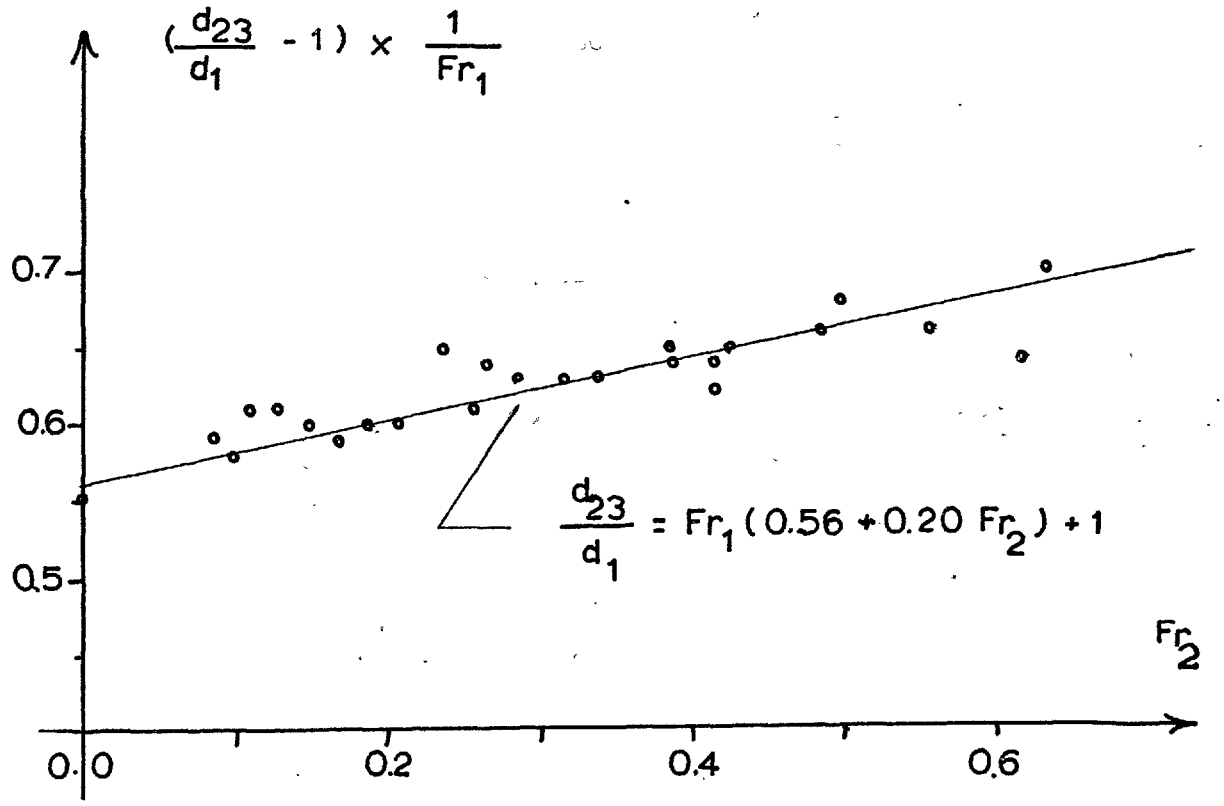


FIG. 3.3-3 JUMP DEPTH IN A COFLOWING STREAM

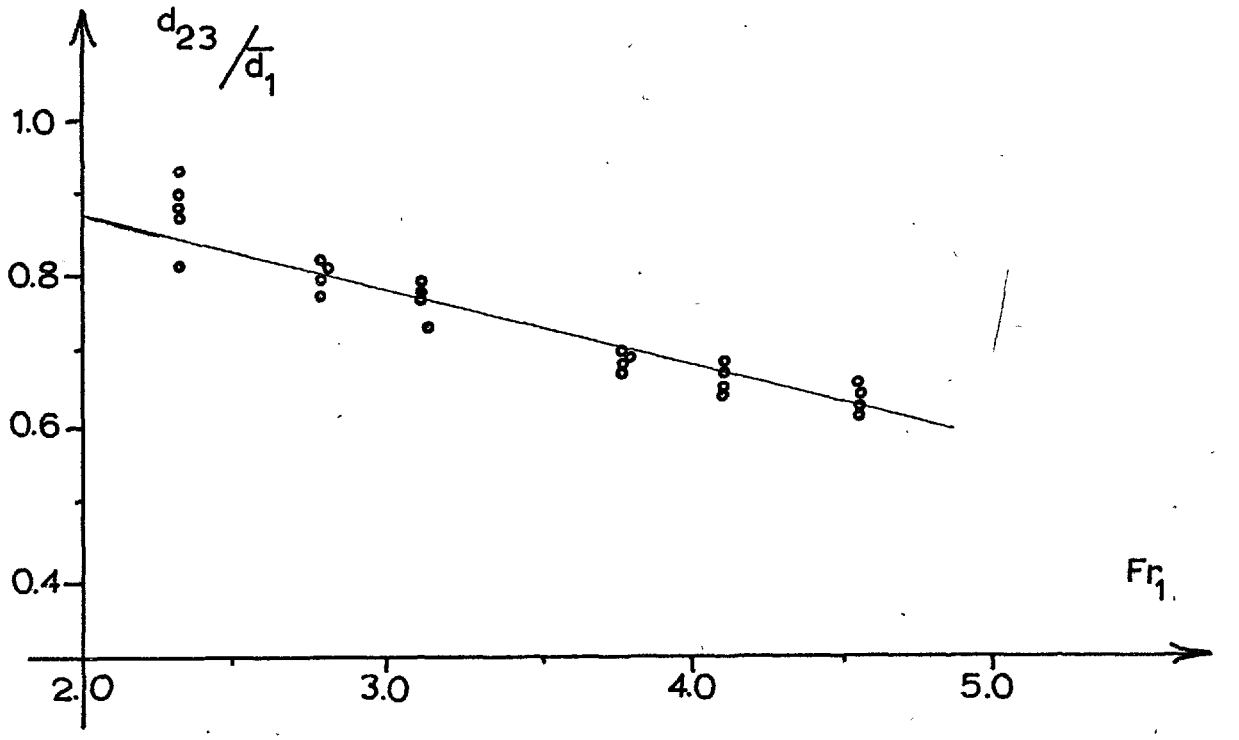


FIG. 3.3-4 JUMP DEPTH AT AN ABRUPT EXPANSION

TABLE 3.3-3 NORMAL HYDRAULIC JUMP DEPTH RATIO AT AN ABRUPT EXPANSION

Fr_1	Fr_2	$\frac{d_{23}}{d_1}$	$\frac{\bar{d}_1}{d_1}$	$\frac{d_{23}}{\bar{d}_1}$	$(\frac{d_{23} - d_1}{d_1} \cdot \frac{1}{Fr_1})$
2.30	0.00	2.27	2.80	0.81	0.55
	0.42	2.43		0.87	0.62
	0.49	2.53		0.90	0.66
	0.62	2.47		0.88	0.64
	0.64	2.60		0.93	0.70
2.77	0.15	2.67	3.45	0.77	0.60
	0.27	2.77		0.80	0.64
	0.56	2.83		0.82	0.66
2.80	0.43	2.83	3.48	0.81	0.65
3.10	0.24	3.00	3.91	0.77	0.65
	0.39	3.00		0.77	0.65
	0.50	3.10		0.79	0.68
3.14	0.13	2.90	3.96	0.73	0.61
3.78	0.11	3.30	4.87	0.68	0.61
	0.21	3.27		0.67	0.60
	0.32	3.40		0.70	0.63
3.82	0.42	3.43	4.93	0.70	0.64
4.11	0.10	3.40	5.34	0.64	0.58
	0.19	3.47		0.65	0.60
	0.29	3.60		0.67	0.63
	0.39	3.63		0.68	0.64
4.56	0.09	3.67	5.97	0.61	0.59
	0.17	3.67		0.61	0.59
	0.26	3.80		0.64	0.61
	0.34	3.87		0.65	0.63

to two ($\gamma = 2$)(5,64,67). In a two-dimensional flow case, a direct analogy exists and the fundamental equations are,

GAS FLOW $\gamma = 2$ (compressible fluid)		WATER FLOW (incompressible fluid)	
1. Speed of propagation of sound waves	$a = (\gamma \frac{p}{\rho})^{\frac{1}{2}}$	Speed of propagation of small gravity waves	$c = (gh)^{\frac{1}{2}}$
2. Mach number	$M_{\text{Ma}} = \frac{V}{(\gamma \frac{p}{\rho})^{\frac{1}{2}}}$	Froude Number	$Fr = \frac{V}{(gh)^{\frac{1}{2}}}$
3. Density ratio	ρ_2/ρ_1	Depth ratio	h_2/h_1
4. Pressure ratio	P_2/P_1	(Depth ratio)^2	$(h_2/h_1)^2$
5. Temperature ratio	T_2/T_1	Depth ratio	h_2/h_1

Since the ratio of specific heats of air is ($\gamma = 1.40$) and the changes of pressure and density across a shock wave occurring in a supersonic flow does not fulfil completely an isentropic law, the direct hydraulic analogy has to be modified to give practical results. This method has been mainly used to predict the aerodynamic characteristics of a given shape or structure in a water flume, where the similarity of boundary conditions and equivalence of the Mach number and Froude number has to be satisfied. Very often the depth ratio of the hydraulic model is only used to find the analogous density ratio, which is used with the

aerodynamic equations to calculate the ratio of temperature, pressure and Mach number (64).

In the discharge of a two-dimensional supersonic jet of gas from an orifice into a free space, where the pressure is greater than the pressure in the jet, a pattern of oblique waves of compression start from each edge of the orifice. These waves cross one another (without disturbing) and they are totally reflected at the boundaries of the free jet as waves of rarefaction. As these advance, they taper away and after crossing the jet are reflected again at the boundary of the jet as waves of compression; the whole process then begins afresh (11).

In the flume, a similar system of standing waves across the diffusing jet was observed in the flow pattern of an oblique jump. The flow conditions were analogous to the ones described above with the wall of the flume as a plane of symmetry. The jet issuing from the sluice gate is diffusing in a deeper mass of water (adverse pressure gradient) and the oblique front wave (similar to a shock wave) is always attached to the edge of the dividing wall. This oblique wave builds up when it approaches the wall of the flume where it is completely reflected. After crossing the jet the wave is reflected again at the shear boundary of the jet and builds up approaching the wall. A pattern of standing waves along the right wall of the flume were observed with a fairly constant wave length and decreasing amplitude, both of them varying with the Froude number of the sluice discharge and the tail-water levels.

Only a qualitative analysis of the waves crossing the jet was possible due to the limited amount of time available to conduct the experimental work. However, the results support a hydraulic analogy of the conditions investigated to the discharge of a two-dimensional supersonic jet.

IV - THE DIFFUSION OF THE JET IN A UNIFORM STREAM

4.0 - INTRODUCTION

In this chapter the properties of a turbulent jet of water diffusing in a uniform stream, flowing in the same direction, are investigated, these being the conditions of the tests described in Section 2.4.4. The experimental results are compared with the results of similar investigations on two-dimensional turbulent jets: free jets and wall-jets spreading throughout a uniform stream or a medium at rest. The flow of a fast fluid spreading throughout an infinite medium of the same fluid is called a free jet. In the particular case in which the medium is at rest, the jet is known as a submerged jet. The flow obtained by blowing a jet parallel to a solid surface (which confines the diffusion of the fast fluid) is a wall-jet. The diffusion of free-jets and wall-jets in a uniform stream flowing in the same direction of the jet are the two types of turbulent jets considered in this chapter.

High velocity flows from a submerged outlet are designed by hydraulic engineers to dissipate the kinetic energy of the fast jet through reaction with the surrounding fluid. In more explicit terms, the difference in velocity between a jet and the region into which it is discharged gives rise to instability in the flow (at the shear boundary), from which eddies are generated and the energy of the jet is steadily converted into turbulent energy which gradually decays through viscous shear. This process involves a decrease in

the velocity of the jet, and in order to fulfil the requirements of continuity the area of the jet cross-section must become greater as the velocity becomes smaller. A detailed knowledge of the velocity distribution within such an expanding stream is essential to many problems of diffusion.

The development of turbulent jets in situations that are of engineering interest was discussed by Newman (52). He confined himself to aeronautical applications and considered a great variety of geometries and boundary conditions, but did not include temperature and compressibility effects. Jets may be blown along aerofoil surfaces to energise the boundary layer and prevent separation. In this way, blowing has been used to reduce the take-off and landing speed of air-craft. Other practical applications of jets are air-cushion vehicles and jet pumps. In the new technology of fluidics, switches, proportional amplifiers and logic elements are produced using fluid jets. The mixing of two coaxial streams is a problem of great importance to the mechanical and chemical industries and the design of combustion chambers, ejectors, disposal of waste gases, dust collectors and others, are some of the practical applications in the respective fields of Engineering. The diffusion of plunging nappes from spillways or of submerged jets from sluice-gates, which require a study in the rate of deceleration of the jet to prevent the scour beyond the apron, are examples of diffusing jets found in the field of river engineering. A theoretical and experimental study of several aspects of jet-forced reservoir circulation was carried out by Sobey (58) at Imperial College, and this is another application of jets to the field

of water quality management in lakes and reservoirs.

A brief introduction to turbulent flow is presented in Section 4.2.2. The turbulent flow is the most complicated case of fluid motion defined exactly by the Navier-Stokes equations, and there is not a general numerical solution for these equations. Bradshaw (3) defines the turbulence studies as "the art of understanding the Navier-Stokes equations without actually solving them". Because we cannot solve these equations for every case, we have to simplify them or to appeal to experiment for qualitative understanding of turbulence, and quantitative information for engineering purposes.

The mean flow pattern of a two-dimensional jet can be derived from an empirical approach, with the exception of a single experimental constant, if the following assumptions are made: (a) the pressure is hydrostatically distributed throughout the flow; (b) the diffusion process is dynamically similar under all conditions; and (c) the longitudinal component of velocity within the diffusion region varies according to a pre-established form of the velocity profile. In this similarity solution approach, which does not require any assumption to the distribution of turbulence, experimental data is required to provide the single numerical value of the constants. The method has been effectively used with submerged jets (by Albertson et al (41)), free jets in an external stream (by Abramovich (1)), wall-jets (by Glauert (48)), and wall-jets in a uniform co-flowing stream (by Kruka and Eskinazi (50)). The diffusion characteristics of a free jet are dynamically similar if the Reynolds number of the fluid efflux at the submerged boundary outlet is not too low, and therefore the viscous action has no influence on

the mixing process.

An empirical solution was investigated for the diffusion of the sluice jet. The analysis of turbulent jets was confined to those in which the fluid is incompressible and its properties are independent of temperature (that is, the case of a jet of water). Only steady state flows were considered. The flow conditions in the merged streams were assumed two-dimensional, and the velocity measurements taken at half depths of the flow were assumed to be the representative value of velocity of the approximated two-dimensional flow. The experimental results were compared with empirical results on submerged jets and free jets diffusing in a uniform stream. Since one of the walls of the flume confined the sluice jet, the results were also compared against a wall-jet spreading throughout an external stream. Most of the experimental work in turbulent jets with which the present results are compared has been carried out with air.

In the present experiments, a Pitot-static tube and a mini-current meter were used to measure velocities in the flow of the two streams which were confined by the walls of the flume. Velocity profiles were drawn at seven cross-sections of the flow and the geometrical similarity of these profiles was investigated. The growth of the jet and the decay of maximum velocity were the two other characteristics of the diffusing jet analysed here. The measurements were confined to the free-mixing region of the flow, because neither the laboratory flume nor the measuring (velocity) equipment was appropriate to investigate the flow conditions in the region near the walls of the flume.

The quality of the measurements was checked through an elementary impulse-momentum analysis of the flow conditions in a fixed control volume. The results proved to be satisfactory and enabled an evaluation of the energy dissipated in the normal hydraulic jump to be performed. When the measurements conducted in the flume were presented in a dimensionless form they were found to be in substantial agreement with the analytical and experimental predictions of two-dimensional turbulent flow jets.

4.1 - IMPULSE - MOMENTUM ANALYSIS

The impulse-momentum principle, along with the continuity and energy principles are the three basic equations of Hydrodynamics. A detailed knowledge of the complex flow process within a control volume is not required when the impulse-momentum principle is applied to it. The elementary analysis is used in this section to establish simple relations among the flow variables directly controlled in the laboratory (the discharges of the orifice plate (Q_{OR}) and Venturi-meter (Q_{VE}), the aperture of the sluice gate (d_{SL}), and the tail water depth of the flume), and to check the quality of the measurements taken during the tests.

4.1.1 - The Impulse - Momentum Balance

The control volume used in the investigation was defined in the following way (see Fig. 4.1-1): (1)-a downstream control section (S_3) at 190 cm from the edge of the dividing wall (x_o = 190 cm); (2)-in the uniform stream the control section (S_2) was at the section containing tapping point P_1 (x_o = -40 cm) (3)-in the fast stream, the control section (S_1) was chosen at the sluice section (x_o = -10 cm). At sections S_2 and S_3 the depth of the flow was

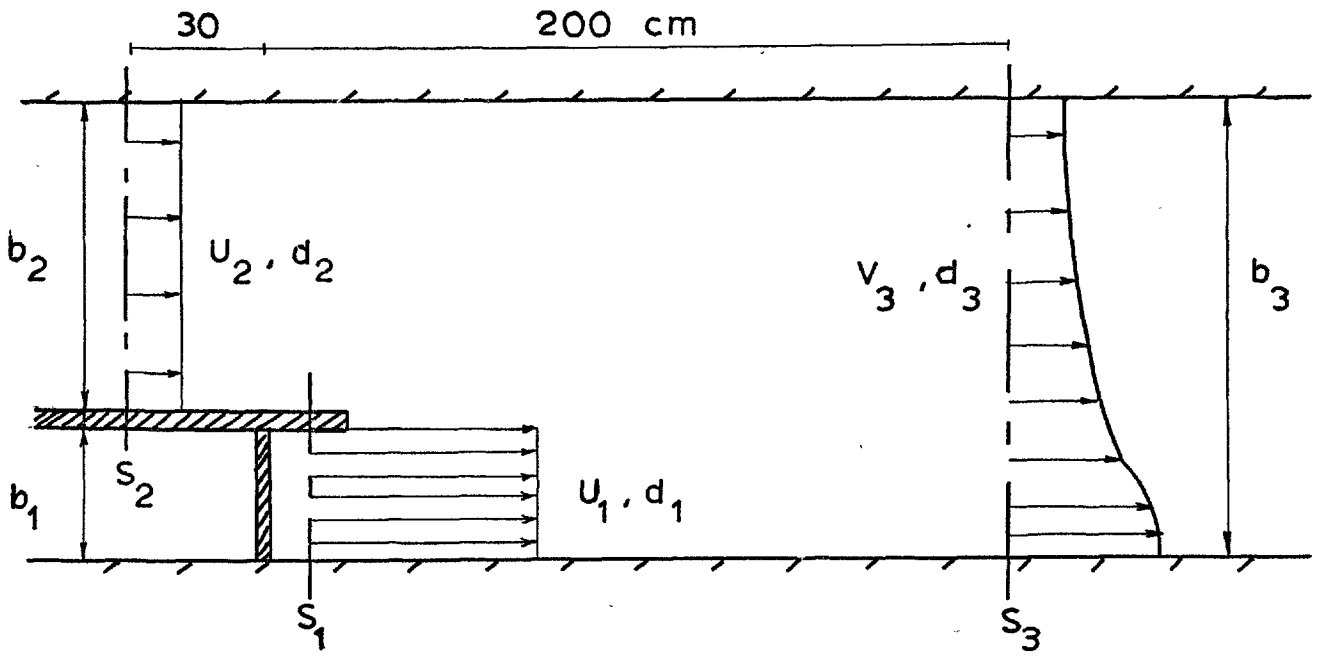


FIG. 4.1-1 TWO-DIMENSIONAL DIFFUSION OF THE SLUICE JET

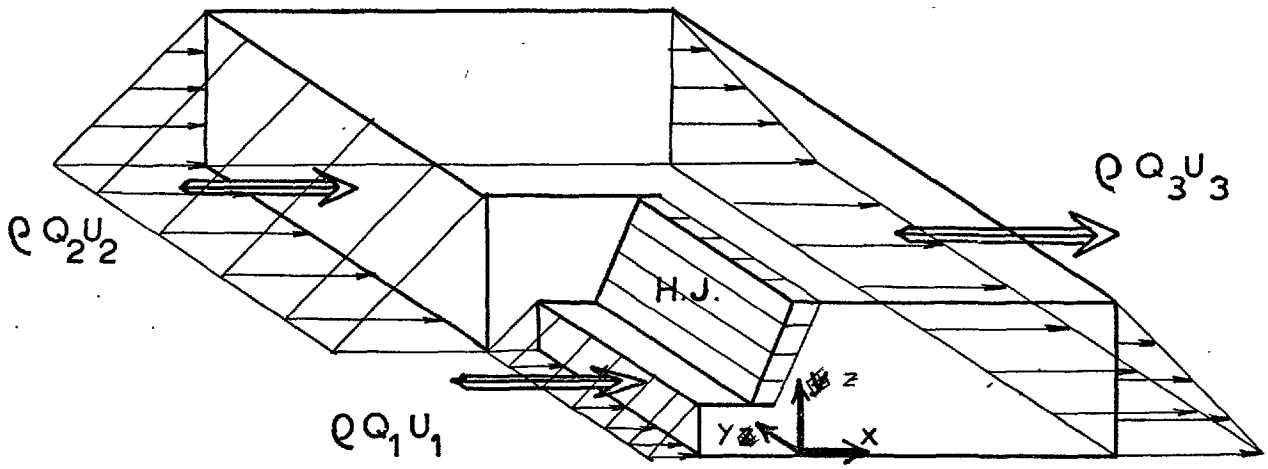


FIG. 4.1-2 THE CONTROL VOLUME

measured by tapping points (P_1, P_2 and P_3), and velocities were measured at several points. The depth (d_1) and the uniform velocity (U_1) at the control section in the fast stream were calculated, but not measured. The bed of the flume was always in the horizontal position.

The effects of viscosity and surface tension in the water, and the wall friction in the flume can be neglected in a first approximation analysis of the two merging streams. Hydrostatic pressure distributions and horizontal surface profiles (this assumption was checked at section P_2) were assumed in all cross-sections of the flow. The velocity distributions were assumed uniform at section S_1 and S_2, and a two-dimensional velocity profile was considered at section S_3. For reasons of simplicity the dividing wall (2 cm thick) was assumed to have had no effect upon the velocity distribution, so that

$$b_3 = b_2 + b_1 \qquad \ldots (4.1\text{-}1)$$

and the continuity equation,

$$Q_3 = Q_2 + Q_1 \qquad \ldots (4.1\text{-}2)$$

where b_i is the width of the channel ($i = 1, 2$ or 3), and Q_i the corresponding flow rate discharge. For the uniform streams, Q_1 and Q_2 can be written as $Q_i = U_i \cdot d_i \cdot b_i$, in which U_i is the uniform velocity of the stream and d_i its mean depth. The flow rate at downstream control section is given by an integral form, where V_3 is the velocity at a point in the

section,

$$Q_3 = \int_0^{b_3} V_3 . d_3 . dy$$

The momentum equation for the same control volume is

$$\left(\rho . Q_1 U_1 + \tfrac{1}{2} \rho . g . d_1^2 . b_1 \right) + \left(\rho . Q_2 . U_2 + \tfrac{1}{2} \rho . g . d_2^2 . b_2 \right) =$$

$$= \beta . \rho . Q_3 . U_3 + \tfrac{1}{2} \rho . g . d_3^2 . b_3 \qquad \ldots (4.1\text{-}3)$$

being, ρ and g the mass density of the fluid and the acceleration of gravity, respectively, and β the momentum coefficient which is defined as

$$\beta = \frac{1}{U_3^2 . A_3} \int V_3^2 . dy . dz \simeq \frac{1}{U_3^2 . A_3} \sum \bar{V}_3^2 . \Delta A \qquad \ldots (4.1\text{-}4)$$

where A_3 is the area of the cross-section, and (y) and (z) are the co-ordinates of the point velocity (V_3). ($\bar{V}_3$) is the mean velocity at an elemental area (ΔA). The coefficient (β) quantifies the non-uniformity of the velocity distribution at the section and any boundary shear forces (which were assumed to be small). The momentum and hydrostatic forces acting in the control volume are sketched in Fig. 4.1-2, in which the velocity distribution at section S_3 is assumed uniform ($\beta = 1.0$).

For a fixed geometry of the flume the variables in the flow of the two merging streams are the three discharges (Q_1, Q_2 and Q_3), and the three corresponding depths of flow (d_1, d_2 and d_3). Fixing the discharges

Q_1 and Q_2 and controlling the depth of the fast stream d_1, Equations 4.1-2 and 4.1-3 relate three unknowns Q_3, d_2 and d_3, and one parameter β. In the tests performed, the depths of the flow in the wider channel and in the flume were both controlled by the tail-water levels in the downstream end of the flume. Both depths were measured and within 3% the following assumption was justified,

$$d_2 = d_3 \qquad \ldots (4.1\text{-}5)$$

With this third equation the momentum coefficient could be estimated if the downstream depth (d_3) was known.

If all the velocities are replaced by the corresponding flow rates (Q_i) and areas ($b_i \cdot d_i$), and if ρ is cancelled in Equation 4.1-3, the pressure hydrostatic terms can be separated from the momentum forces in the following way,

$$\tfrac{1}{2}g(d_3^2 \cdot b_1 - d_1^2 \cdot b_1) = \frac{Q_1^2}{b_1 \cdot d_1} + \frac{Q_2^2}{b_2 \cdot d_2} - \beta \frac{Q_3^2}{b_3 \cdot d_3}$$

or
$$d_3^2 - d_1^2 = \frac{2}{g \cdot b_1}\left(\frac{Q_1^2}{b_1 \cdot d_1} + \frac{Q_2^2}{b_2 \cdot d_2} - \beta \frac{Q_3^2}{b_3 \cdot d_3}\right) \qquad \ldots (4.1\text{-}6)$$

The hydraulic jump equation for a two-dimensional flow can be derived from Equation 4.1-6, making: $\beta = 1.0$; $Q_1 = Q_3 = Q$; $Q_2 = 0$; $Q = q_1 \cdot b_1 = q_3 \cdot b_3$; $q_1 = q_3$; and $b_1 = b_3 = b$.

$$d_3^2 - d_1^2 = \frac{2q_1^2}{g}\left(\frac{1}{d_1} - \frac{1}{d_3}\right)$$

$$d_3^2 \cdot d_1 + d_1^2 \cdot d_3 = \frac{2q_1^2}{g}$$

q_1 and q_3 are the discharges per unit width at the corresponding sections. The solution of this quadratic equation in d_3 leads to the well known Belanger momentum equation for a two-dimensional normal hydraulic jump (4,12).

$$\frac{d_3}{d_1} = \tfrac{1}{2}\left(\left(1 + 8Fr_1^2\right)^{\frac{1}{2}} - 1\right) \qquad \ldots (4.1\text{-}7)$$

in which the Froude number of the approaching flow is $Fr_1 = q_1/(g \cdot d_1^3)^{\frac{1}{2}}$.

4.1.2 - Experimental Results

The momentum coefficient of the velocity profiles measured in the flow was calculated through Equation 4.1-4. Twenty-one points of the velocity distribution at section S_3 were measured by a mini-current meter (three velocity profiles, each with seven measurements, at depths 1.0, 3.8 and 6.0 cm from the bed of the flume), giving a three-dimensional distribution of velocity at that particular section. The corresponding momentum coefficient was $\beta_a = 1.49$. The coefficient calculated by the momentum Equation 4.1-6 was $\beta = 1.51$. These two results are in very good agreement, which suggests that the current meter measurements were reliable, and confirms that the simplifications made (assuming the shear forces to be small, neglecting the width of the dividing wall, and assuming $d_2 = d_3$)

in the analysis were satisfactory.

The momentum coefficients of the velocity profiles measured at half depth of the flow by both the mini-current meter ($\beta_b = 1.48$) and the Pitot-static tube ($\beta_c = 1.31$) were also calculated. The bigger value of β_b proved that the propeller meter was a more sensitive instrument than the Pitot-static tube in the range of velocities measured which tended to damp the maximum and minimum values of flow velocity.

The fact that the values of the momentum coefficient β_a and β_b are practically the same (1.49 and 1.48, respectively) can be used as an argument to justify the approximation, considered in this chapter, that the flow conditions in the flume were effectively two-dimensional and the velocities measured at half-depth were characteristics of the cross-section.

Inside the control volume, 12.8% of the hydraulic energy transported by the two parallel streams was dissipated (see Appendix G), and we will assume that all this loss of energy was due to the action of the normal hydraulic jump formed in the narrower channel of the supercritical stream (in fact, only part of the energy is dissipated by the jump). According to Ven Te Chow (4) the relative loss of energy in a two-dimensional hydraulic jump with a Froude number of 2.58 (the Froude number of the sluice discharge) is 18.7%. The energy dissipated in a normal hydraulic jump formed in a channel expanding in a coflowing stream is considerably smaller than the energy dissipated in a two-dimensional hydraulic jump. This result agreed with the empirical observations of other authors (25,38) that the downstream depth required for the formation of a normal hydraulic

jump in an abrupt expanded channel is smaller than in a two-dimensional rectangular channel.

The amount of energy dissipated in the jump must be smaller than the calculated 12.8%, since some energy had to be dissipated at the walls of the flume confining the control volume, and at the shear boundary of the diffusing jet. It was also observed that there were gravity waves travelling in the free surface of the flow, which radiated a small amount of energy.

4.2 - THEORETICAL ANALYSIS OF TURBULENT SHEAR FLOWS

Fig. 4.2-1 shows the mean flow pattern of a turbulent jet (with an initial uniform velocity U_o) spreading through an infinite medium, of the same fluid, at rest. The understanding of this simple example of a submerged jet is essential to the theory of turbulent jets. A typical velocity profile of a turbulent wall-jet diffusing in a free stream is shown in Fig. 4.2-2. The experimental results of the present research will be compared with two-dimensional flows of free jets and wall-jets diffusing in a medium at rest or in a uniform stream flowing in the same direction of the jet.

4.2.1 - General Considerations on Submerged Jets

In the diffusion of a jet there is a pronounced velocity discontinuity ($\Delta V = U_o$) between the jet and the surrounding fluid. A shear boundary separates the two zones of the flow, and the shearing surface is unstable and generates eddies in the flow, which move in disorderly fashion both along and across the stream, resulting in a transverse transfer of momentum

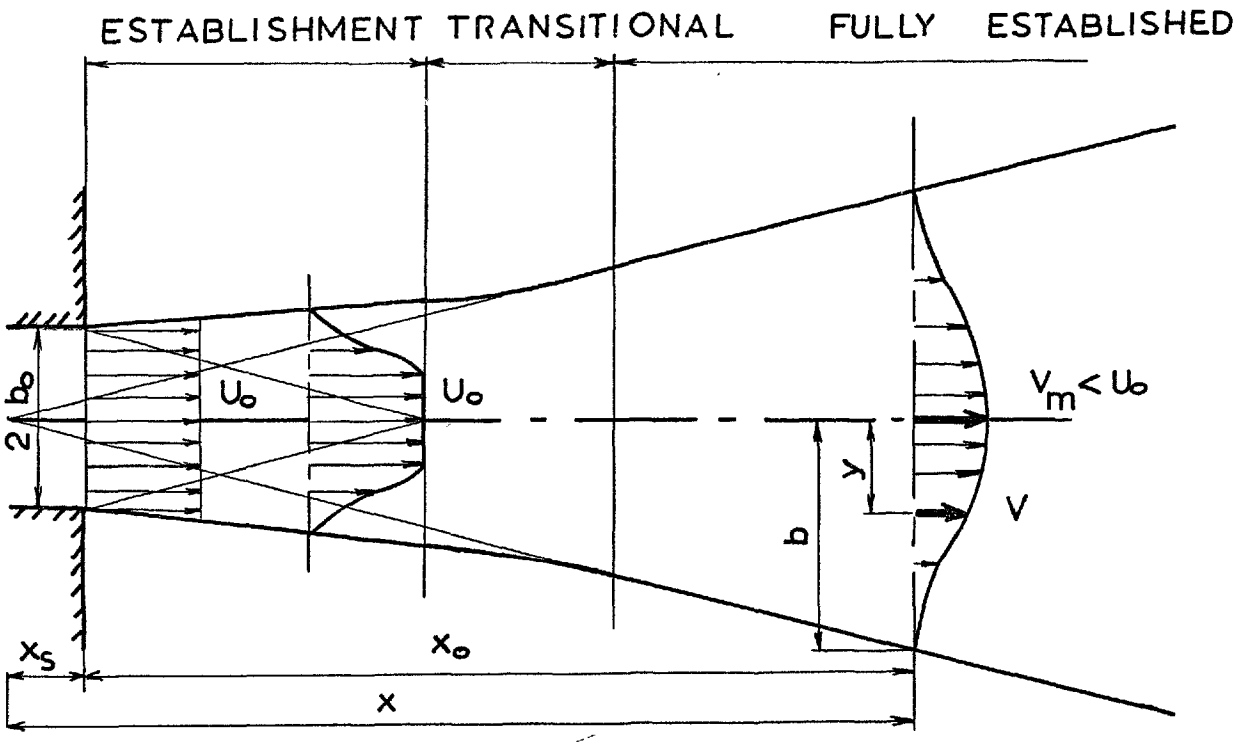


FIG. 4.2-1 THE DIFFUSION OF A TURBULENT JET

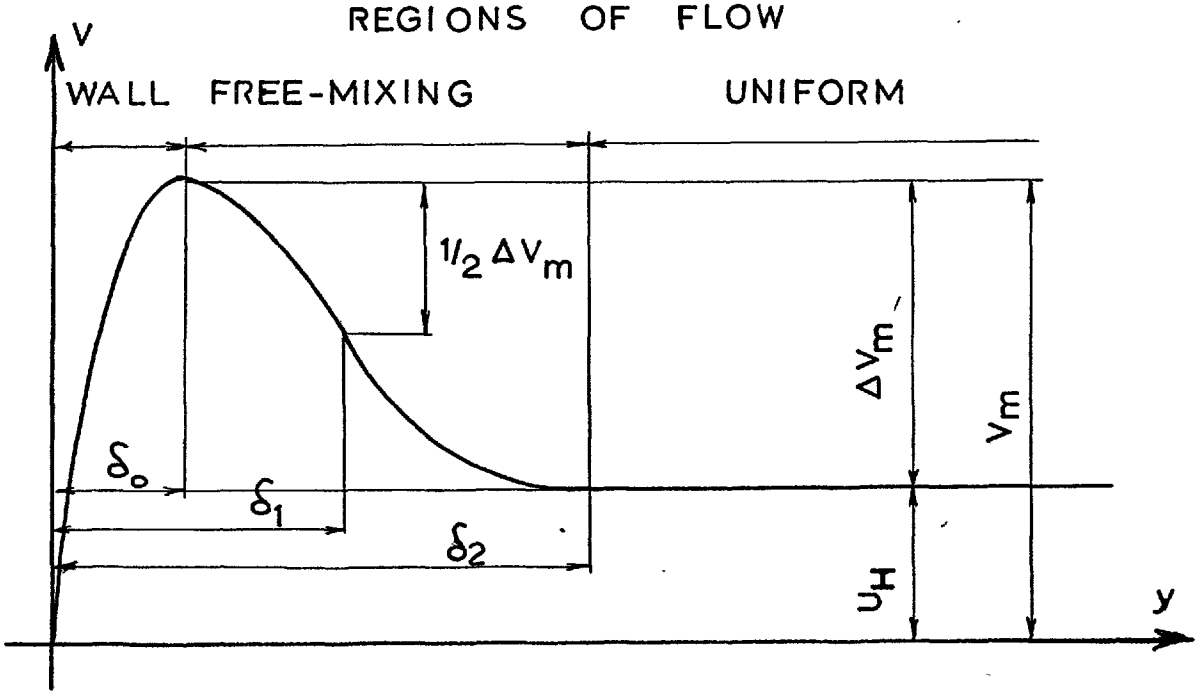


FIG. 4.2-2 TYPICAL VELOCITY PROFILE OF A WALL-JET DIFFUSING IN A UNIFORM STREAM

and mass. As a result of this lateral mixing process a region of finite thickness with a continuous distribution of velocity is formed between the core of the jet and the surroundings at rest. The width of the constant-velocity core steadily decreases and, at the same time, both the rate of flow and the overall breadth of the jet increases in magnitude with distance from the efflux section. The limit of this initial "zone of flow establishment" is reached when the mixing region has penetrated to the centre line of the jet. A small transitional zone separates the zone of flow establishment from the zone where the turbulent flow is fully established, and the jet then diffuses throughout the medium at rest without any essential change in character. The pole of a turbulent jet with finite thickness does not coincide with the efflux section, and a virtual origin has to be considered. Typical velocity profiles in the zones of the flow establishment and fully established flow is shown in Fig. 4.2-1.

The following analysis is confined to two-dimensional turbulent jets and to the zone of fully established flow. There is no theoretical value for the limit of this zone, and the experimental values given by several authors varies widely. According to Newman (52), the width of the core of a submerged jet (two-dimensional) diminishes to vanish at $(12b_o)$, being b_o the half width of the plane jet, and the fully established jet develops at about $(50b_o)$ for high Reynolds number. Albertson et al (41) put the limit to the zone of the fully established flow at $(10.4\ b_o)$. Narasimha (51) suggests a value of $(30\ b_o)$ for two-dimensional wall-jets diffusing in still air, but Rajaratnam (32) accepts just half of that value.

Two-dimensional turbulent jets

If viscous action is presumed to have no influence on the mixing process, i.e. the Reynolds number for fluid efflux of the outlet is not too low, the diffusion characteristics of a turbulent two-dimensional submerged jet should be dynamically similar under all conditions. Then the mean value of the longitudinal velocity (V) at any point in the diffusion region only depends upon the position of the point (coordinates x,y) with respect to the efflux section, the linear dimension characterising the particular outlet form ($2\,b_o$), and the initial efflux velocity (U_o). These variables may be grouped in the following dimensionless relationship

$$\frac{V}{U_o} = f_1\left(\frac{x}{b_o}, \frac{y}{x}\right) \qquad \ldots (4.2\text{-}1)$$

A large number of experiments have been carried out to define the formal expression of this relationship (1, 41). They have proved that beyond a certain distance from the outlet section (where the turbulent flow is fully developed), the velocity distribution profiles at all sections of the jet are of the same general form, changing only in their relative proportions. Different authors accept different expressions for the universal velocity profile, as will be seen later in the Chapter.

The volume flux (Q) of the diffusing jet increases with the longitudinal distance (x) due to entrainment of the surrounding fluid. The ratio of the rate of flow (Q) at any section of the flow pattern to the efflux rate at the initial section (Q_o) may be expected to have the

form

$$\frac{Q}{Q_o} = \frac{\int_0^{A} V \cdot dA}{U_o \cdot A_o} = f_2\left(\frac{x}{b_o}\right)$$

where (A_o) is the cross-section area of the outlet section and (dA) an elemental area normal to the direction of the flow.

Similarly, the ratio of momentum flux (M) at any cross-section of the flow to the momentum flux of the uniform jet (M_o) can be written as,

$$\frac{M}{M_o} = \frac{\int_0^{A} V^2 \cdot dA}{U_o^2 \cdot A_o} = f_3\left(\frac{x}{b_o}\right)$$

The energy of the jet decreases with the distance to the outlet section. The ratio of the energy flux (E) at any section to the energy flux at the outlet section (E_o) should take, as well, the non-dimension form

$$\frac{E}{E_o} = \frac{\int_0^{A} V^3 \cdot dA}{U_o^3 \cdot A_o} = f_4\left(\frac{x}{b_o}\right)$$

On the basis of experimental evidence it may be safely presumed that the pressure distribution is essentially hydrostatic throughout the zone of motion. This implies that the sole force producing the deceleration of the jet and the acceleration of the surrounding fluid is the tangential shear within the mixing region. Because this process

is wholly internal, it follows that the momentum flux must be a constant for all the cross-sections of the jet.

$$\frac{M}{M_o} = f_3\left(\frac{x}{b_o}\right) = 1$$

In the analysis of submerged jets, Albertson et al (41) used a Gaussian normal probability function for the similar velocity profiles of the diffusing jet.

$$\frac{V}{V_{max}} = \exp\left(-\frac{y^2}{2\sigma^2}\right) \qquad \ldots (4.2\text{-}2)$$

In this approximation, only two parameters are required to define the velocity profile of the mean flow pattern at any section: the velocity at the axis of the jet (V_{max}), and the standard deviation (σ). Now Equation 4.2-1 can be reduced to

$$\frac{V_{max}}{U_o} = f_5\left(\frac{x}{b_o}, \frac{\sigma}{x}\right) \qquad \ldots (4.2\text{-}3)$$

and the condition of dynamic similarity requires that at all cross-sections, regardless of the efflux velocity,

$$\frac{\sigma}{x} = C \qquad \ldots (4.2\text{-}4)$$

In other words, the jet spreads at a linear rate defined by the value of the constant C.

Using the last three equations, the characteristics of the mean flow pattern for any specific boundary conditions may be determined analytically, with the exception of a single experimental coefficient.

In a two-dimensional submerged jet the fact that the momentum is constant can be expressed by the following relationship.

$$V_{max}^2 \cdot x \cdot \int_0^{b/x} \left(\frac{V}{V_{max}}\right)^2 \cdot \frac{dy}{dx} = C_1$$

in which b is the semi-thickness of the section. On account of the universal nature of the velocity profiles

$$\int_0^{b/x} \left(\frac{V}{V_{max}}\right)^2 \cdot \frac{dy}{dx} = C_2$$

which implies that the decay of velocity along the axis of a plane jet is

$$V_{max} = \frac{C_3}{x^2} \qquad \ldots (4.2\text{-}5)$$

4.2.2 - Turbulent Flow Equations of a Jet of Incompressible Fluid.

A brief and simple summary of the theory available on turbulent shear flow is introduced in this section. The theoretical analysis is confined to fluids which are viscous (Newtonian type) and incompressible (ρ = const), because such is the case of the water which was used in the experimental work carried out in the Hydraulics Laboratory. The temperature effects were completely neglected and only steady state flows in respect to time will be considered.

Equations of motion of a viscous-incompressible flow

The conservation of mass in an homogeneous incompressible fluid is expressed by means of the continuity equation, which in differential form is (13)

$$\frac{\partial u}{\partial x} + \frac{\partial v}{\partial y} + \frac{\partial w}{\partial z} = 0 \qquad \ldots (4.2\text{-}6)$$

being (u,v,w) the three velocity components in a referential system of Cartesian coordinates (x,y,z).

The Navier-Stokes equations of a viscous (Newtonian) fluid which are applicable to laminar and turbulent flows, are (13)

$$\rho\left(\frac{\partial u}{\partial t} + u\frac{\partial u}{\partial x} + v\frac{\partial u}{\partial y} + w\frac{\partial u}{\partial z}\right) = \rho X - \frac{\partial p}{\partial x} + \mu\nabla^2 u$$

$$\rho\left(\frac{\partial v}{\partial t} + u\frac{\partial v}{\partial x} + v\frac{\partial v}{\partial y} + w\frac{\partial v}{\partial z}\right) = \rho Y - \frac{\partial p}{\partial y} + \mu\nabla^2 v$$

$$\rho\left(\frac{\partial w}{\partial t} + u\frac{\partial w}{\partial x} + v\frac{\partial w}{\partial y} + w\frac{\partial w}{\partial z}\right) = \rho Z - \frac{\partial p}{\partial z} + \mu\nabla^2 w \qquad \ldots (4.2\text{-}7)$$

where (t) is the variable time, (ρ) the fluid density, (p) the pressure, (X,Y,Z) the components of the body force per unit mass, and (μ) the dynamic viscosity of the fluid. (∇^2) is the Laplacian operator

$$\nabla^2 = \frac{\partial^2}{\partial x^2} + \frac{\partial^2}{\partial y^2}\,\frac{\partial^2}{\partial z^2}$$

The solution of this system of four differential equations in four unknowns (u,v,w and p) requires in each particular problem the definition

of the initial conditions in the flow and the formulation of the boundary conditions. Owing to the non-linearity of the Navier-Stokes equations, no general method of solution is available, the only exceptions being simple cases of laminar flows.

Reynolds equations

In the analysis of turbulent flows it is convenient to represent each independent variable (velocity as well as the normal and tangential stresses) as a sum of a time-averaged mean value and an instantaneous turbulent fluctuation value,

$$A = \bar{A} + A'$$

where A' is the fluctuating component with a mean value of zero, and $\bar{A}$ is the time-averaged component defined in the following way,

$$\bar{A} = \lim_{T\to\infty} \frac{1}{T} \int_0^T A \, dT \qquad \ldots (4.2\text{-}8)$$

Using the Cartesian tensor notation, Equations 4.2-6 and 4.2-7 become,

$$\frac{\partial u_i}{\partial x_i} = 0 \qquad \ldots (4.2\text{-}9)$$

$$\frac{\partial u_i}{\partial t} + u_j \frac{\partial u_i}{\partial x_j} = X_i - \frac{1}{\rho}\frac{\partial p}{\partial x_i} + \frac{\mu}{\rho}\frac{\partial^2 u_i}{\partial x_j \partial x_j} \qquad \ldots (4.2\text{-}10)$$

being the subscript (i) a free index, indicating which component is considered and (j) a dummy index, which indicates repeated operation.

In the following analysis, only steady state flow conditions with respect to time will be considered, so that $\frac{\partial \bar{u}_i}{\partial t} = 0$. The instantaneous values of u,v,w and p can be replaced by the equivalents $\bar{u} + u'$, $\bar{v} + v'$, $\bar{w} + w'$, and $\bar{p} + p'$, in Equations 4.2-9 and 4.2-10. If the same equations are averaged with respect to time they become, respectively (13),

$$\frac{\partial \bar{u}_i}{\partial x_i} = 0 \qquad \ldots (4.2\text{-}11)$$

$$\bar{u}_j \frac{\partial \bar{u}_i}{\partial x_j} + \overline{u'_j \frac{\partial u'_i}{\partial x_j}} = X_i - \frac{1}{\rho}\frac{\partial \bar{p}}{\partial x_i} + \frac{\mu}{\rho}\frac{\partial^2 \bar{u}_i}{\partial x_j \partial x_j} \qquad \ldots (4.2\text{-}12)$$

where the overbar represents a time-average mean value defined in the manner of Equation 4.2-8.

A new set of equations can be established when the mean-value equations are subtracted from the fully expanded equations (with the instantaneous values of the variables). These new equations represent the fundamental relationships among the components of the turbulent fluctuations (13),

$$\frac{\partial u'_i}{\partial x_i} = 0$$

$$\frac{\partial u'_i}{\partial t} + \bar{u}_j \frac{\partial u'_i}{\partial x_j} + u'_j \frac{\partial \bar{u}_i}{\partial x_j} + u'_j \frac{\partial u'_i}{\partial x_j} - \overline{u'_j \frac{\partial u'_i}{\partial x_j}} = -\frac{1}{\rho}\frac{\partial p'}{\partial x_i} + \frac{\mu}{\rho}\frac{\partial^2 u'_i}{\partial x_j \partial x_j}$$

The equation of continuity for the velocity fluctuations can be multiplied by the appropriate component of fluctuation, and then averaged,

$$\overline{u_i' \frac{\partial u_j'}{\partial x_j}} = 0$$

If these equations of zero value are added to the equations of motion, the Reynolds equations for the mean flow can be obtained after a convenient re-arrangement of the terms and differential expressions.

$$\rho \bar{u}_j \frac{\partial \bar{u}_i}{\partial x_j} = \rho X_i - \frac{\partial \bar{p}}{\partial x_i} + \frac{\partial}{\partial x_j} \left(\mu \frac{\partial \bar{u}_i}{\partial x_j} - \rho \overline{u_i' u_j'} \right) \qquad \ldots (4.2\text{-}13)$$

These equations differ from the Navier-Stokes equations for laminar flow only in the terms involving the velocity fluctuations. The nine products $\rho \overline{u_i' u_j'}$ are equivalent to apparent shear stresses, and they are called the Reynolds stress (τ'_{ij}),

$$\tau'_{ij} = -\rho \overline{u_i' u_j'} \qquad \ldots (4.2\text{-}14)$$

Although these apparent (turbulent) shear stresses may be quite large compared to the mean viscous shear, they cannot account for the dissipation of energy in the flow; the entire energy of the flow, both mean and turbulent is eventually dissipated by the action of viscosity.

The fundamental equations just presented are exact and have some value in helping to describe the mechanism of turbulence. The addition of six more unknowns (the independent components of the turbulence stress tensor) to the four usual ones (u,v,w, and p) increases to ten the number of variables of the equations of motion. The three Reynolds equations and the equation of continuity are insufficient in number to yield a solution.

of any problem (indeterminate solution) unless either greatly simplified or suplemented by additional relationships between the characteristics of the turbulence and the mean flow.

Turbulent shear flow model

It was Taylor who first developed a statistical theory of turbulence satisfying the equations of motion. He assumed the turbulence in the flow to be homogeneous (i.e. the same at every point) and isotropic (i.e. statistically independent of the orientation as well as the location of the co-ordinate axis). With this simplification, he reduced the six independent components of the stress tensor to a single one, which could be determined experimentally.

The essential characteristic of a turbulent motion is that its turbulent fluctuations are random in nature. In order to understand the turbulent flow field, it is necessary to know the properties of the turbulent fluctuations (intensity, correlation, spectrum, probability densities, etc). Since no complete statistical theory on turbulent shear flow is now available, it is necessary to rely on experimental evidence to solve the engineering problems.

Semi-empirical theories, sometimes known as phenomono-logical theories, have been applied to fully developed turbulent flows. These theories are based on the observation that in turbulent shear flow there is a lateral transport of fluid between zones of high and low velocity, and that the mixing process is related to the velocity gradient. The first attempt to express turbulent shear stress (τ'_{xy}) in mathematical form was made by Boussinesq who introduced the coefficient of eddy viscosity ε and assumed it to be a constant property of the flow depending upon the structure of

the turbulence.

$$\tau'_{xy} = \varepsilon \frac{\partial \bar{u}}{\partial y}$$

The total shear stress in turbulent flow is usually written as (17),

$$\tau_{xy} = \mu \frac{\partial \bar{u}}{\partial y} + \varepsilon \frac{\partial \bar{u}}{\partial y}$$

where (ε) is the eddy viscosity by analogy with (μ), which is the molecular viscosity of the flow. At higher Reynolds numbers, the viscous stress are negligible in comparison with the apparent turbulent stresses ($\mu \ll \varepsilon$).

Prandtl succeeded in relating the velocity components of turbulence to the general flow characteristics by proposing that small fluid mass elements are transported by turbulence inside the fluid a certain mean distance (l), the mixing length, from regions of one velocity to regions of another before they lose their increment of momentum in the new region. He suggested the following model of turbulence,

$$\tau'_{xy} = \rho l^2 \left(\frac{\partial \bar{u}}{\partial y}\right)^2$$

This expression, although satisfactory in many respects, had the disadvantage that (l) was a function of (y), the mixing length becoming larger at greater distance from the boundary wall. This disadvantage was partially overcome by von Karman, who proposed a more complex model of turbulence,

$$\tau'_{xy} = \rho k^2 \frac{(\partial \bar{u}/\partial y)^2}{(\partial^2 \bar{u}/\partial y^2)^2}$$

in which k is a (dimensionless) constant of the turbulence.

The first successful analysis in the diffusion of turbulent jets of incompressible fluid was made by Tollmien, who applied Prandtl's mixing length theory. The mixing length was assumed constant across the sections of the jet and proportional to a characteristic length (the width of the jet) in the longitudinal direction of the flow, $\varepsilon = \rho l^2 \frac{\partial \bar{u}}{\partial y}$). Tollmien solved the following three problems (1,10):

1. The diffusion of a parallel stream throughout an adjacent fluid at rest.

2. The diffusion of a two-dimensional jet issuing from a very narrow slot in a medium at rest.

3. The diffusion of an axially symmetric jet issuing from a very small orifice with a medium at rest.

Görtler used also Prandtl's theory of free turbulence, but he assumed that the eddy viscosity was proportional to the product of the velocity difference $(V_m - U_H)$ and the jet thickness (b), and that the coefficient of turbulent viscosity (χ) was constant over the cross-sections of the jet, ($\varepsilon = \chi \rho x b(V_m - U_H)$), instead of the mixing length (1). Görtler applied this theory to an infinitely narrow plane jet and obtained an asymptotic velocity profile at the cross-sections of the diffusing jet.

The velocity profiles predicted by both theories for a two-dimensional plane jet issuing from a very narrow slot in an infinite medium at rest are very similar, but the main advantage of the Prandtl'-Görtler theory is that the velocity profile is described by a relatively simple analytic formula, while in the Prandtl'-Tollmien theory the profile only can be determined

numerically (1). Görtler's expression for the velocity profile is (1 ,52),

$$\frac{V}{V_m} = \operatorname{sech}^2\left(\frac{\theta y}{x}\right) \qquad \ldots (4.2\text{-}15)$$

in which (x) is the distance to the hypothetical origin of the jet (the pole of the jet), and not the distance to the exit section (x_o), (y) the distance to the axis of the jet of any point of the cross-section, (V) is the corresponding component of velocity in the direction of the flow, and (V_m) the maximum velocity. The value of the empirical constant (θ), according to Abramovich (1), is $\theta = 7.67$, and Newman (52), $\theta = 8.46$.

4.2.3 - Dimensional Analysis of Two-Dimensional Jets.

The integration of the equations of motion for turbulent shear flow is impossible for the great majority of practical problems. It is necessary then to use dimensional arguments and approximate methods to indicate possible physical laws of the mean flow, and then to discriminate between them with the aid of experimental data. The variation of mean velocity across sections of a fully developed jet is usually found to exhibit geometrical "similarity". This implies that the mean velocity distribution and the turbulent structure on which it depends are completely determined by a velocity scale and a length scale. These scales in a free submerged jet are the maximum velocity (U_m) and the local half width (b), given by the distance from the axis to the point at which the mean velocity falls to half its maximum value in the section. A further assumption which finds some experimental support is that of "self preservation" which implies a continuing similarity in turbulent structure during the decay or development of a turbulent flow.

Such a situation is to be expected in a steady state brought about by the equilibrium between viscous decay and the generation of turbulent energy through turbulent shear stresses. These considerations apply to flow with sufficiently large Reynolds number so that viscous effects on the mean velocity are negligible. In this section, only two-dimensional plane turbulent jets will be considered and the overbars in the variables of the flow (which represent a time average value defined in the manner of Equation 4.2-8) will be omitted in the subsequent discussion as all mean flow dependent variables are assumed to be time averaged.

The equations of motion for a two-dimensional jet (in which $X_i = 0$ and $\frac{\partial p}{\partial x} = 0$) may be deduced from Equations 4.2-11 and 4.2-13,

$$\frac{\partial u}{\partial x} + \frac{\partial v}{\partial y} = 0 \qquad \ldots (4.2\text{-}16)$$

$$u \frac{\partial u}{\partial x} + v \frac{\partial u}{\partial y} = - \frac{\partial \overline{u' v'}}{\partial y} + \frac{\mu}{\rho} \frac{\partial^2 u}{\partial y^2} \qquad \ldots (4.2\text{-}17)$$

The conditions under which the mean velocity profiles are similar and the turbulent structure of the flow are self preserved in the motion are (8 , 16)

$$u = U_m f(y/b)$$

$$\overline{u'v'} = U_m^2 \, g_{12}(y/b)$$

$$u^2 = U_m^2 \, g_1(y/b); \; v^2 = U_m^2 \, g_2(y/b)$$

In these equations $U_m(x)$ is the maximum velocity in the (x) direction (at the axis of the jet) and b(x) the half width of the same jet. The similarity

function is $f(y/b)$ and g_1, g_2 and g_{12} are the self preserving functions.

Free submerged jets

The main stream flow in the discharge of a two-dimensional jet is in the direction of the jet axis. The mean velocity component (v) at right angles to the axis is found to be very small by comparison with the main stream velocity (u) itself and can sometimes be neglected. At high Reynolds number the viscous stresses are negligible in comparison with turbulent stresses. Equation 4.2-12 may be integrated across half the jet, and because the shear stress ($\rho\ \overline{u'v'}$) is zero at the limit of integration, then

$$\int_0^b \rho . \frac{\partial u^2}{\partial x} . dy = -\left[\rho . \overline{u'v'}\right]_0^b = 0$$

and, integrating this equation, it will be found that the momentum flux of the jet is constant at all sections.

$$\int_0^b \rho\, u^2\, dy = \text{constant} \qquad \ldots (4.2\text{-}18)$$

Equation 4.2-12 may be multiplied, as well, by the mean velocity u and integrated with respect to y,

$$\int_0^b \rho . u^2 . \frac{\partial u}{\partial x} . dy = -\int_0^b u . \rho . \frac{\partial (u'v')}{\partial y} . dy \qquad \ldots (4.2\text{-}19)$$

If the conditions for similarity and self-preservation of the flow are satisfied the momentum and energy equations in the flow (Equations

4.2-13 and 4.2-14, respectively) become (10),

$$\rho . U_m^2 . b . \int_0^1 f^2(\eta) . d\eta = \text{constant}$$

$$\rho . U_m^2 . b . \frac{\delta U_m}{\delta x} \int_0^1 f^3(\eta) . d\eta = \rho . U_m^3 . \int_0^1 f(\eta) . g_{12}'(\eta) . d\eta$$

where ($\eta = y/b$). From the foregoing equations and because the velocity profiles are similar,

$$\rho U_m^2 \, b = \text{constant} \; ; \quad b \frac{\delta U_m}{\delta x} = U_m$$

which implies that (b) is proportional to distance (x) and the velocity at the axis of the jet is inversely proportional to the square root of the distance. Both results were found before in Equations 4.2-4 and 4.2-5 and the values of the constants of proportionality have to be determined from experimental data.

The distance (x_o) in the region of fully established flow is usually measured from the hypothetical pole of the jet (x), being (x_s) the distance between the pole of the jet and the exit section

$$x_o = x - x_s$$

In the remainder of this chapter we will use capital (U) to designate a uniform velocity, and capital (V) for a point velocity. The rate of growth of the turbulent jet (Equation 4.2-4) and the decay of maximum velocity (Equation 4.2-5) can be re-written, respectively,

$$\frac{b}{x - x_s} = C_1 \qquad \ldots (4.2\text{-}10)$$

$$\frac{V_m}{U_O} = \frac{C_2}{(x - x_s)^{\frac{1}{2}}} \qquad \ldots (4.2\text{-}11)$$

Free jets in a co-flowing stream

A momentum jet spreading in a parallel stream flowing in the same direction can be treated in an analogous manner as a submerged jet. The assumption of a similar velocity distribution function must be written in terms of the excess velocity $V - U_H$, (1)

$$\frac{V-U_H}{V_m-U_H} = f_1\left(\frac{y}{b}\right) \qquad \ldots (4.2\text{-}12)$$

where (U_H) is the uniform velocity of the external stream, (V_m) the maximum velocity at the axis of the jet and (b) the width of the jet. (V) is the velocity at distance (y) from the axis in any point of the section. The velocity profiles in a turbulent jet spreading through an external stream are similar to the profiles of a submerged jet (1). An empirical Gaussian distribution is often used to represent the velocity profile

$$f_1\left(\frac{y}{b}\right) = \exp(-\ 0.693\ \left(\frac{y}{b}\right)^2)$$

If $U_H < V_m$, Abramovich (1) gives the rate of growth of a two-dimensional jet in a co-flowing fluid as

$$\frac{db}{dx} = C\,\frac{V_m - U_H}{V_m + U_H} \qquad \ldots (4.2\text{-}13)$$

where the constant (C) is determined experimentally. Since the velocity at the axis of the jet (V_m) varies with (x), the boundary of the jet in a coflowing stream must be curved according to Equation 4.2-28.

Wall-jets in a free stream

A typical velocity profile of a plane two-dimensional turbulent wall-jet in a free stream was sketched in Fig. 4.2-2. The uniform velocity of the free stream is U_H and V_m is the maximum velocity in the profile. The distances from the wall to the point of maximum velocity and to the point of the flow at which the velocity is equal to half the maximum velocity difference in the free mixing region are (δ_o) and (δ_1), respectively.

The similarity solution approach to boundary value problems had been effectively used by Glauert (48) for the solution of the wall-jet in a still medium. Based on physical reasoning he was the first to postulate that, in strict sense, the entire flow of the wall jet cannot conform to one overall similarity solution. He divided the flow into an inner "wall region" and an outer "free mixing region" on either side of the maximum velocity and treated the two regions separately.

Kruka and Eskinazi (50) investiaged a plane steady turbulent wall-jet with negligible longitudinal pressure gradient in a constant moving stream, with varying ratios of jet to free stream velocity. They also divided the flow into an inner wall region and an outer free mixing region, but they suggested that the division of the two regions should be the point of zero shear, which may not coincide with the location of the maximum velocity. The inner layer is constantly losing momentum due to frictional stresses at the wall, while the outer layer tends to preserve its momentum. Similarity was found to exist in both regions of the flow, but the same scales do not apply to both layers.

The "similar" velocity profile in the free-mixing region of the flow can be defined in terms of the maximum excess velocity and a characteristic width of the wall jet. Kruka and Eskinazi (46,50) chose for the width scale the distance from the point of maximum velocity (δ_o) to the point of the flow where the excess velocity of the jet ($V - U_H$) is half the maximum excess velocity ($V_m - U_H$).

$$\frac{V - U_H}{V_m - U_H} = f_2\left(\frac{y - \delta_o}{\delta - \delta_o}\right) \qquad \ldots (4.2\text{-}29)$$

4.3 - MEASURED MEAN FLOW PATTERN

The mean flow pattern of a turbulent jet issuing from a sluice gate and merging with a deeper and slower co-flowing stream is investigated in this section. The growth of the jet, the decay of the maximum velocity, and the velocity distribution are the specific flow characteristics considered. The sluice jet was discharged along one of the lateral walls of the flume. If the effect of the boundary layer on the wall is disregarded and the wall of the flume is assumed to be a plane of symmetry, the jet can be treated as a free jet and the results compared with the equivalent characteristics of free turbulent jets diffusing in a still medium or in a parallel stream. Alternatively, when the effect of the wall is taken into account, the flow can be considered as a particular case of a wall-jet.

The flow conditions in the laboratory were arranged to give a stable and well defined normal hydraulic jump inside the sluice channel. The fast sluice discharge, after passing through the jump, diffused into a slow and uniform stream flowing in the same direction, the details of the experiments being given in Section 2.4-4. The flow pattern with an oblique jump was unstable (the jump and the shear boundary of the jet had no fixed position) and the free surface was highly disturbed by waves propagating on the surface of the flow and reflecting in both walls of the flume. Due to the instability of the flow and the waves, the measurements of velocity and depths were difficult. The normal hydraulic jump flow pattern was more stable and it was decided to investigate this steadier flow instead of the oblique jump case. The initial aim of the work was to investigate the flow behaviour of a fast stream intersecting a slow stream, so that the diffusion of the jet in a normal jump case was preferred to a submerged discharge of

the sluice gate.

At the exit section of the fast channel the depth of the flow was approximately the same as that of the main channel, where the depth was controlled by the downstream conditions in the flume. Uniform velocity distributions were assumed for both parallel streams at the section of the sluice gate. The flow conditions downstream in the flume were assumed to be two-dimensional and the results of the tests were compared with equivalent conditions on two-dimensional turbulent jets. In the interpretation of the results, the three-dimensional characteristics of the real flow (since the two parallel streams had different depths and velocities), the free surface, and the confinement of the jet by the two walls and bed of the metal flume were taken into account.

4.3-1 - Growth of the Jet

The growth of the sluice jet was calculated from the velocity profiles measured with the Pitot-tube at different cross-sections in the flume (see Fig. 4.3-1). The characteristic width of the jet (δ_1) in a cross-section was assumed to be the distance from the right wall of the flume to the point with velocity $V_1 = U_H + \frac{1}{2}(V_m - U_H)$. The mean velocity of the uniform stream was (U_H = 22.8 cm/s) and (V_m) was the maximum velocity in the section. The characteristic velocity (V_1) was calculated for each section where velocity measurements were taken and the corresponding (δ_1) was measured from the velocity profiles.

A simple linear relationship for the growth of the jet thickness with the distance to the edge of the dividing wall was investigated. The

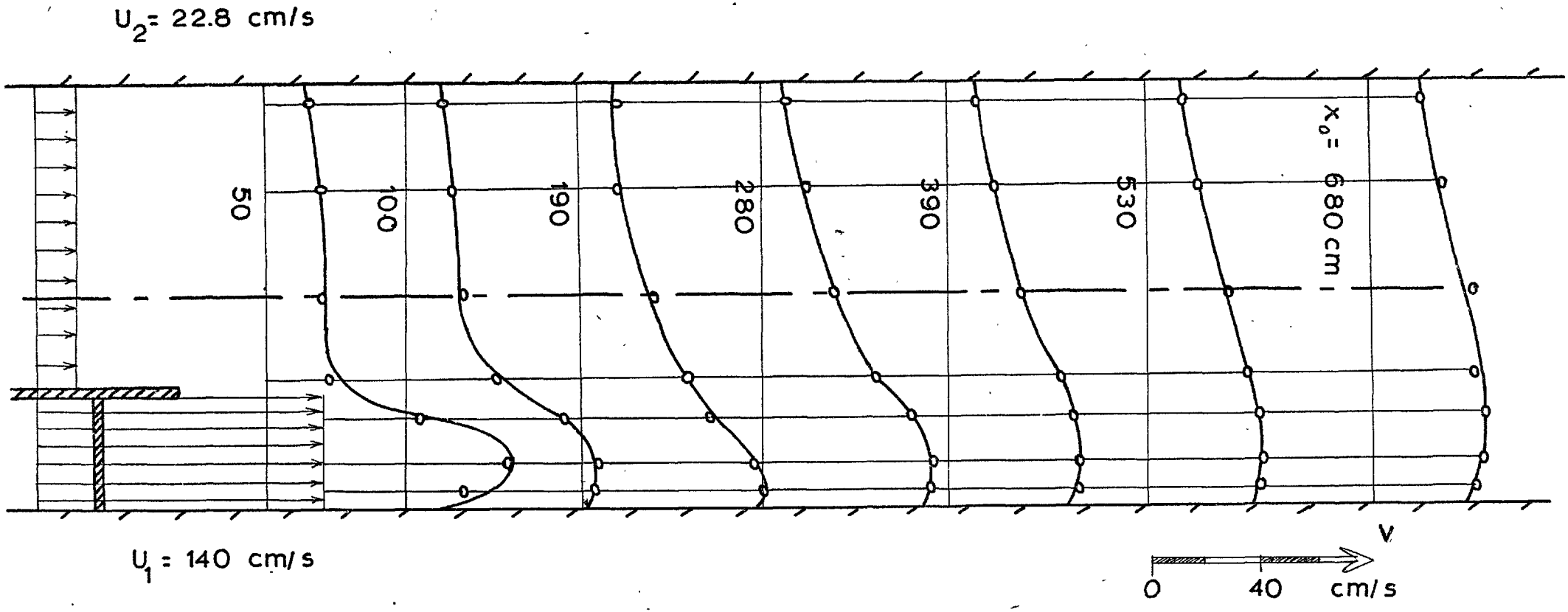


FIG. 4.3-1 THE DIFFUSION OF THE JET

results were made non-dimensional by the width of the sluice gate (b_o = 20 cm).

$$\frac{\delta_1}{b_o} = c + m. \frac{x_o}{b_o} \qquad \ldots (4.3\text{-}1)$$

In this expression (m) is the rate of growth of the jet ($m = d\delta_1/dx$), and (c) a constant value depending on the geometry of the exit section. The experimental points were plotted in Fig. 4.3-2 and compared with the growth of two-dimensional free-jets and wall-jets. A straight line with coefficients c=0.70 and m=0.035 fitted well the measured values of the jet thickness except for the far downstream point in the flume. This point was close (100 cm) to the weir controlling the tail-water levels of the flume. It was possible for the jet to separate from the wall at that section due to the presence of the weir. This separation was observed when there was no flow (U_H=0) in the main channel.

The rate of growth (m=0.109) of a submerged jet of air issued from a two-dimensional slot was measured by Albertson et al (41). Bradbury (42) quoted the same value, but Newman (52) used a slightly smaller value (m=0.104). The measured value in the jet (m=0.035) was about 66-68% lower than that of a free jet. This small rate may be due partly to the external stream flowing in the same direction of the jet and partly to the difference in depth between the fast and slow streams. The difference in the depth of the two-flows creates a pressure gradient along the shear boundary pushing the jet against the ~~left~~ right wall of the flume, which explains, as well, why the virtual width of the jet, at the exit section, was 0.70 of the width of the sluice gate.

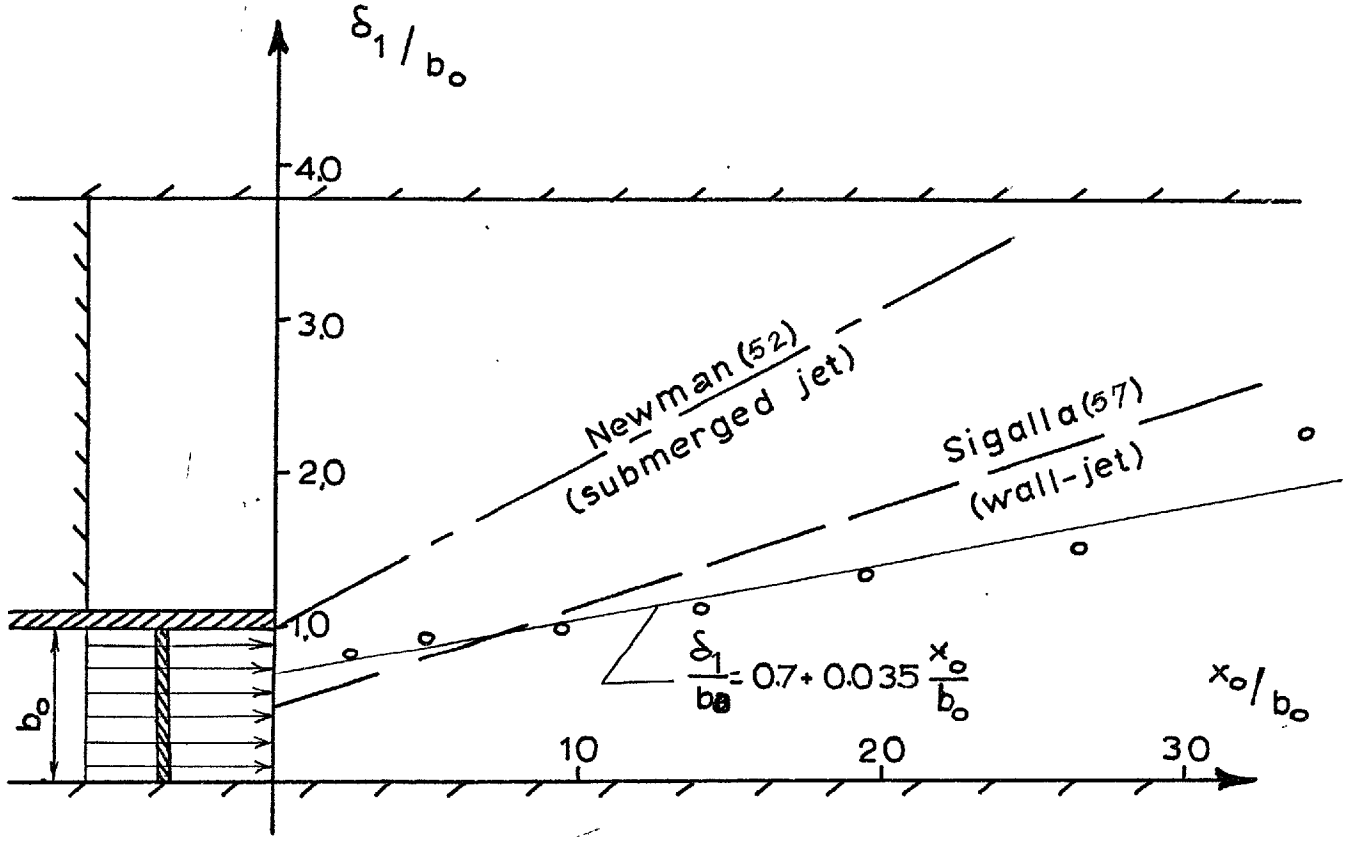


FIG. 4 3 2 JET DIFFUSION IN A MEDIUM AT REST

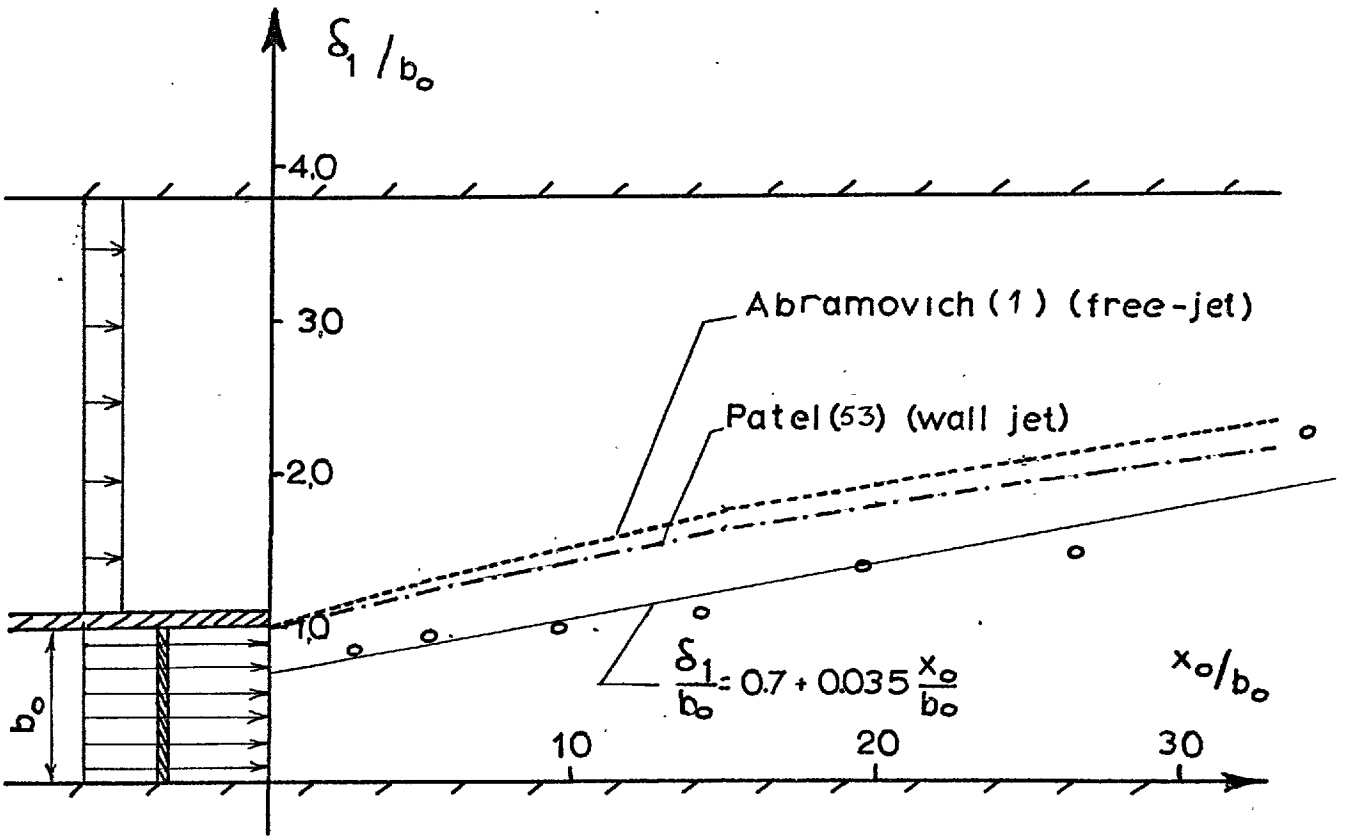


FIG. 4.3-3 JET DIFFUSION IN A UNIFORM STREAM

In an experimental investigation of a plane turbulent wall jet of air, Sigalla (57) found out that the points lie close to a line drawn from the centre of the nozzle and inclined at an angle 3.7^{o} to the wall (c=0.5; m=0.065). Rajaratnam (32), who studied the submerged hydraulic jump as a case of a plane turbulent wall jet under adverse pressure gradient, concluded that (c) and (m) are weak functions of the supercritical Froude number (F_1), and essentially independent of the submergence factor. The rate of growth of a wall jet is about 37-40% lower than that of a free submerged jet (52,53). This is attributed to a reduction in large eddy length scale associated with the presence of the wall.

A simplified analysis of a free jet in a uniform flow was developed by Abramovich (1) in which the rate of growth of the jet is related to that with still surroundings by a transformation of the (x) co-ordinate. If ($U_H < V_m$), he assumed the rate of growth of a two-dimensional jet to be,

$$\frac{d\delta_1}{dx} = C. \frac{V_m - U_H}{V_m + U_H} \qquad \ldots (4.3\text{-}2)$$

This equation is equivalent to Equation 4.2-23. In the analyses of free shear flows and wall-jet flows in uniform streams, Patel (53) assumed a simple empirical law (similar to the one used by Abramovich) for the rate of growth of the jet,

$$\frac{d\delta_1}{dx} = C_1. \frac{V_m - U_H}{V_m} \qquad \ldots (4.3\text{-}3)$$

TABLE 4.3-1 - THE GROWTH OF THE JET.

x_o	V_m	$V_m - U_H$	V_1	δ_1	$\frac{x_o}{b_o}$	$\frac{\delta_1}{b_o}$	$0.004 \frac{V_m - U_H}{V_m + U_H}$	$0.065 \frac{V_m - U_H}{V_m}$	$\Delta \frac{\bar{x}_o}{b_o}$	$\frac{\bar{x}_o}{b_o}$	δ_{11}	δ_{12}
cm	cm/s	cm/s	cm/s	cm	-	-	-	-	-	-	cm	cm
50	74.8	52.0	48.8	17.0	2.5	0.85	0.0554	0.0452	3.75	3.75	1.21	1.17
100	69.6	46.8	46.2	18.7	5.0	0.94	0.0527	0.0437	3.50	7.25	1.39	1.32
190	64.2	41.4	43.5	19.8	9.5	0.99	0.0495	0.0419	4.50	11.75	1.61	1.51
280	60.2	37.4	41.5	22.3	14.0	1.12	0.0469	0.0404	5.00	16.75	1.84	1.71
390	46.9	24.1	34.8	28.6	19.5	1.43	0.0360	0.0334	6.25	23.0	2.06	1.92
530	40.8	18.0	31.8	30.1	26.5	1.50	0.0294	0.0287	7.25	30.25	2.27	2.13
680	39.4*	16.6	31.1	46.2	34.0	2.31	0.0278	0.0274				

Notes: (1) δ_{11} - characteristic width of free jet diffusing in a uniform stream calculated from Eq. 4.3-2.

(2) δ_{12} - characteristic width of a wall-jet diffusing in a uniform stream calculated from Eq. 4.3-3.

(3) V_m^* - check of the velocity measurement.

(C_1 = 0.065) for wall-jets in streaming flow. Both equations of jet growth were integrated along the flume, and it was assumed (C = 0.104). The measured velocities (V_m) were used to calculate the values of $(V_m - U_H)/(V_m + U_H)$ and $(V_m - U_H)/V_m$. Abramovich curve is plotted in Fig. (4.3-3) and the results of the calculations are given in Table 4.3-1, and for sake of simplification, it was assumed that the jet spreads from the edge of the dividing wall, and ($x = x_o$). Both curves predicted well the rate of growth of the sluice jet in the flume. These results confirmed the observations of other authors that the general effects of the streaming flow is to reduce the rate of entrainment in the jet of the surrounding flow and reduce the jet rate of growth (52).

Both integrations, one for a free jet and the other for a wall-jet both diffusing in a uniform stream, gave very similar results, suggesting that the solid boundary had little effect on the growth of the turbulent jet.

4.3-2 - Decay of the Maximum Jet Velocity

The decay of maximum velocity (V_m) in a two-dimensional jet is inversely proportional to the square root of the distance (x) from the pole of the jet (see Equation 4.2-5), the constant of proportionality being determined experimentally. Abramovich (1) plotted in a non-dimensional form the variation of the axial velocity in a plane jet, using the initial velocity of the jet (U_o) and half width (b_o) of the exit section as scales,

$$\frac{V_m}{U_o} = \frac{C_4}{\left(\frac{x}{b_o}\right)^{\frac{1}{2}}}$$

and quoted values from several authors for the constant (C_4) varying between (3.5 and 4.0). Albertson et al (41) used the distance from the exit section (x_o) to plot their results in submerged jets,

$$\frac{V_m}{U_o} = \frac{C_5}{\left(\frac{x_o}{b_o}\right)^{\frac{1}{2}}}$$

The distance (x_o) is easier to measure in practical situations and is smaller than (x), which explains why the empirical value of C_5 at 3.22 is smaller than the values of C_4 (3.5 to 4.0) for the same values of the velocity ratio. A similar expression of velocity decay was used by Siggala (57) on two-dimensional wall-jets, and he found C_3 to be 3.45.

If the boundary is smooth, momentum from the free shear layer is transferred towards the wall region to compensate for the viscous dissipation near the wall, and the effect of the wall layer in the free mixing region is to decelerate the flow. Therefore, the rate of decay of the maximum velocity should be greater than in a free jet. The experiments done by Schwarz and Cosart (56) indicate the above fact, with the expression for maximum velocity decay as $V_m \propto (1/x^{0.55})$. However, for simplicity, a square root law for the decay of velocity will be used for comparison in the present results.

The experimental results in the decay of the jet velocity are plotted in Fig. 4.3-4. The width of the sluice channel (b_o) was used to calculate non-dimensional ratios of the distance to the edge of the dividing wall

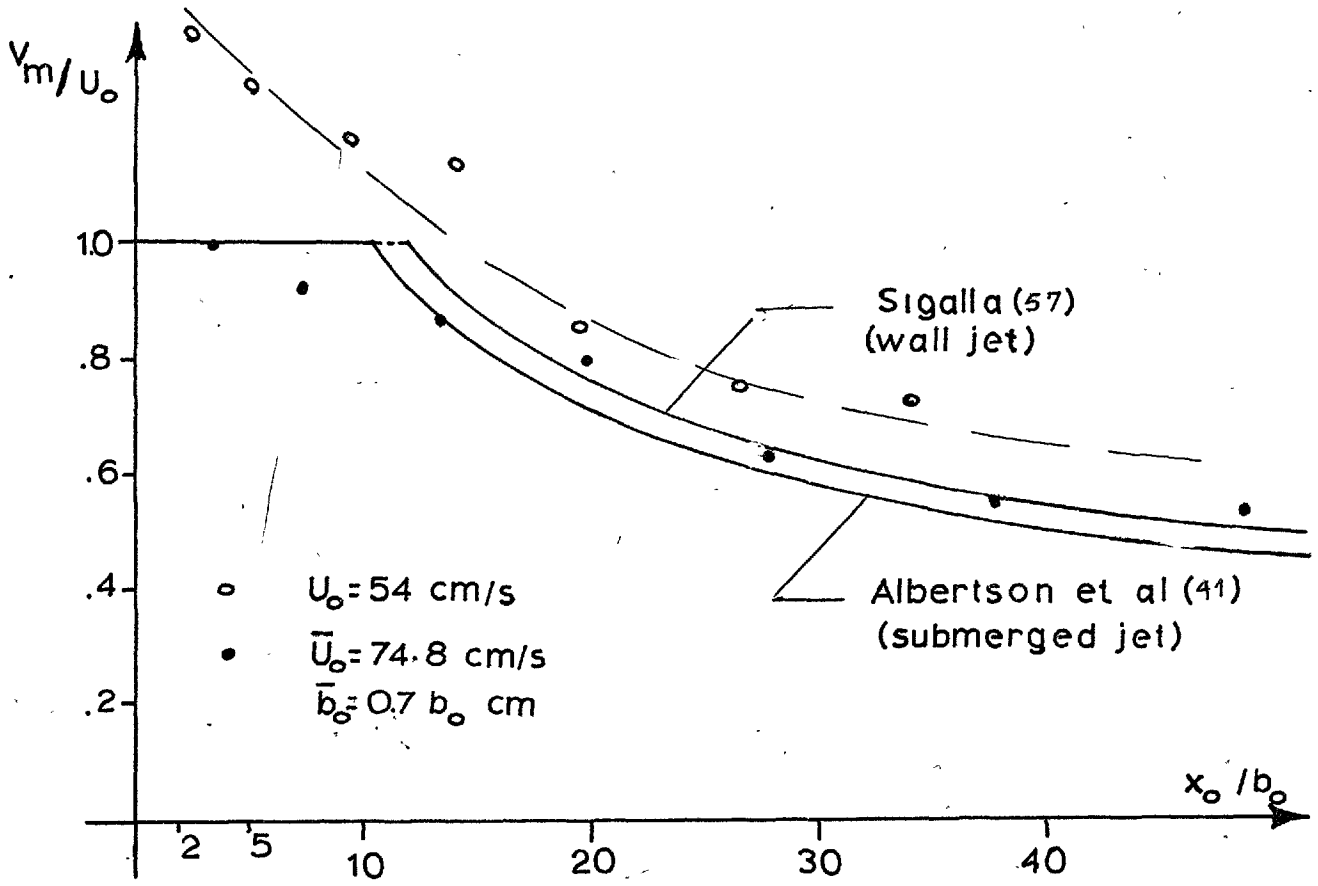


FIG. 4.3-4 DECAY OF THE MAXIMUM JET VELOCITY

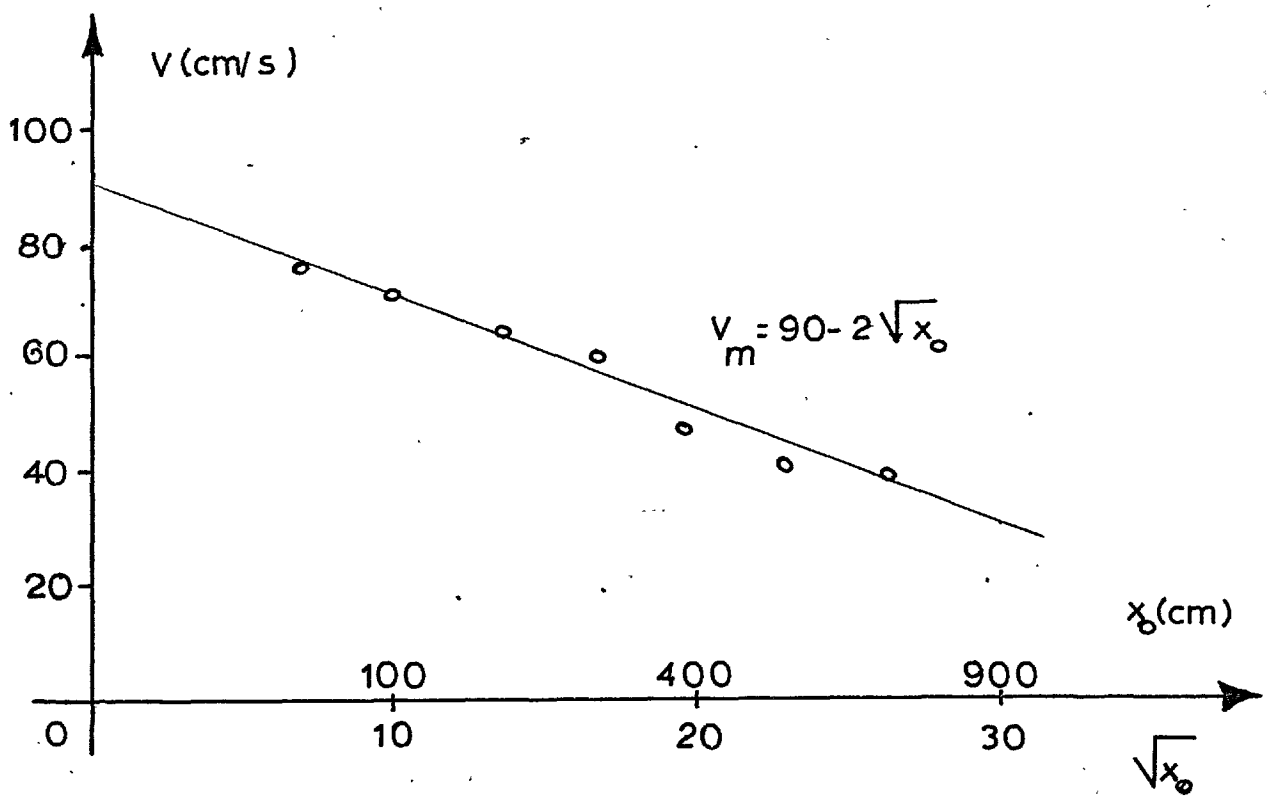


FIG. 4.3-5 LINEAR VELOCITY DECAY

TABLE 4.3-2 - MAXIMUM VELOCITY DECAY.

x_o	V_m	$\frac{V_m}{140}$	$\frac{V_m}{54}$	$\frac{x_o}{b_o}$	$\frac{x_o}{0.7b_o}$	$\frac{V_m}{74.8}$	$\frac{V_m}{U_o}$	$\frac{V_m}{U_o}$	$x_o^{\frac{1}{2}}$	$90 - 2x_o^{\frac{1}{2}}$
cm	cm/s									cm/s
							Sigalla	Albertson	$cm^{\frac{1}{2}}$	
50	74.8	0.534	1.385	2.5	3.57	1.00	2.18	2.04	7.06	76.0
100	69.6	0.497	1.289	5.0	7.14	0.93	1.54	1.44	10.00	70.0
190	64.2	0.459	1.189	9.5	13.57	0.86	1.12	1.05	13.80	62.4
280	60.2	0.430	1.115	14.0	20.00	0.80	0.92	0.86	16.73	56.5
390	46.9	0.335	0.869	19.5	27.86	0.63	0.78	0.73	19.74	50.5
530	40.8	0.291	0.756	26.5	37.86	0.55	0.67	0.63	23.02	44.0
680	39.4*	0.281	0.730	34.0	48.57	0.53	0.59	0.55	26.25	37.5

in the flume (x_o), but difficulties were found in defining a velocity scale (U_o). The first velocity used to make the flow dimensionless was the mean velocity of the flow downstream of the jump (U_o = 54 cm/s), but this gave results well above the predictions of Albertson (41) and Sigalla (57) as shown in Fig. 4.3-4. It had already been observed that the effective width of the jet was 0.7 times the width of the sluice gate. Making this assumption, altering the length scale of the jet and using the maximum velocity measured in the jet (74.8 cm/s) was obtained reasonable agreement with the empirical curve of Sigalla. The use of the maximum velocity for scaling is virtually identical to assuming that the jet after the jump only occupies 0.7 of the sluice channel width as (54 ÷ 0.7 = 77 cm/s). Fig. 4.3-5 shows how the decay in the maximum jet velocity approximates quite closely to a square root law.

4.4-3 - Geometrical Similarity in the Mean Velocity Profiles

The velocity distribution in the flow of a two-dimensional turbulent jet can be predicted from the equation of motion if simplifying assumptions are made about the turbulent structure of the flow. Tollmien and Görtler using slightly different assumptions on the mixing length characteristics of the flow derived similar velocity distribution functions. (Görtler's velocity profile given in Equation 4.2-15).

The similarity solution approach to boundary-value problems in Fluid Mechanics has proved to be a useful method of studying turbulent jets. The approximate characteristics of the mean flow pattern of the jet can

be derived analytically, with the exception of a single experimental constant, if conditions of dynamical similarity are observed in the flow. These similarity conditions were investigated in the discharge of the sluice gate into a parallel stream. The flow pattern was assumed two-dimensional and the results compared with two-dimensional theories and experimental work on plane turbulent jets. An adequate functional form for the velocity profile was specifically investigated.

The velocity measurements at half depth and in seven cross-sections of the flow were used to draw velocity profiles of the flow. The velocity ratio of each measurement (V) to the maximum velocity (V_m) measured at the same section was calculated, as well as the ratio of the distance from the wall (y) to a characteristic distance of the jet (δ_1), defined as the distance to the wall of the flume of a point with a characteristic velocity $V_1 = U_H + \frac{1}{2}(V_m - U_H)$. These results are plotted in Fig. 4.3-6, and suggest the possibility of a universal velocity profile in the flow conditions measured if adequate scales for velocity and width are found. The maximum velocity was found to occur between ($y/\delta_1 = 0.2$ and 0.4) from the wall, at each section, which showed that the diffusing jet is feeling the presence of the confining wall of the flume. Because, on the side away from the wall, the jet was diffusing in a uniform stream the velocity ratio tended towards a constant value of V/V_m.

Fig. 4.3-6 showed some scatter among the experimental points. As only a limited number of velocity measurements were made at each section (to be precise, seven), it was unlikely that the maximum velocity measured (V_m) in the section was the real maximum value of the velocity profile (V_{max}). The difference between V_m and V_{max} is a possible explanation for

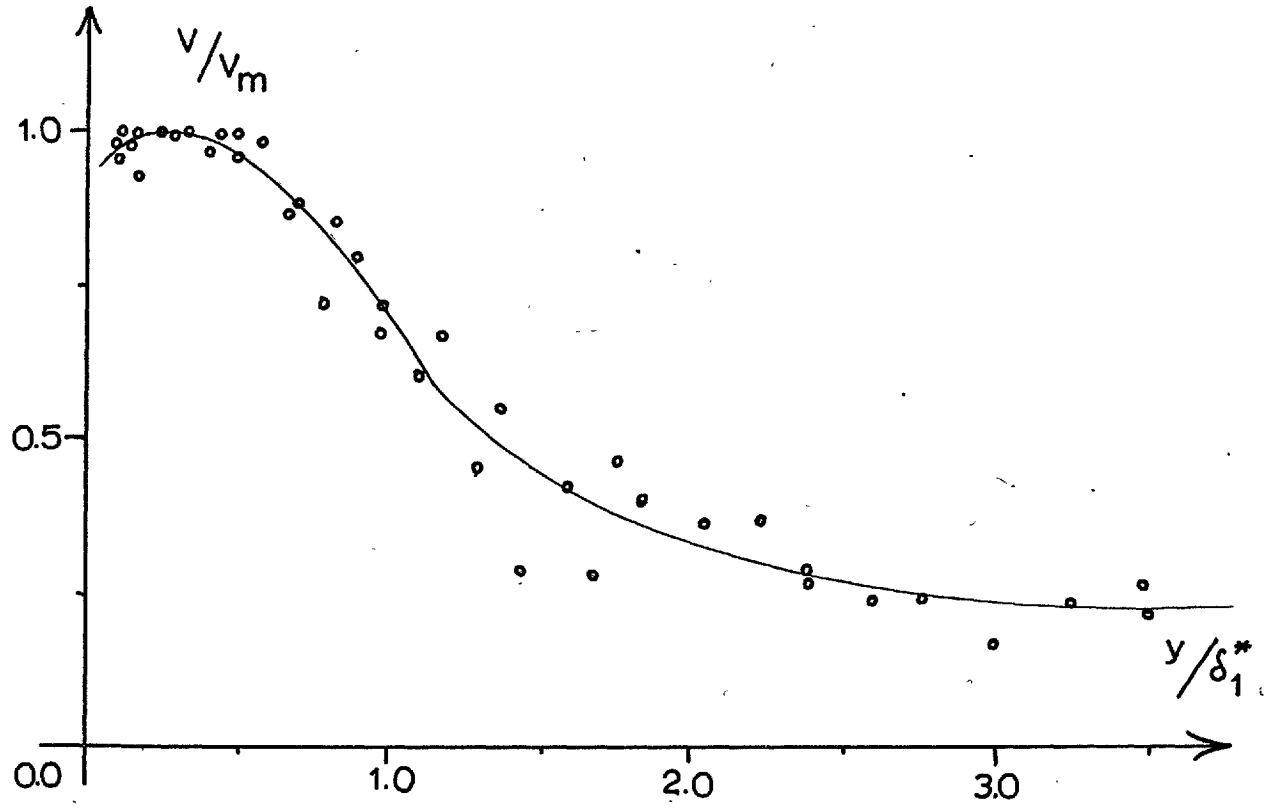


FIG. 4.3-6 JET VELOCITY PROFILES

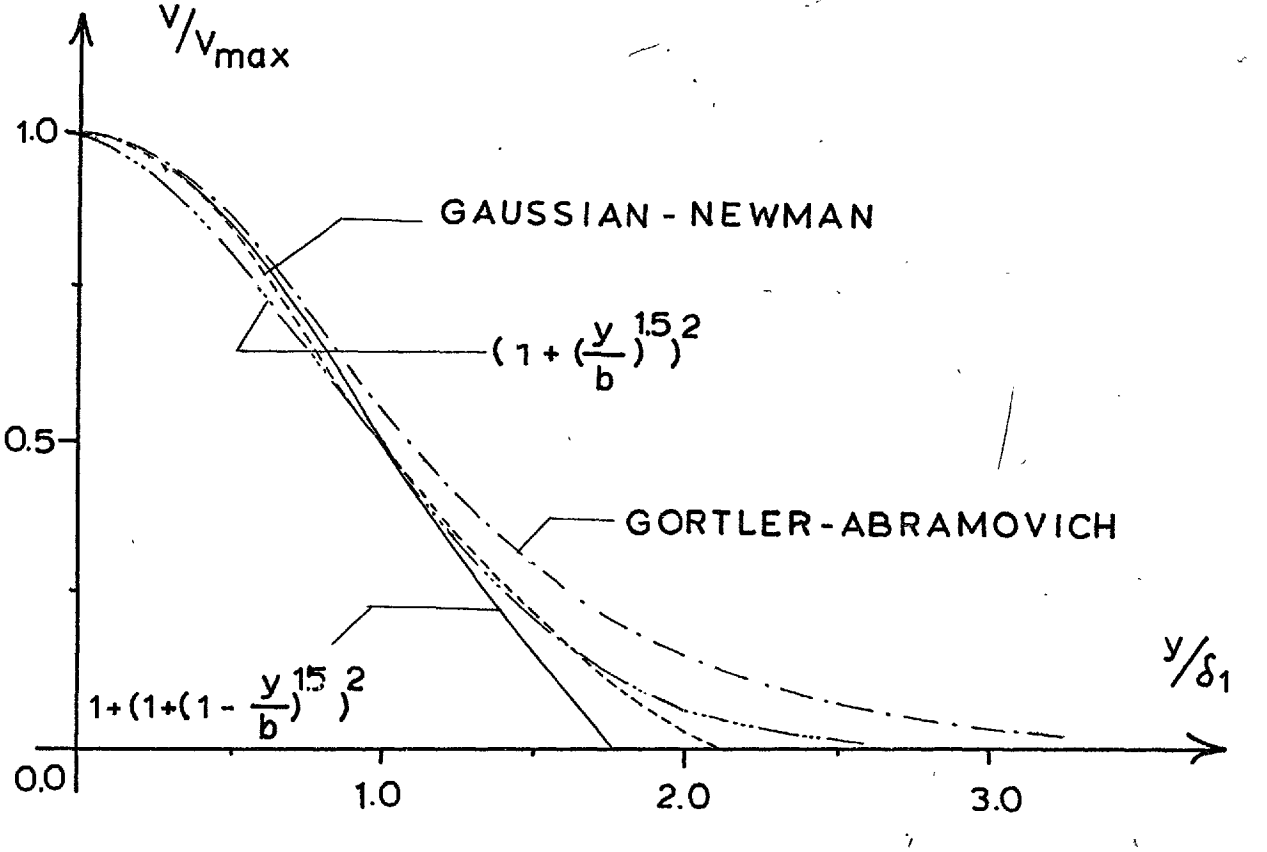


FIG. 4.3-7 ANALITICAL VELOCITY PROFILES

the observed scatter of the points. The same arguement could be applied to the width scale. In spite of the scatter, both values (V_m,δ_1) were found to be reasonable engineering scales as only one experimental section (x_o = 50 cm) did not fit the velocity profile. This is the nearest section to the edge of the dividing wall at which measurements were taken and lies in a region where strong transverse flow was observed. It can also be argued that the turbulent flow is not fully established at this cross section (x_o/d_o = 2.5), and therefore the velocity is unlikely to conform to the universal profile of velocity. Experimental errors in the measurement of the velocity at that section due to the three-dimensional nature of the flow is also possible.

In the analysis of two-dimensional free jets spreading throughout a co-flowing stream, Abramovich (1) plotted the velocity profiles in terms of dimensionless value of excess velocities ($V - U_H$), (see Equation 4.2-22). As characteristic width of the jet (b) he used the distance (b_1) between the axis and the point at which the velocity difference is half its maximum ($V_1 - U_H = 0.5(V_m - U_H)$). The distribution function $f(y/b_1)$ is the same as in a plane submerged jet (1), and the Gaussian normal probability function is very often chosen to represent the velocity profile in submerged jets (13,41,52,58)

$$\frac{V}{V_m} = \exp(-0.693(\frac{y}{b_1})^2) \qquad \ldots (4.3\text{-}4)$$

Abramovich (1) suggested two other simple expressions for the velocity profiles in the main region of a two-dimensional jet with and without an

external flow

$$\frac{V - U_H}{V_m - U_H} = (1 - (\frac{y}{b})^{1.5})^2 \qquad \ldots (4.3\text{-}5)$$

and

$$\frac{V - U_H}{V_m - U_H} = 1 - (1 - (1 - \frac{y}{b})^{1.5})^2 \qquad \ldots (4.3\text{-}6)$$

where (b) is the half thickness of the jet. The velocity profile of Equation 4.3-5 corresponded to a somewhat larger thickness of the jet than the profile of Equation 4.3-6.

Görtler's theoretical velocity profile for a two-dimensional turbulent jet diffusing in a medium at rest is given in Equation 4.2-16. Using Newman's values (52) of ($\theta = 8.46$) and ($b/x = 0.104$), the expression for the velocity profile is approximately,

$$\frac{V}{V_m} = \text{sech}^2(0.88 \frac{y}{\delta_1}) \qquad \ldots (4.3\text{-}7)$$

The velocity profiles corresponding to Equations 4.3-4, 4.3-5, 4.3-6 and 4.3-7 were calculated, and the results are presented in Appendix (H), and plotted in Fig. 4.3-7. The profiles are very similar in the central region of the jet, but the Newman-Görtler profile and the Gaussian distribution have the advantage of being asymptotic profiles.

Two simple models of the jet diffusing in the flume, which is assumed to be two-dimensional, will be discussed now. To start with, it will be assumed that the flow in the flume is similar to half a jet diffusing

in a uniform stream. Among other things, this model implies that the wall of the flume is a plane of symmetry of the plane jet. In the second model the flow pattern will be assumed equivalent to a wall-jet, which is a more realistic assumption, but in this case, only the flow characteristics in the free-mixing region of the jet will be investigated. Excess velocity profiles ($V - U_H$) were calculated from the mean velocity of the uniform stream ($U_H = 22.8$ cm/s), and also the ratio of excess velocity to the maximum value of excess velocity measured at the section. The results are plotted in Fig. 4.3-8, but no improvement in the similarity profile was found. Some of the values of the excess velocity ratio (30%) were negative (points where the velocity was smaller than the uniform velocity due to the resistance offered by the left wall of the flume), and the scatter of points was bigger than before, especially in the zone of negative velocity ratios.

A better excess velocity profile was found (Fig. 4.3-8) when the value of the minimum velocity (V_{min}) measured at ($y = 72$ cm), in each cross-section, was used to calculate the excess velocity ($V - V_{min}$) of the points in the section. The excess velocity ratios, calculated from ($V_m - V_{min}$), were always positive or zero, and the velocity profile tended asymptotically to zero. The agreement between Görtler velocity profile (Equation 4.3-7), and the experimental points was quite satisfactory, especially if the profile was shifted from the wall by $0.3(y/\delta_1)$. This artifice is equivalent to assume that the boundary layer displacement thickness is about $0.3(y/\delta_1)$. This observation suggested an analysis of the flow as a wall-jet.

The flow pattern of a wall-jet can be divided into an outer region

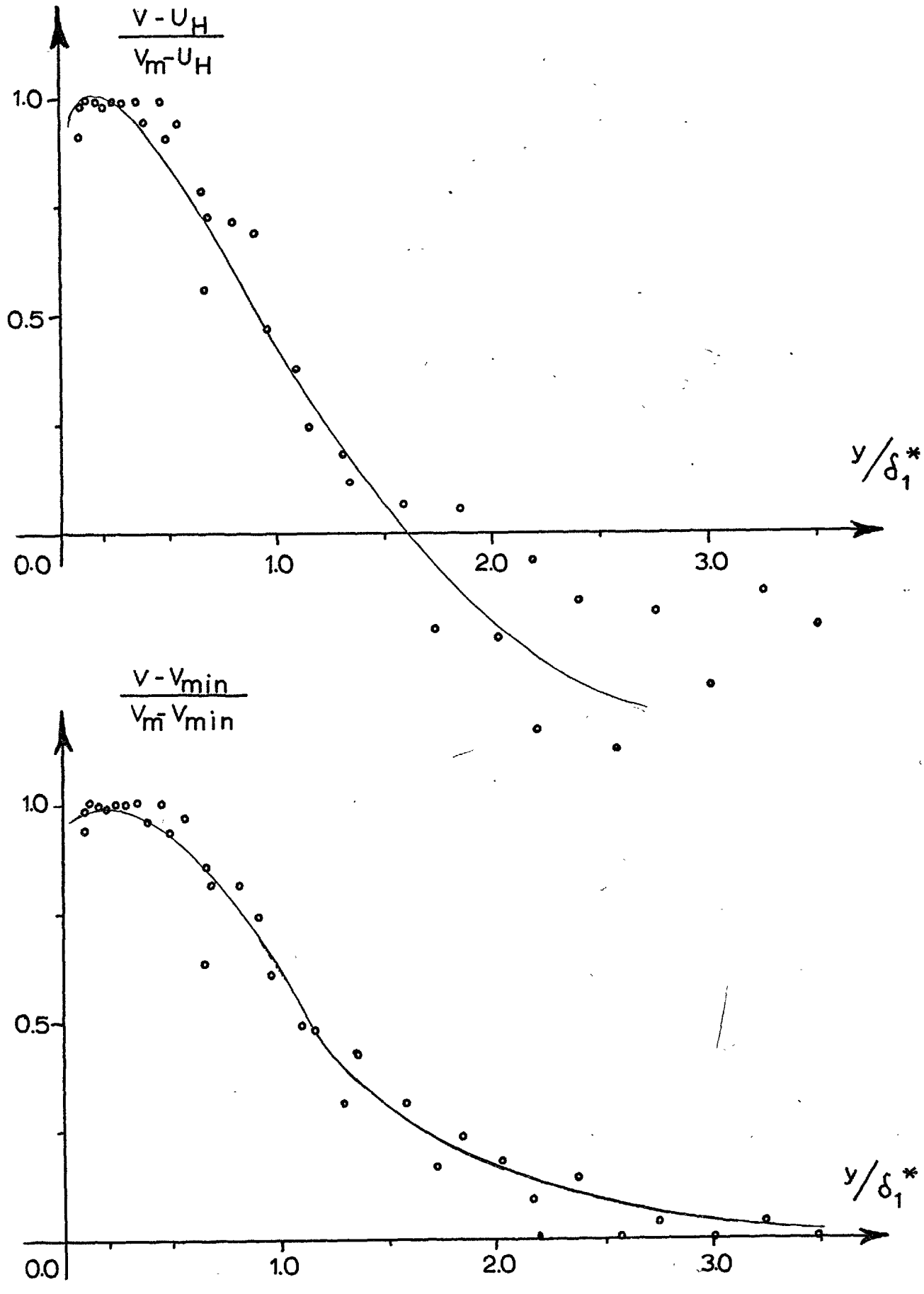


FIG. 4.3-8 EXCESS VELOCITY PROFILES

of free mixing flow and an inner region, near the wall, where the flow is controlled by the growth of the wall boundary layer (Section 4.2.3). Kruka and Eskinazi (50) investigated the similarity conditions in both regions of a wall-jet in a uniform stream. In the inner layer the maximum velocity (V_m) and its location (δ_o) reduced the mean velocity to a universal boundary layer velocity profile. (V_m) varied with the longitudinal distance (x) to a power which was a function of free stream to jet velocity ratio. The boundary layer thickness was found to be proportional to ($x^{4/5}$) (45,50), and the corresponding width scale (δ_o) independent of free stream to jet velocity ratio.

$$\delta_o = 0.0109\, x \qquad \ldots (4.3\text{-}8)$$

In the free-mixing region of the jet, the maximum excess velocity ($V_m - U_H$) and a characteristic half width ($\delta_1 - \delta_o$) were used as scales to find the similarity conditions in the flow. (δ_1) was the distance from the wall to a point in the cross-section where the excess velocity is half its maximum value.

In order to compare the experimental results with the equivalent conditions in a two-dimensional wall-jet, the distance to the shear boundary of the jet ($y - \delta_o$) had to be calculated, and the width of the wall region (δ_o) was estimated by Equation 4.3-8. The distance to the pole of the jet (x_o) was approximately ($x = x_o + 400$ cm). The results were plotted in ~~three~~ two sets of velocity profiles (Fig. 4.3-9) and they fit better a similar velocity profile than the corresponding results presented for half a free jet diffusing in a parallel stream. In Fig. 4.3-9, the experimental points with a positive excess velocity ratio fit a Gaussian

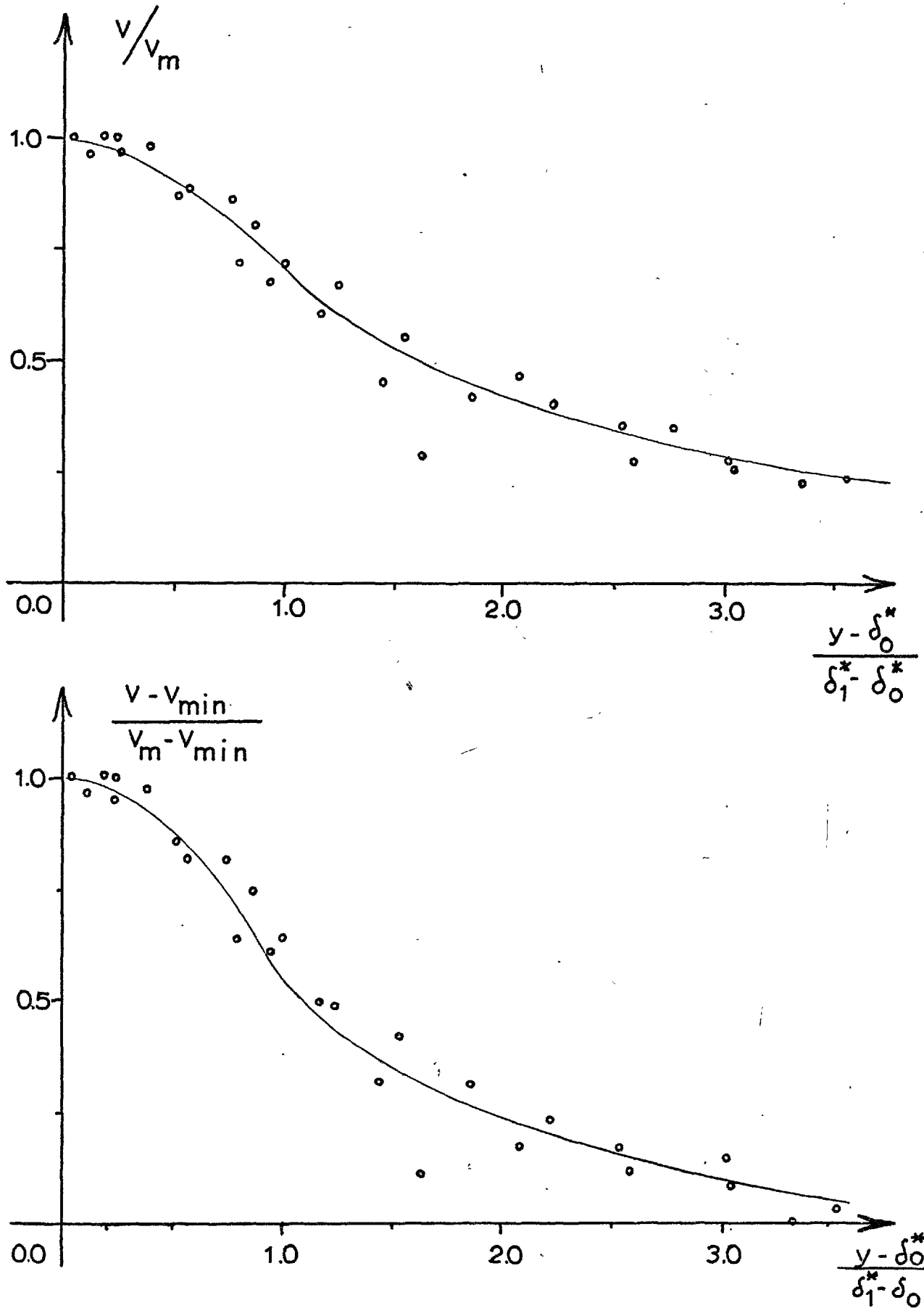


FIG. 4.3-9 WALL-JET VELOCITY PROFILES

curve. In Fig. 4.3-9 , where (V_{min}), (the minimum velocity measured at each cross-section) was used to calculate the excess velocity, the experimental points fit a Görtler-Newman profile.

4.3-4 - An Engineering Solution

The rate of growth of the jet issuing from the sluice gate and diffusing in the flume was calculated in Section 4.3-1 as,

$$\frac{\delta_1^*}{b_o} = 0.70 + 0.035 \frac{x_o}{b_o} \qquad \ldots (4.3\text{-}9)$$

From this equation the virtual pole of the turbulent jet can be estimated (x_s = 400 cm). In this section the asterisk (*) will be used with quantities calculated through empirical equations developed from the experimental results.

A simple expression for the decay of the maximum velocity was found to be (see Fig. 4.3-5)

$$V_m^* = 90 - 2 \cdot x_o^{\frac{1}{2}} \qquad \ldots (4.3\text{-}10)$$

This equation is not dimensionless and (V_m^*) is expressed in (cm/s) and (x_o) in (cm). The point of maximum velocity separating the wall region and the free-mixing region of the flow and (δ_o^*) can be calculated from Equation (4.3-8),

$$\delta_o^* = 0.0109(x_o + 400 \text{ cm}) \qquad \ldots (4.3\text{-}11)$$

The maximum velocity (V_m^*) was used to draw a new set of velocity profiles. The results are plotted in free jet form in Fig. 4.3-10. The velocity profile tends asymptotically to a value of $U_H/V_m^* = 0.2$ in the region of the uniform velocity of the parallel stream. Three regions of flow were observed in the discharge of the sluice gate in a parallel uniform stream: a wall region confined to approximately 30% of the characteristic width of the jet ($\delta_o^*/\delta_1^* = 0.31$)(under the particular experimental conditions), a free-mixing region of turbulent flow, where the universal velocity profile could be represented by an exponential curve,and an outer part of the jet where the velocity profile tends towards the uniform velocity of the stream into which the sluice discharge was merged.

Finally, the results are also plotted, in terms of the excess velocity profile of a free jet diffusing in a parallel stream in Fig. 4.3-11. The excess velocity ($V - U_H^*$) was calculated from the experimental value ($U_H^* = 0.2V_m$) observed in Fig. 4.3-10. A simple exponential expression,

$$\frac{V - U_H^*}{V_m^* - U_H^*} = \exp\left(-0.4\left(\frac{y}{\delta_1}\right)^2\right) \qquad \ldots (4.3\text{-}12)$$

was used to fit the experimental results. Good agreement was observed among the measurements carried out in the flume at different cross-sections of the flow, and Equation 4.3-12, which demonstrated that similarity conditions existed in the flow of the fast sluice discharge, merged with a uniform stream investigated for this research work.

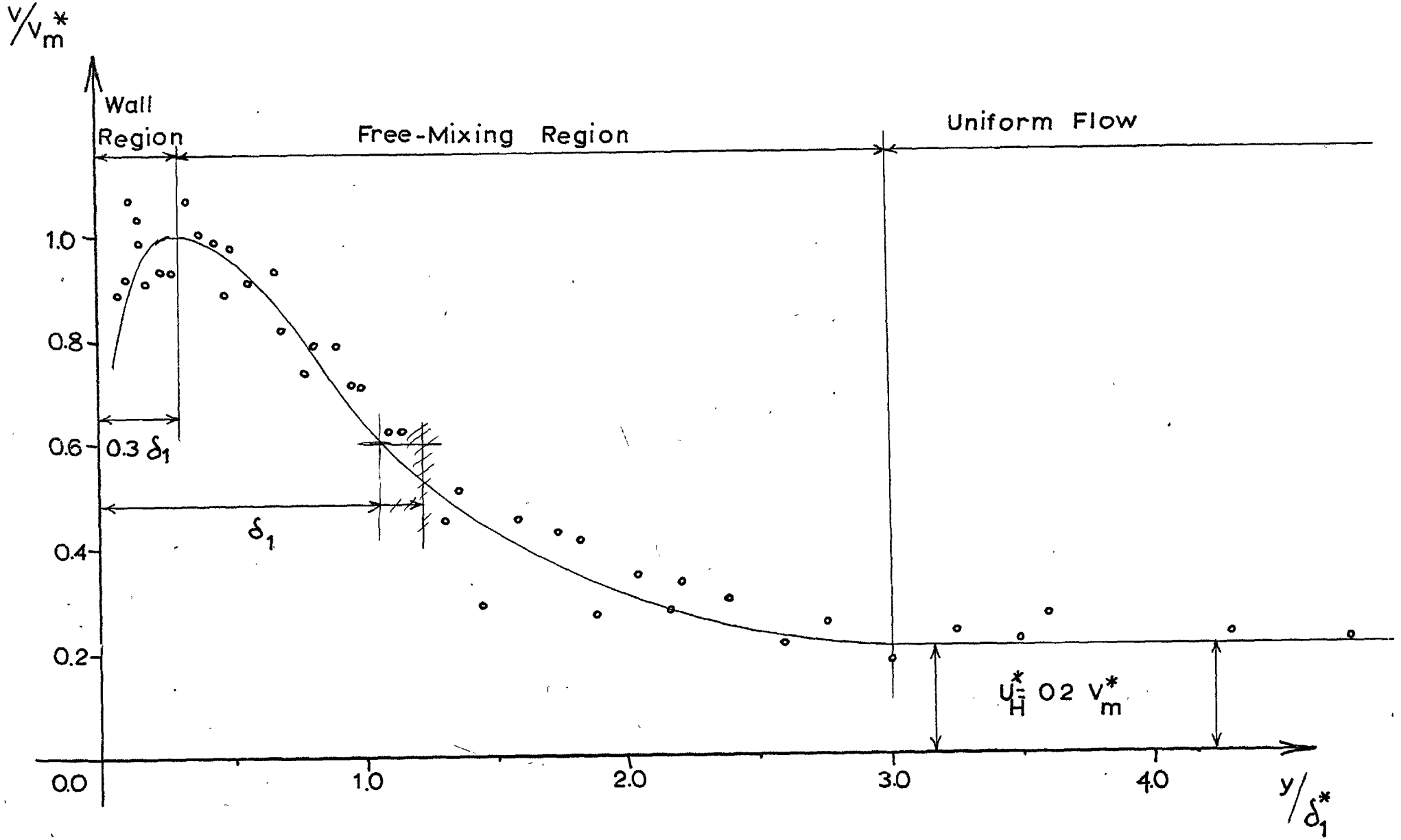


FIG. 4.3-10 SLUICE JET FLOW

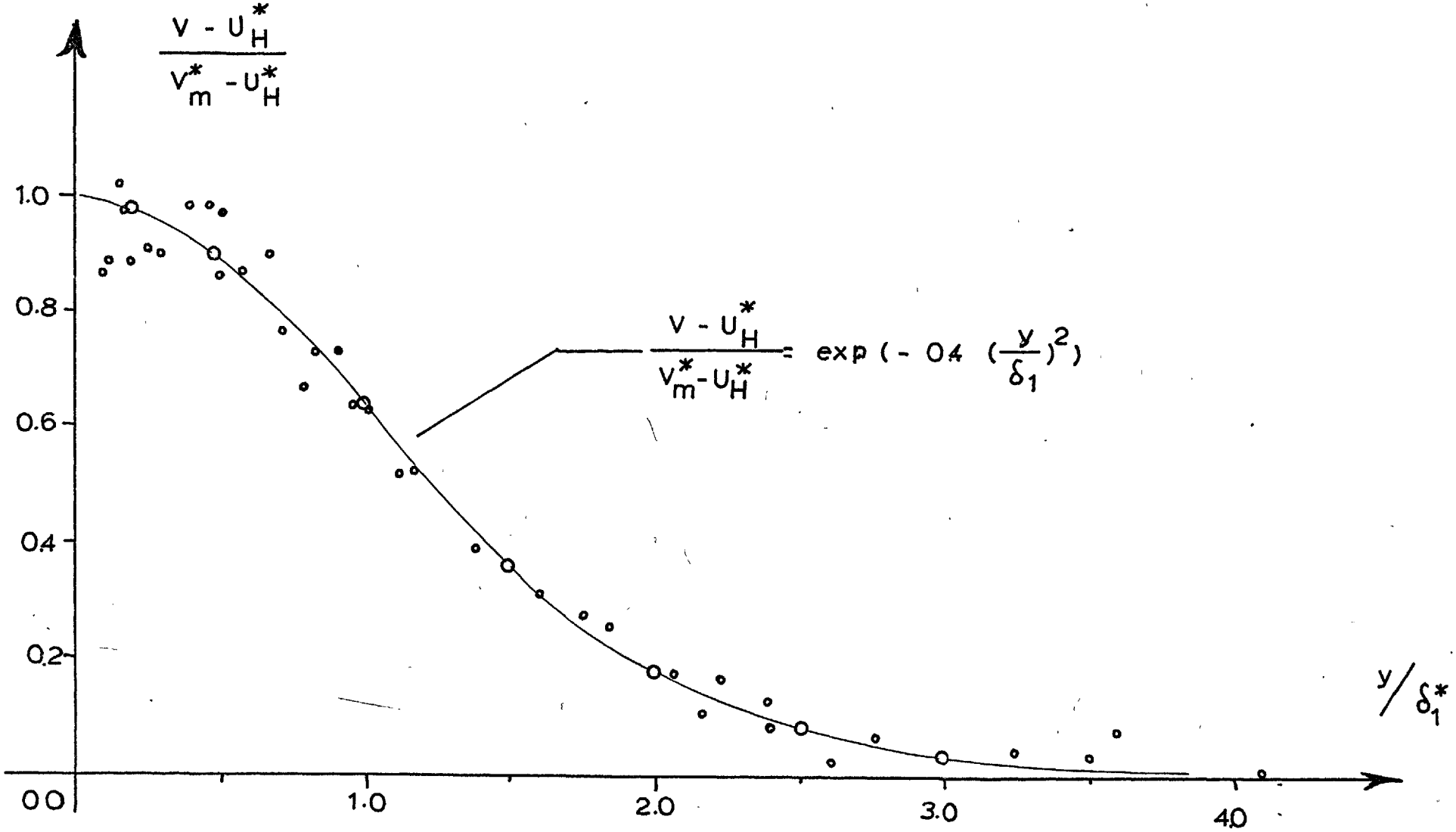


FIG 4.3-11 EXCESS VELOCITY PROFILE

V - SUMMARY OF RESULTS AND CONCLUSIONS. SUGGESTIONS FOR FUTURE RESEARCH WORK.

An investigation into the flow of a sluice gate discharge merging with a deeper and uniform stream flowing in the same direction has been recorded in the preceding chapters. The experimental work was concerned with the particular characteristics of the hydraulic jump forms and the sluice jet diffusing downstream in the flume. A summary of the results and conclusions reached in this study are now presented:

(1) Three basic forms of the hydraulic jump were observed in the flow patterns of the merging streams. For the same initial conditions of the supercritical stream increasing the tail-water level resulted in first oblique, then normal and finally submerged forms of the jump.

(2) The tail-water levels (d_{23}) required in the formation of normal jumps inside or at the abrupt expansion of the sluice channel were smaller than the conjugate depth ($\bar{d}_1$) of the classical two-dimensional hydraulic jump. This effect is attributed to the spatial characteristics of the jump and the formation of side eddies.

(3) The existing empirical equations to predict the depth ratio in normal hydraulic jumps at an abrupt expansion of rectangular channels were reviewed (Fig. 3.2-5). The width expansion ratio (b/B) of the channels (Kuznetzow and Rajaratnam) and a depth parameter (d_1/b) (introduced by Unny) were used to correlate the particular experimental results of each author. In the range of Froude numbers tested (Fr_1 = 2.0 to 6.0), the disagreement among the empirical equations is important (up to 100%)

and the present measurements are better represented by a Unny type of curve (Equation 3.2-6).

(4) The experimental apparatus was inadequate to measure the characteristics of oblique jumps due to the three-dimensional nature of the jump and the interference of the side wall of the flume with the oblique front of the jump.

(5) The effect of a uniform stream on the hydraulic jump was small (an increase of the order of 10% in the downstream depth for an increase in the uniform stream Froude number from zero to 0.6). However, the uniform stream affected the diffusion of the jet (reducing its rate of growth by more than 60%) and eliminated the waves travelling downstream in the flume.

(6) A linear relationship was derived (Equation 3.3-1) to relate the increasing downstream depth of the normal jumps with the Froude number of the two-merging streams (Fr_1 and Fr_2). It was also found that the ratio of the downstream depth of the jump (d_{23}) to the conjugate depth ($\bar{d}_1$) of the equivalent two-dimensional jump decreased from 85% to 63% when the Froude number of the sluice stream (Fr_1) was increased from 2.3 to 4.6. Both results are valid for the particular conditions of the tests and the channel width ratio of 0.264, but similar behaviour of the jumps is expected in other conditions or in a full-scale model.

(7) Scale effects were investigated in the depth of the fast stream (d_1). It was found that d_1 should be at least 3.0 cm in order to avoid the

undesirable scale effects due to the growth of the flume bed boundary layer.

Velocity measurements taken in the flow of the two merged streams with a Pitot-static tube and a mini-current meter showed that the flow conditions downstream in the flume were approximately two-dimensional. The propeller meter proved to be a more sensitive and reliable instrument in the range of velocities from 10 to 80 cm/s. Velocity profiles drawn at different cross-sections of the flow were used to calculate the rate of growth and the decay of the maximum velocity of the sluice jet. The similarity of the velocity profiles was also investigated. The characteristics of the diffusing jet were compared with equivalent results on other two-dimensional turbulent jets and the following conclusions were drawn:

(8) A simple linear equation to predict the growth of the jet was produced (Equation 4.3-9). The rate of growth of the jet (m) was 0.035 and its effective width was 70% of the actual width of the sluice channel which is explained as a three-dimensional effect of the deeper water of the main channel flowing across the shallower water of the fast jet at the channel exit section.

(9) The rate of growth of the diffusing jet is 66% and 46% smaller than the same value of a two-dimensional turbulent free jet or a wall-jet, respectively, both of them diffusing in a medium at rest. This reduction in the jet growth was due to the effect of the uniform stream. The experimental points are in good agreement with the predictions of

Abramovich and Patel on free jets and wall-jets diffusing in a uniform stream. It seems that the left wall of the flume had little effect in the diffusion of the jet.

(10) A square root law was investigated (Equation 4.3-10) for the decay of maximum velocity of the sluice jet, but since the equation is not dimensionless the results are only valid in the context of this research. It was attempted to compare the experimental points with the results of Albertson et al in submerged jets, and Sigalla in wall-jets, but it was found difficult to find an adequate scale for velocity (U_o).

(11) Several sets of velocity profiles were calculated to investigate the best correlation for the velocity measurements. Similarity conditions among the velocity profiles in the flow of the fast sluice discharge merging with a uniform stream were found. Three different regions of flow were observed inside the flume: (a) a wall region confined to approximately 30% of the characteristic width (δ_1) of the jet; (b) a free mixing region of turbulent flow where the velocity profile could be represented by an exponential curve (Equation 4.3-12); and (c) an outer region of uniform flow.

(12) The energy dissipated in the normal hydraulic jump formed inside the sluice channel was evaluated in the particular conditions of the jet diffusing tests. The calculations showed that less than 12.8% of the total hydraulic energy transported by the two parallel streams was

dissipated by the jump which is smaller than the equivalent value of energy dissipated (18,7%) in a two-dimensional normal jump with the same initial conditions (d_1=3.0 cm; Fr_1=2.58).

(13) The free surface of the flow was disturbed by waves travelling or standing inside the flume. The undulation was particularly important for their size in the flow patterns with oblique jumps, which were characterised by a system of standing waves crossing the diffusing jet and being reflected, alternately, at the wall of the flume and the shear boundary of the jet.

There is still a need for research work in the general problem of the flow through a channel junction under any conditions of the combining or dividing streams. A few suggestions for the extension of the present work in merging streams will be made:

(a) The analysis of the hydraulic jump forms and the diffusion of the same sluice jet merging with a uniform stream flowing in the opposite direction has still to be attempted.

(b) The generality of the present results can be checked in a similar investigation under different geometry and scale conditions, or extended with a wider range of Froude numbers of the two-parallel streams. A long dividing wall is particularly recommended.

(c) A new study of the characteristics of the oblique jump forms could be made with a sluice channel abruptly expanding in a symmetrical uniform stream.

The so-called oblique jumps investigated by Ippen were controlled by the deflection of a side wall in the flume and the flow downstream of the oblique front of the jump was still supercritical. In the study suggested, the jump would be produced by a difference in depth of the two streams and with control of the downstream water levels it would be possible to get subcritical flow downstream of the jump. It would be instructive to compare such results with those of Ippen.

(d) An investigation into the characteristics of the waves travelling or standing in the free surface of the merged flows, which are important for their size in the flow patterns involving an oblique jump, could well be carried out. The characteristics of the analogy of the standing waves over the diffusing jet with the shock waves of a supersonic jet could also be further investigated.

APPENDIX A - DISCHARGE CALIBRATION CURVES

A.1 - Orifice Plate

The orifice plate was calibrated against a mercury and a water manometer. The results of both calibration tests (Table A.1) were plotted, manometer heads on a semi square root scale (against discharge), and straight lines were fitted to the experimental points. Simple coefficients for the straight lines were calculated and the agreement between the measurements and the simple empirical equation was good (Fig. A-1). Discharges up to 9.5 l/s were calibrated against the water manometer, and the straight line fitted corresponds to the equation

$$Q_{OR} = 0.98 \ (\Delta h_{H_2O})^{\frac{1}{2}}$$

A mercury manometer was used to measure discharges ranging from 6.9 l/s to 27.3 l/s

$$Q_{OR} = 3.43 \ (\Delta h_{Hg})^{\frac{1}{2}}$$

In both equations discharges are expressed in litres per second (l/s), and manom eter heads in centimetres (cm).

A.2 - Check in the Venturi Meter Calibration Curve

The calibrated discharges of the orifice plate (Q_{OR}) were used to find the depth-discharge curve of the weir at the downstream end of the flume (Fig.A-2). The corresponding heads of water over the crest of the weir (H) were measured by a point gauge at (P_4). Results of these tests are presented in Table A.2. Eight points of the existing calibration curve

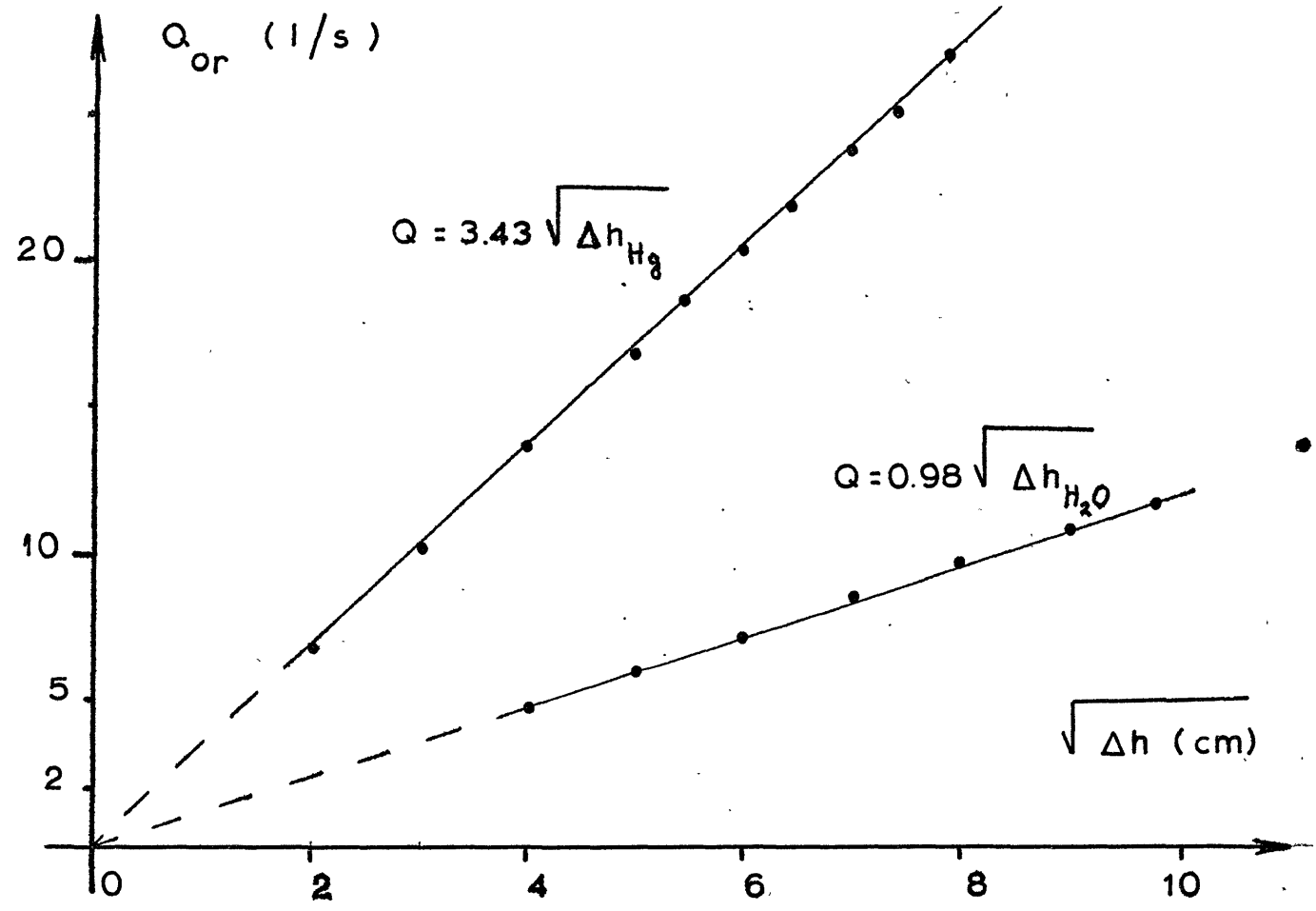


FIG. A - 1 ORIFICE PLATE CALIBRATION CURVES

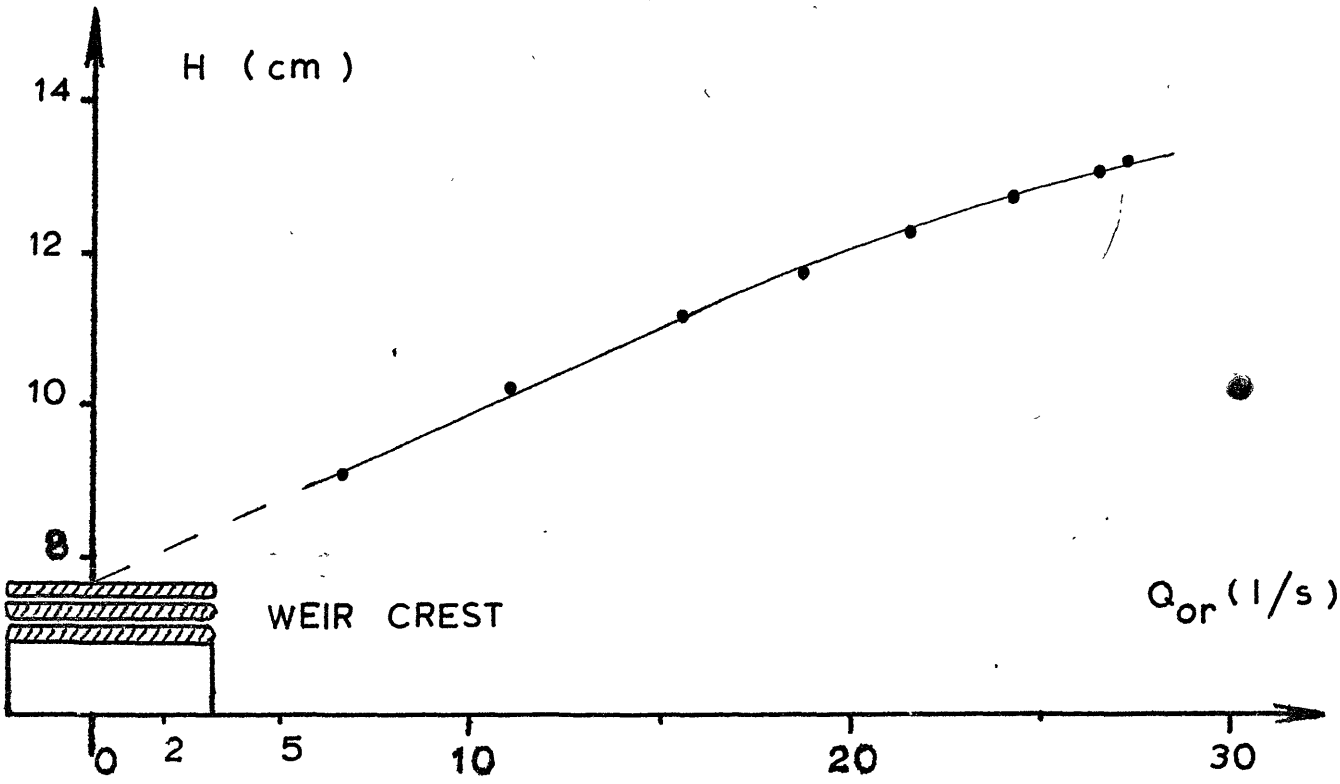


FIG. A - 2 RODS WEIR DEPTH-DISCHARGE CURVE.

TABLE A.1 - RESULTS OF ORIFICE CALIBRATION TESTS

TIME (sec)	Δh (cm)	ΔL (cm)	VOL (m^3)	VOL/TIME (l/s)	$(\Delta h)^{\frac{1}{2}}$ ($cm^{\frac{1}{2}}$)
		MANOMETER FILLED WITH MERCURY			
1033.5	3.9	30	7.08	6.85	1.97
1386.8	8.8	60	14.16	10.21	2.97
1027.6	16.1	60	14.16	13.78	4.01
1107.1	24.7	80	18.88	17.05	4.97
1036.3	29.6	82	19.35	18.67	5.44
918.9	35.7	80	18.88	20.55	5.97
856.5	41.1	80	18.88	22.04	6.41
791.1	48.3	80	18.88	23.87	6.95
743.8	54.5	80	18.88	25.38	7.38
691.2	63.1	80	18.88	27.34	7.49
		MANOMETER FILLED WITH WATER			
1217.3	15.7	20	4.72	3.88	3.96
963.7	25.4	20	4.72	4.90	5.04
819.3	35.3	20	4.72	5.76	5.94
677.1	50.0	20	4.72	6.97	7.07
903.5	64.5	30	7.08	7.84	8.03
809.5	81.6	30	7.08	8.75	9.03
719.1	96.3	29	6.84	9.52	9.81

Notes: (1) Δh-manometer head;

(2) ΔL-depth of water measured in the volumetric tank;

(3) cross-section area of the volumetric tank - 23.6 m^2;

(4) tests carried out between 3/1/72 and 8/1/72.

TABLE C.1 (contd.)

(x_o)	390		530		680	
y	V	Q_x	V	Q_x	V	Q_x
3	46.6	1.82	39.3	1.53	37.0	1.44
8	46.9	2.59	40.8	2.23	39.4	2.15
16	45.8	2.50	39.3	2.15	43.2	2.36
23	40.1	3.44	35.9	3.08	37.0	3.17
38	25.8	3.42	27.3	3.62	35.7	4.73
57	17.1	2.27	18.8	2.49	25.0	3.31
72	10.8	1.01	14.7	1.38	18.3	1.71
Σ		17.02		16.48		18.87
(18.0) : ΣQ_x		1.058		1.092		0.954

(x_o)			190		280	
y	Δy	A_y	V	Q_x	V	Q_x
3	5	39.0	63.2	2.46	55.9	2.18
8	7	54.6	63.4	3.46	54.8	2.99
16	7	54.6	50.2	2.74	50.7	2.77
23	11	85.8	37.7	3.23	40.3	3.46
38	17	132.6	22.1	2.93	25.1	3.33
57	17	132.6	12.1	1.60	13.9	1.84
72	12	93.6	6.0*	0.56	4.9	0.46
Σ	76	592.8		16.98		17.03
(18.0) : ΣQ_x				1.060		1.057

Note: (1) 6.0* - averaged value.

(2) mini-current meter velocities in the last table.

 OUT OF ORDER! (see 138)

of the Venturi meter were checked against the depth discharge curve of the weir (Table A.3), and good agreement was found between these points and the simple equation calculated from Gill's (65) results (Fig. 2.3-1) being the maximum difference 2.79%. A difference of 4.05% was also found at the highest discharge, but this difference was disregarded because the discharge of the weir was extrapolated from the depth discharge curve.

APPENDIX B - SCALE EFFECTS IN THE DEPTH OF THE FAST STREAM

According to Schlichting (14), the boundary layer thickness variation in turbulent flow is given by the equation

$$\frac{\delta}{l} = 0.37 \left(\frac{U_\infty \, l}{\nu}\right)^{-1/5} = 0.37 \, (Re)^{-1/5}$$

The thickness of the boundary layer in the fast stream was calculated assuming l to be the length of the dividing wall (0.10 m), U_∞ the uniform velocity of the stream (U_1), and ν the kinematic viscosity of the water at 20°C (1.01×10^{-6} m^2/sec). The thickness of the boundary layer in flows with different depths (d_1 = 2.0; 2.6; and 3.0 cm), but all of them with the same (Fr_1 = 4.8), was calculated. A constant value of 0.32 cm was found in the three cases. For flows with depths of 2.0 and 3.5 cm and a constant (Fr_1 = 2.2), the thickness was 0.37 and 0.35 cm, respectively.

A complete list of the results of the tests is given in Table B.1, where the symbols are:

- d_{SL} - aperture of the sluice gate
- Q_1 - discharge of the orifice plate
- d_1 - depth of the fast stream
- d_2 - depth in the wider channel at (P_1)
- d_{23} - characteristic downstream depth of the normal jump
- U_1 - uniform velocity of the fast stream
- Fr_1 - Froude number of the fast stream
- Q_2=0 - no uniform stream
- NOR - normal hydraulic jump
- Su-Ob - the characteristic depth of the normal jump was estimated

TABLE B.1 - SCALE EFFECTS IN THE DEPTH OF THE FAST STREAM

JUMP (form)	d_{SL} (cm)	Q (l/s)	d_1 (cm)	d_2 (cm)	d_{23} (cm)	U_1 (m/s)	Fr_1 -	$\frac{d_{23}}{d_1}$ -	DATE
Su-Ob	6.3	17.0	3.8	11.4	11.1	2.24	3.67	2.92	19/3/73
Su-Ob		12.5		9.2	9.1	1.64	2.69	2.40	19/3/73
NOR		10.6		8.5	8.4	1.40	2.29	2.21	20/3/73
Su-Ob		14.2		10.0	9.9	1.87	3.06	2.60	1/6/73
Su-Ob		15.6		10.2	10.0	2.06	3.37	2.63	1/6/73
Su-Ob	5.0	11.6	3.0	8.9	8.7	1.93	3.56	2.90	30/3/73
NOR		6.8		6.6	6.6	1.13	2.08	2.20	5/4/73
Su-Ob		15.7		10.5	9.7	2.62	4.83	3.24	6/4/73
Su-Ob		14.1		9.6	9.2	2.35	4.34	3.07	11/4/73
NOR		9.5		8.1	8.0	1.58	2.92	2.67	12/4/73
NOR		8.3		7.1	7.0	1.38	2.54	2.34	2/5/73
Su-Ob		11.3		9.0	8.8	1.88	3.46	2.94	17/5/73
NOR	5.8	8.9	3.5	7.3	7.3	1.27	2.17	2.09	22/5/73
Su-Ob		14.1		9.8	9.6	2.01	3.43	2.74	22/5/73
Su-Ob		17.9		11.1	10.8	2.56	4.37	3.10	22/5/73
Su-Ob		16.1		10.6	10.3	2.30	3.93	2.93	23/5/73
Su-Ob		12.8		9.3	9.2	1.83	3.12	2.64	23/5/73
NOR		10.9		8.3	8.2	1.56	2.66	2.34	23/5/73
Su-Ob	4.2	13.8	2.6	10.3	9.8	2.66	5.26	3.81	24/5/73
Su-Ob		10.9		8.9	8.6	2.10	4.16	3.42	24/5/73
NOR		5.65		5.9	5.8	1.09	2.16	2.23	24/5/73
NOR		7.75		7.4	7.2	1.49	2.95	2.77	25/5/73
Su-Ob		9.5		8.5	8.3	1.83	3.62	3.19	25/5/73
Su-Ob		12.2		9.6	9.2	2.44	4.83	3.54	25/5/73
NOR	3.2	5.4	2.0	6.1	6.1	1.35	3.05	3.05	31/5/73
NOR		7.3		7.7	7.6	1.83	4.13	3.80	31/5/73
Su-Ob		9.75		9.1	8.9	2.44	5.51	4.45	31/5/73
Su-Ob		10.8		9.4	9.0	2.70	6.10	4.50	1/6/73
Su-Ob		8.5		8.4	8.2	2.12	4.78	4.20	1/6/73
NOR		6.25		6.8	6.6	1.56	3.52	3.30	1/6/73
NOR		3.9		4.8	4.8	0.98	2.22	2.40	1/6/73

APPENDIX C - VELOCITY MEASUREMENTS TAKEN WITH A PITOT-STATIC TUBE

The characteristics of the two merging streams:

(1) Slow stream: 7.8 cm deep; 54 cm wide; mean velocity - 22.8 cm/s; discharge - 9.6 l/s (Δh_{VE} = 1.0 cm).

(2) Fast stream: 3.0 cm deep; 20 cm wide; mean velocity - 140 cm/s; discharge 8.4 l/s (Δh_{OR} = 6.0 cm).

(3) The two parallel streams are confined by the walls and bed of the metal flume, which is 76 cm wide.

All the symbols used below have been defined in Chapter 2, and the values of the tables represent the measured manometer heads.

C.1 - The Diffusion of the Jet

Test 1 - Date: 6 July 1973
h_{SL} : 13.6 cm
d_2 : 7.7 cm

Test 2 - Date: 9 July 1973
h_{SL} : 13.7 cm
d_2 : 7.6 cm

$\frac{y}{x_o}$	3	16	23	8	38
50	2.6 2.61*	1.6 1.63*	0.25 0.39*	3.15 2.87*	0.29 0.42*
100	2.7 2.47*	1.7 1.72*	0.6 0.73*	2.65 2.59*	0.30 0.40*
280	2.0	1.55	1.05 0.94*	2.0	0.48
680	0.85	1.1	0.85	0.95	0.80

Notes: (1) - x_o and y are in cm;
(2) - Δh^* - repeated measurements on 6/8/73.

Test 3 - Date: 11th July 1973

h_{SL} : 13.8 cm

d_2 : 7.7 cm

x_o \ y	3	8	16	23	38	57	72
190	2.25	2.12	1.22	0.94 0.88*	0.48	0.27	(0.25)

Notes: (1) Δh* - repeated measurement;

(2) (0.25) measurement taken on 31/7/73

Test 4 - Date: 31 July 1973

h_{SL} : 13.5 cm

d_2 : 7.6 cm

x_o \ y	16	23	57	72
50	1.42*	0.39	0.36	0.27
100	1.63*	0.66	0.29	0.26
190	1.40*	0.88	-	0.25
280	1.35*	0.94	0.30	0.20
390	1.21*	-	-	(0.21)
530	1.06*	-	-	(0.26)
680	0.95*	-	0.47	0.32

Notes: (1) Δh* - check in previous measurements;

(2) (0.21) and (0.26) measurements taken on 16/6/73

Test 5 - Date: 16th July 1973

h_{SL} : 13.6 cm

d_2 : 7.7 cm

x_o \ y	3	8	16	23	38	57	72
390	1.26	1.27	1.22	0.97	0.49	0.30	0.21
530	0.94	1.00	0.94	0.81	0.53	0.33	0.26

C.2 - Vertical Velocity Profiles

Position	(z=)	1.0	2.5	3.8	5.0	6.0	7.0	Date
(x_o=)	110	2.31	2.61	2.80	2.96	3.07	3.08	10/7/73
(y=)	8	65.10	69.50	72.10	74.30	75.70	75.80	
	290	1.25	1.56	1.70	1.69	1.74	1.88	18/7/73
	12	46.50	52.60	55.20	55.00	55.90	58.30	
	290	0.29	0.35	0.45	0.45	0.57	0.55	18/7/73
	45	16.80	19.80	24.30	24.30	28.70	28.00	

Notes: (1) the first value is the manometer head in (cm);

(2) the second value is the velocity in cm/s.

TABLE C.1 - CALCULATION OF THE FLOW RATES FROM THE VELOCITY PROFILES

	(x_o)		50		100		280	
y	Δy	A_y	V	Q_x	V	Q_x	V	Q_x
cm	cm	cm^2	cm/s	l/s	cm/s	l/s	cm/s	l/s
3	5	39.0	69.5	2.71	69.1	2.69	60.2	2.35
8	7	54.6	74.8	4.08	69.6	3.80	60.2	3.29
16	7	54.6	53.6	2.92	55.4	3.02	52.4	2.86
23	11	85.8	21.7	1.86	31.6	2.71	40.3	3.46
38	17	132.6	20.3	2.69	19.8	2.62	25.5	3.38
57	17	132.6	20.3	2.69	16.5	2.19	17.1	2.27
72	12	93.6	15.3	1.43	14.7	1.38	9.9	0.93
Σ	76	592.8		18.38		18.41		18.41
18.0 : ΣQ_x				0.979		0.978		0.978

Notes: (1) A_y - elementary area ($A_y = 7.8 \quad \Delta y \ cm^2$);
(2) V - velocity in the middle of area A_y;
(3) Q_x - flow rate through A_y ($Q_x = A_y.V$);
(4) Q_x - flow rate across the section;
(5) The measured flow rate in the flume was 18.0 l/s.
(6) The velocity measurements were taken with a Pitot-static tube.

/contd.....

TABLE A.2 - WEIR DEPTH-DISCHARGE CURVE

Δh_{OR} (cm)	H (cm)	Q_{OR} (l/s)
3.65	9.2	6.55
10.6	10.3	11.2
20.6	11.15	15.6
30.2	11.75	18.8
39.9	12.3	21.7
50.1	12.7	24.3
60.3	13.05	26.6
63.3	13.2	27.3

Notes: (1) Δh_{OR} - orifice manometer head
(2) H - head of water over the crest of the weir
(3) Q_{OR} - $3.43\ (\Delta h_{OR})^{\frac{1}{2}}$

TABLE A.3 - VENTURI METER CALIBRATION CHECK

Δh_{VE} (cm)	H (cm)	Q_{WR} (l/s)	Q_{VE} (l/s)	$1 - \frac{Q_{WR}}{Q_{VE}}$ (%)
1.85	10.7	13.2	13.1	-0.76
3.75	11.7	18.4	18.6	+1.08
4.6	12.1	20.5	20.6	+0.49
5.5	12.4	22.4	22.5	+0.44
6.65	12.8	25.0	24.8	-0.81
7.75	13.1	26.8	26.7	-0.37
8.95	13.5	29.5	28.7	-2.79
13.0	14.3	36.0*	34.6	-4.05*

* extrapolated value

Notes: (1) Δh_{VE} - Venturi manometer head
(2) Q_{WR} - Weir discharge
(3) Q_{VE} - $9.6\ (\Delta h_{VE})^{\frac{1}{2}}$
(4) Tests carried out on 29/2/72 and 1/3/72.

OUT OF ORDER ! (see 130)

APPENDIX D - VELOCITY MEASUREMENTS MADE WITH A MINI-CURRENT METER.

D.1 - Current meter tests

Test 1 - Date : 16 July 1973

Beginning of the test : 14h 40 m

h_{SL} = 13.6 cm; d_2 = 7.7 cm

x_o = 290 cm; y = 16 cm; z = 3.8 cm
(position of the propeller in the flume)

Time	N (revolutions in 10 sec)					$\bar{N}$	$\frac{\bar{N}}{871}$	$1 - \frac{N_{min}}{N_{max}}$
14 h 50 m	897	909	934	846*	878	901	1.034	0.108
55	949*	857	891	966	888			
15 05	888	955*	901	863*	874	909	1.044	0.096
10	891	894	899	933	904			
15 40	911*	884	896	895	863	879	1.009	0.082
45	836*	891	902	874	840			
17 45	880	862	912*	822*	878	871	1.000	0.099
50	847	878	860	890	886			
18 25	867	876	889	907	849	871	1.000	0.090
30	875	848	837*	847	920*			

Note: (1) N - number of revolutions of the propeller read by electronic counter unit in 10 seconds.

(2) $\bar{N}$ - mean averaged value of the ten readings.

(3) N*- maximum (N_{max}) or minimum (N_{min}) values of the readings.

D.2 - Check on the measurements of the Pitot-static tube

Test 2 - Measurements taken at z = 3.8 cm

x_o \ y	3	8	16	23	38	57	DATE
190	1118	1120	875	643	354	178	16/7/73
	63.2	63.4	50.2	37.7	22.1	12.1	
	64.2*	62.1*	45.8	38.5*	25.5*	15.3*	
280	982	961	885	691	410	203	11/7/73
	55.9	54.8	50.7	40.3	25.1	13.9	
	60.2*	62.2*	52.4*	40.3*	25.5*	17.1*	

Notes: (1) first value - number of revolutions of the propeller;
(2) second value - the velocity calculated from a calibration curve (cm/s);
(3) third value - corresponding velocity of the Pitot-static tube (V*);
(4) the measurements at (x_o=190 cm) and (y=3 and 8 cm) were repeated on 6/8/73, and were 1141 and 1133, respectively.

Test 3 - Measurements taken at z = 3.8 cm

y \ x_o	190	280	390	530	680	DATE
16	900	886	825	777	690	31/7/73
	51.6	50.7	47.6	44.9	40.2	
	45.8*	52.4*	45.8*	39.3*	43.2*	
72	80	50	-	-	239	31/7/73
	6.8	4.9	-	-	15.8	
	14.0*	9.9*	10.8*	14.7*	16.3*	

Notes: the same as in Test 2.

D.3 - Velocity measurements at the control sections

Test 4 - The downstream section (x_o= 190 cm)

z \ y	3	8	16	23	38	57	72	DATE
1.0	1018*	948*	720	464	232	134	50	18/7/73
	57.8	54.1	41.9	28.0	15.4	9.9	4.9	
3.8	1118	1130	875	643	354	178	-	16/7/73
	63.2	63.4	50.2	37.7	22.1	12.1		
6.0	1143*	1188*	999	761	477	245	58	18/7/73
	64.6	66.9	56.9	44.0	28.7	16.1	5.3	

Notes: (1) first value - number of revolutions of the propeller;
(2) second value - velocity in cm/s;
(3) N* - values measured on 6/8/73.

Test 5 - The control section in the slow (uniform) stream (x_o= -40 cm)

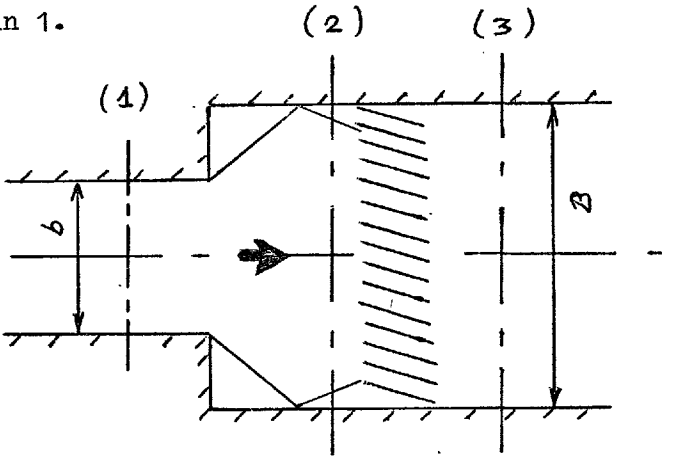
z \ y	1.0	3.8	6.0	DATE
36	368	428	425	6/8/73
	22.8	26.1	26.0	
62	351	423	447	
	22.0	25.9	27.1	

Notes: the same as in Test 4.

APPENDIX E - CRITICAL ANALYSIS ON R-JUMPS (33)

The characteristics of a supercritical stream freely expanding in an abrupt expansion can be predicted by the method of characteristics (62,63,66). As the fast stream expands the depth of the flow gradually decreases and the flow surface assumes a three-dimensional shape. The contour lines of equal depths have smaller ratios of d/d_1 (d_1 is initial flow depth) as an observer moves downstream or transversely to the direction of the flow (62). As the Froude number (Fr_1) increases, the more the contour of constant depth are displaced downstream and transversely (62).

Below an abrupt expansion of a rectangular cross-section channel the supercritical flow does not expand freely, because the fast stream is confined downstream by the side walls of the channel. However, the depth of the flow decreases gradually in the region where the flow is expanding. For sake of simplicity it will be assumed that the expanded supercritical stream at section 2 has a uniform depth (d_2) and consequently the depth ratio (n) is greater than 1.



$$n = \frac{d_1}{d_2} \qquad \ldots (E\text{-}1)$$

From continuity,

$$U_1 \cdot d_1 \cdot b = U_2 \cdot d_2 \cdot B \qquad \ldots (E\text{-}2)$$

Equation 3.2-4, which was derived by Rajaratnam and Subramanya (33) for a R-jump can be written as,

$$\frac{d_2}{d_1} = (0.30 + \frac{b}{B})Fr_1 - 0.85\,\frac{b}{B} + 0.495 \qquad \ldots (E\text{-}3)$$

This equation was derived for width expansion ratios (b/B) of 0.17; 0.33; 0.50; 0.67 and 0.83; and for Froude numbers (Fr_1) varying from 2.2 to 8.9.

The conjugate depth ($\bar{d}_2$) of the flow conditions at section 2 is,

$$\frac{\bar{d}_2}{d_2} = 0.5\ ((1 + 8Fr_2^2)^{\frac{1}{2}} - 1) \qquad \ldots (E\text{-}4)$$

Using equations (E-1) and (E-2) and taking into account that ($\bar{d}_2 = d_3$), the conjugate depth equation can be rewritten in terms of the initial conditions,

$$\frac{d_3}{d_1} = \frac{0.5}{n}\ ((1 + 8Fr_1^2.n^3.(b/B)^2)^{\frac{1}{2}} - 1) \quad \ldots (E\text{-}5)$$

Comparing the results of Equations E-3 and E-5, the value n can be estimated for different expansion ratios and Froude numbers:

(a) For (b/B) = 0.83, n varied from 1.0 (Fr_1=9) to 1.1 (Fr_2=2)

(b) For (b/B) = 0.50, n varied from 1.4 to 1.8

(c) For (b/B) = 0.33, n varied from 2.1 to 3.0

(d) For (b/B) = 0.17, n varied from 4.6 to 8.0

These results showed that the depth ratio (n) was greater when the expanding stream spread in a wider channel, or when the initial Froude number was smaller. Since similar results were observed by Abu-Sayf (62) and the estimated values of n varied between 1.0 and 3.0 for a width expansion ratio (b/B) bigger than 0.33, it seems that the so-called R-jump is just a normal two-dimensional hydraulic jump forming in the wider channel of the ~~from an~~ expanded stream.

APPENDIX F - CALCULATION OF THE MOMENTUM COEFFICIENT IN THE DOWNSTREAM CONTROL SECTION (S_3).

The impulse momentum balance in the control volume defined in Section 4.1.1 was calculated for the following particular conditions of the flow:

$Q_1 = 0.0084\ m^3/s$; $Q_2 = 0.0096\ m^3/s$

$d_1 = 0.030\ m$; $d_2 = d_3 = 0.078\ m$

$b_1 = 0.20\ m$; $b_2 = 0.54\ m$; $b_3 = 0.76\ m$

The values used for the constants were: $\rho = 1000\ Kg/m^3$ and $g = 9.8\ m/s^2$.

Momentum equation

Assuming uniform velocity and hydrostatic pressure distributions at control sections (S_1) and (S_2), the corresponding momentum forces can be calculated,

$$F_i = \rho.Q_i.U_i + \tfrac{1}{2}\rho.g.d_i^2.b_i$$

and, $F_1 = 11.76 + 0.88 = 12.64$ N

$F_2 = 2.19 + 16.10 = 18.29$ N

At sections (S_3), a two-dimensional velocity profile was considered and a momentum correction coefficient (β) introduced to take into account the non-uniformity of the velocity profile,

$$F_3 = 5.47\beta + 22.66 \quad N$$

The momentum coefficient calculated from the momentum-force balance equation was ($\beta = 1.51$);

$$F_3 = F_1 + F_2$$

$$5.47\beta + 22.66 = 12.64 + 18.29$$

Velocity profiles

The momentum coefficient was also calculated from the velocity profiles measured with the Pitot-tube and the propeller meter at control section (S_3). These experimental coefficients, which were designated by (β) with an index (corresponding to the test) to differentiate from the previous value of the momentum coefficient, were calculated by Equation 4.1-4. Three different tests were considered:

(a) a set of twenty-one velocity measurements (seven measurements in each velocity profile taken at three different depths) made with a mini-current meter, giving a three-dimensional velocity distribution at the control section. In Table (F.1) are given all the results.

$$\beta_a = 1.49$$

(b) a set of seven measurements made at half depth of the flow with the current-meter (two-dimensional velocity distribution).

$$\beta_b = 1.48$$

TABLE F.1 - CALCULATION OF THE MOMENTUM AND ENERGY COEFFICIENTS IN THE DOWNSTREAM CONTROL SECTION (S_3).

F.1-1 - Three-Dimensional Velocity Profiles. Current Meter Measurements.

y	Δy	z = 1.0 cm; Δz = 2.0 cm					z = 3.8 cm; Δz = 3.0 cm					z = 6.0 cm; Δz = 2.8 cm				
		A_{yz}	V	VA	V^2A	V^3A	A_{yz}	V	VA	V^2A	V^3A	A_{yz}	V	VA	V^2A	V^3A
cm	cm	cm^2	cm/s	cm^3/s	cm^4/s^2	cm^5/s^3	cm^2	cm/s	cm^3/s	cm^4/s^2	cm^2/s^2	cm^2	cm/s	cm^3/s	cm^4/s^2	cm^5/s^3
					(x 10^3)	(x 10^3)				(x 10^3)	(x 10^3)				(x 10^3)	(x 10^3)
3	5	10.0	57.8	578	33.4	1931	15.0	63.2	948	59.9	3787	14.0	64.6	904	58.4	3774
8	7	14.0	54.1	757	41.0	2217	21.0	63.4	1331	84.4	5352	19.6	66.9	1311	87.7	5869
16	7	14.0	41.9	587	24.6	1030	21.0	50.2	1054	52.9	2657	19.6	56.9	1115	63.5	3611
23	11	22.0	28.0	616	17.3	483	33.0	37.7	1244	46.9	1768	30.8	44.0	1355	59.6	2624
38	17	34.0	15.4	524	8.1	124	51.0	22.1	1127	24.9	550	47.6	28.7	1366	39.2	1125
57	17	34.0	9.9	337	3.3	33	51.0	12.1	617	7.5	90	47.6	16.1	766	12.3	199
72	12	24.0	4.9	118	0.6	3	36.0	5.1*	184	0.9	5	33.6	5.3	178	0.9	5
Σ	76	152.0		3517	128.3	5821	228.0		6505	277.4	14209	212.8		6995	321.6	17207

Note: (1) V = 5.1* - estimated value.

F.1-2 - Two-Dimensional Velocity Profiles. Pitot-tube and Current-Meter Measurements.

y	A_{yz}	Current-meter				Pitot-static tube			
		V	VA	V^2A	V^3A	V	VA	V^2A	V^3A
cm	cm^2	cm/s	cm^3/s	cm^4/s^2	cm^5/s^3	cm/s	cm^3/s	cm^5/s^2	cm^5/s^3
				$(\times 10^3)$	$(\times 10^3)$			$(\times 10^3)$	$(\times 10^3)$
3	39.0	63.2	2465	155.8	9849	64.2	2504	160.8	10323
8	54.6	63.4	3462	219.5	13916	62.1	3391	210.6	13078
16	54.6	50.2	2741	137.6	6907	45.8	2501	114.5	5244
23	85.8	37.7	3235	122.0	4598	38.5	3303	127.2	4897
38	132.6	22.1	2930	64.8	1431	25.5	3381	86.2	2198
57	132.6	12.1	1604	19.4	235	15.3	2029	31.0	474
72	93.6	6.0	562	3.4	20	14.0	1310	18.3	256
$\sum$	592.8		16999	722.5	36956		18419	748.6	36470

a) Momentum coefficient

$$\beta = \frac{\sum V^2 . A_{yz}}{U_3^2 . A_3}$$

b) Energy coefficient

$$\alpha = \frac{\sum V^3 . A_{yz}}{U_3^3 . A_3}$$

(c) the same set of seven values of velocity, but measured with the Pitot-static tube at half depth of the flow (two-dimensional velocity distribution).

$$\beta_c = 1.31$$

APPENDIX G - EVALUATION OF THE ENERGY DISSIPATED INSIDE THE CONTROL VOLUME.

The dissipation of energy inside the control volume (which was 230 cm long and 76 cm wide) was calculated in order to estimate the amount of energy dissipated by the normal hydraulic jump formed inside the sluice channel for the particular flow conditions defined in Section 4.1.1. The specific energy (energy per unit weight) at each control section (S_i) is given by,

$$E_i = d_i + \frac{Q_i^2}{2g(b_i.d_i)^2}$$

The balance of hydraulic energy in the control volume can be written as

$$W_1 + W_2 = W_3 + \Delta W$$

where $W_i = \rho.g.Q_i.E_i$ is the energy of the flow at each control section and ΔW is the hydraulic energy dissipated inside the control volume. Since the velocity distribution at section (S_3) is non-uniform, the specific energy (E_3) had to be corrected by an energy coefficient α defined in the following way

$$\alpha = \frac{\int V^3.dy.dz}{U_3^3.A_3} \simeq \frac{\Sigma \bar{V}_3^3.\Delta A_3}{U_3^3.A_3}$$

$$\text{and } E_3 = d_3 + \alpha \frac{Q_3^2}{2g(b_3.d_3)^2}$$

In the calculation of the energy coefficient ($\alpha = 2.65$), the results of the twenty-one velocity measurements made with the current meter at section (S_3) were used (see Table F.1).

Assuming uniform velocity and hydrostatic pressure distributions at sections (S_1) and (S_2), the hydraulic energy at these sections was, respectively

$$W_1 = \rho.g.Q_1.(E_1) = 82.32\ (0.030 + 0.100) = 10.71 \quad J$$

$$W_2 = \rho.g.Q_2.(E_2) = 94.08\ (0.078 + 0.0027) = 7.59 \quad J$$

The energy at the downstream control section with a two-dimensional velocity profile was

$$W_3 = \rho.g.Q_3.(E_3) = 176.4\ (0.078 + 2.65(0.0047)) = 15.96 \quad J$$

The hydraulic energy dissipated in the control volume was

$$\Delta W = 10.71 + 7.59 - 15.96 = 2.34 \quad J$$

The ratio of energy dissipated inside the control volume to the energy transported by the two parallel streams was,

$$\frac{\Delta W}{W_1 + W_2} = \frac{2.34}{18.30} = 0.128$$

APPENDIX H - SIMILARITY IN THE VELOCITY PROFILES OF THE DIFFUSING JET.

Cross-Section (x_o = 50 cm)

(Characteristic values of the velocity profile)

U_H = 22.8 cm/s (velocity of the uniform stream)

V_m = 74.8 cm/s (maximum velocity measured in the section)

V_{min} = 15.3 cm/s (minimum velocity measured at y = 72 cm)

δ_1^* = 15.8 cm (characteristic width calculated from Eq. 4.3-9)

V_m^* = 76.0 cm/s (maximum velocity calculated from Eq. 4.3-10)

δ_o^* = 4.9 cm (growth of the boundary layer from Eq. 4.3-11)

y	V	$\frac{y}{\delta_1^*}$	$\frac{V}{V_m}$	$V-U_H$	$\frac{V-U_H}{V_m-U_H}$	$V-V_{min}$	$\frac{V-V_{min}}{V_m-V_{min}}$	$\frac{y-\delta_o^*}{\delta_1^*-\delta_o^*}$	$\frac{V}{V_m^*}$
cm	cm/s	-	-	cm/s	-	-	-	-	-
3	69.5	0.19	0.93	46.7	0.90	54.2	0.91	-	0.91
8	74.8	0.51	1.00	52.0	1.00	59.5	1.00	0.28	0.98
16	53.6	1.01	0.72	30.8	0.59	38,3	0.64	1.02	0.71
23	21.7	1.46	0.29	-1.1	-0.02	6.4	0.11	1.66	0.29
38	20.3	2.40	0.27	-2.5	-0.05	5.0	0.08	3.04	0.27
57	20.3	3.61	0.27	-2.5	-0.05	5.0	0.08	4.78	0.27
72	15.3	4.56	0.20	-7.5	-0.14	0.0	0.00	6.16	0.20

Cross-Section (x_o = 100 cm):

U_H = 22.8 cm/s V_m = 69.6 cm/s V_{min} = 14.7 cm/s

δ_1^* = 17.5 cm V_m^* = 70.0 cm/s δ_o^* = 5.5 cm

y	V	$\frac{y}{\delta_1^*}$	$\frac{V}{V_m}$	$V-U_H$	$\frac{V-U_H}{V_m-U_H}$	$V-V_{min}$	$\frac{V-V_{min}}{V_m-V_{min}}$	$\frac{y-\delta_o^*}{\delta_1^*-\delta_o^*}$	$\frac{V}{V_m^*}$
3	69.1	0.17	0.99	46.3	0.99	54.4	0.99	-	0.99
8	69.6	0.46	1.00	46.8	1.00	54.9	1.00	0.21	0.99
16	55.4	0.91	0.80	32.6	0.70	40.7	0.74	0.88	0.79
23	31.6	1.31	0.45	8.8	0.19	16.9	0.31	1.46	0.45
38	19.8	2.17	0.28	-3.0	-0.06	5.1	0.09	2.71	0.28
57	16.5	3.26	0.24	-6.3	-0.13	1.8	0.03	4.29	0.24
72	14.7	4.11	0.21	-8.1	-0.17	0.0	0.00	5.54	0.21

Cross-Section (x_o = 190 cm):

U_H = 22.8 cm/s V_m = 64.2 cm/s V_{min} = 14.0 cm/s

δ_1^* = 20.6 cm V_m^* = 62.4 cm/s δ_o^* = 6.4 cm

y	V	$\frac{y}{\delta_1^*}$	$\frac{V}{V_m}$	$V-U_H$	$\frac{V-U_H}{V_m-U_H}$	$V-V_{min}$	$\frac{V-V_{min}}{V_m-V_{min}}$	$\frac{y-\delta_o^*}{\delta_1^*-\delta_o^*}$	$\frac{V}{V_m^*}$
3	64.2	0.15	1.00	41.4	1.00	50.2	1.00	-	1.03
8	62.1	0.39	0.97	39.3	0.95	48.1	0.96	0.11	1.00
16	45.8	0.78	0.71	23.0	0.56	31.8	0.63	0.80	0.73
23	38.5	1.11	0.60	15.7	0.38	24.5	0.49	1.17	0.62
38	25.5	1.84	0.40	2.7	0.06	11.5	0.23	2.22	0.41
57	15.3	2.77	0.24	-7.5	-0.18	1.3	0.03	3.56	0.25
72	14.0	3.50	0.22	-8.8	-0.21	0.0	0.00	4.62	0.22

Cross-Section (x_o = 280 cm)

U_H = 22.8 cm/s V_m = 60.2 cm/s V_{min} = 9.9 cm/s

δ_1^* = 23.8 cm V_m^* = 56.5 cm/s δ_o^* = 7.4 cm

y	V	$\frac{y}{\delta_1^*}$	$\frac{V}{V_m}$	$V-U_H$	$\frac{V-U_H}{V_m-U_H}$	$V-V_{min}$	$\frac{V-V_{min}}{V_m-V_{min}}$	$\frac{y-\delta_o^*}{\delta_1^*-\delta_o^*}$	$\frac{V}{V_m^*}$
3	60.2	0.13	1.00	37.4	1.00	50.3	1.00	-	1.07
8	60.2	0.34	1.00	37.4	1.00	50.3	1.00	0.04	1.07
16	52.4	0.67	0.87	29.6	0.79	42.5	0.85	0.52	0.93
23	40.3	0.97	0.67	17.5	0.47	30.4	0.60	0.95	0.71
38	25.5	1.60	0.42	2.7	0.07	15.6	0.31	1.87	0.45
57	17.1	2.40	0.28	-5.7	-0.15	7.2	0.14	3.02	0.30
72	9.9	3.02	0.16	-12.9	-0.35	0.0	0.00	3.94	0.18

Cross-Section (x_o = 390 cm):

U_H = 22.8 cm/s V_m = 46.9 cm/s V_{min} = 10.8 cm/s

δ_1^* = 27.6 cm V_m^* = 50.5 cm/s δ_o^* = 8.6 cm

y	V	$\frac{y}{\delta_1^*}$	$\frac{V}{V_m}$	$V-U_H$	$\frac{V-U_H}{V_m-U_H}$	$V-V_{min}$	$\frac{V-V_{min}}{V_m-V_{min}}$	$\frac{y-\delta_o^*}{\delta_1^*-\delta_o^*}$	$\frac{V}{V_m^*}$
3	46.6	0.11	0.99	23.8	0.99	35.8	0.99	-	0.92
8	46.9	0.29	1.00	24.1	1.00	36.1	1.00	-	0.93
16	45.8	0.58	0.98	23.0	0.95	35.0	0.97	0.39	0.91
23	40.1	0.83	0.86	17.3	0.72	29.3	0.81	0.76	0.79
38	25.8	1.38	0.55	3.0	0.12	15.0	0.42	1.55	0.51
57	17.1	2.06	0.36	-5.7	0.24	6.3	0.17	2.55	0.34
72	10.8	2.61	0.23	-12.0	0.50	0.0	0.00	3.34	0.21

Cross-Section (x_o = 530 cm):

U_H = 22.8 cm/s V_m = 40.8 cm/s V_{min} = 14.7 cm/s

δ_1^* = 32.5 cm V_m^* = 44.0 cm/s δ_o^* = 10.1 cm

y	V	$\frac{y}{\delta_1^*}$	$\frac{V}{V_m}$	$V-U_H$	$\frac{V-U_H}{V_m-U_H}$	$V-V_{min}$	$\frac{V-V_{min}}{V_m-V_{min}}$	$\frac{y-\delta_o^*}{\delta_1^*-\delta_o^*}$	$\frac{V}{V_m^*}$
3	39.3	0.09	0.96	16.5	0.92	24.6	0.94	-	0.89
8	40.8	0.25	1.00	18.0	1.00	26.1	1.00	-	0.93
16	39.3	0.49	0.96	16.5	0.92	24.6	0.94	0.26	0.89
23	35.9	0.71	0.88	13.1	0.73	21.2	0.81	0.58	0.82
38	27.3	1.17	0.67	4.5	0.25	12.6	0.48	1.25	0.62
57	18.8	1.75	0.46	-4.0	-0.22	4.1	0.16	2.09	0.43
72	14.7	2.22	0.36	-8.1	-0.45	0.0	0.00	2.76	0.33

B I B L I O G R A P H Y

BASIC REFERENCES

(1) Abramovich, G. N. (1963), "The Theory of Turbulent Jets". MIT Press, Cambridge, Massachusetts.

(2) Birkhoff, G. and Zarantonelo, E.H. (1957), "Jets, Wakes and Cavities". Academic Press, New York.

(3) Bradshaw, P. (1971), "An Introduction to Turbulence and its Measurements". Pergamon Press, Oxford.

(4) Chow, V.T. (1959), "Open-Channel Hydraulics". McGraw-Hill Book Company, New York.

(5) Ferri, A. (1949), "Elements of Aerodynamics of Supersonic Flows". The MacMillan Company, New York.

(6) Goldstein, S. (1965), "Modern Developments in Fluid Dynamics". Dover Publications Inc., New York.

(7) Howarth, L. (Editor) (1953), "Modern Developments in Fluid Dynamics - High Speed Flow", Vol. 1, Clarendon Press, Oxford.

(8) Hunt, J.N. (1964), "Incompressible Fluid Dynamics". Longmans, Green & Co. Ltd., London.

(9) Lin, C.C. (Editor) (1959), "Turbulent Flows and Heat Transfer". Oxford University Press, London.

(10) Pai, S. (1954), "Fluid Dynamics of Jets". Van Nostrand, New York.

(11) Prandtl, L. (1949), "Essential of Fluid Dynamics", Blackie & Son Ltd., London.

(12) Rajaratnam, N. (1967), "Advances in Hydroscience-Hydraulic Jumps", Vol. 4, edited by Ven Te Chow. Academic Press, New York.

(13) Rouse, H. (Editor) (1959), "Advanced Mechanics of Fluids". John Wiley & Sons, New York.

(14) Schlichting, H. (1960), "Boundary-Layer Theory", 4th edition. McGraw-Hill Book Company, New York.

(15) Taylor, G.I. (1960), "Scientific Papers", edited by G.H. Batchelor. Cambridge University Press, Cambridge.

(16) Townsend, A.A. (1956), "The Structure of Turbulent Shear Flow". Cambridge University Press, Cambridge.

(17) Vennard, J.K. (1961), "Elementary Fluid Mechanics", 4th edition. John Wiley & Sons, New York.

HYDRAULIC JUMPS

(21) Arbhabhirama, A. and Abella, A.U. (1971), "Hydraulic Jump Within Gradually Expanding Channel". Proc. Am.Soc.Civil Engrs., Vol. 97, HY1, pp 31-42.

(22) Flôres, J.O.M. (1954), "Le Ressault". Houille Blanche, Vol. 9, No. 6, pp 811-822.

(23) Garg, S.P. and Sharma, H.R. (1971), "Efficiency of Hydraulic Jump". Proc. Am.Soc. Civil Engrs., Vol. 97, HY3, pp 409-420.

(24) Herbrand, K. (1973), "The Spatial Hydraulic Jump". J. Hydraul.Res., Vol. 11, No. 3, pp 205-218.

(25) Herbrand, K. and Knauss, J. (1973), "Computation and Design of Stilling Basin with Abruptly or Gradually Enlarged Boundaries", Proc. 11th Congr. on Large Dams, Vol 2, pp 57-79.

(26) Ippen, A.T. (1951), "Mechanics of Supercritical Flow". Trans.Am.Soc. Civil Engrs., Vol. 116, pp 268-295.

(27) Ippen, A.T. and Harleman, D.R.F. (1956), "Verification of Theory for Oblique Standing Waves". Trans.Am.Soc. Civil Engrs., Vol. 121, pp 678-694.

(28) Kulavaratharajah, K. (1973), "Oblique Hydraulic Jump". M.Sc. Thesis, University of London (Imperial College of Science & Technology).

(29) Leutheusser, H.J. and Kartha, V.C. (1972), "Effects of Inflow Condition on Hydraulic Jump". Proc.Am.Soc. Civil Engrs., Vol. 98, HY8, pp. 1367-1385.

(30) Naas, S.L. (1972), "The Characteristics of the Hydraulic Jump Over a Rock Sausage Basin". M.Sc. Thesis, University of Colorado.

(31) Rajaratnam, N. (1965), "Submerged Hydraulic Jump". Proc.Am.Soc. Civil Engrs., Vol. 91, HY4, pp 71-96.

(32) Rajaratnam, N. (1965), "The Hydraulic Jump as a Wall-Jet". Proc.Am.Soc. Civil Engrs., Vol. 91, HY5, pp 107-132.

(33) Rajaratnam, N. and Subramanya, K. (1968), "Hydraulic Jump Below Abrupt Symmetrical Expansions", Proc.Am.Soc. Civil Engrs., Vol. 94, HY2, pp 481-503.

(34) Rao, N.S.G. and Rajaratnam, N. (1963), "The Submerged Hydraulic Jump". Proc.Am.Soc. Civil Engrs., Vol. 89, HY1, pp 139-162.

(35) Resch, F.J. and Leutheusser, H.J. (1972), "Reynolds Stress Measurements in Hydraulic Jumps". J. Hydraul.Res., Vol. 10, No. 4, pp 409-430.

(36) Rouse, H., Siao, T.T. and Nagaratnam, S. (1958), "Turbulence Characteristics of the Hydraulic Jump". Proc.Am.Soc. Civil Engrs., Vol. 84, HY1, pp 1-30.

(37) Ten-Yu Kao (1971), "Hydraulic Jump assisted by a Cross-Jet". Proc.Am.Soc. Civil Engrs., Vol. 97, HY12, pp 2037-2050.

(38) Unny, T.E. (1961), "The Spatial Hydraulic Jump". Proc. 9th Congr. I.A.H.R., pp 32-42.

(39) Wilson, E.H. and Turner, A.A. (1972), "Boundary Layer Effects on Hydraulic Jump Location". Proc.Am.Soc. Civil Engrs., Vol. 98, HY7, pp 1127-1142.

TURBULENT JETS

(41) Albertson, M.L., Dai, Y.B., Jensen, R.A. and Rouse, H. (1950), "Diffusion of Submerged Jets". Trans.Am.Soc.Civ. Engrs., Vol. 115, pp 639-664.

(42) Bradbury, L.J.S. (1965), "The Structure of a Self-Preserving Turbulent Plane Jet". J. Fluid Mech., Vol. 23, part 1, pp 31-64.

(43) Bradbury, L.J.S. and Rilley, J. (1967), "The Spread of a Turbulent Plane Jet issuing into a Parallel Moving Airstream". J. Fluid Mech., Vol. 27, part 2, pp 381-394.

(44) Bradshaw, P. and Gee, M.T. (1962), "Turbulent Wall-Jets with and without an External Stream". Aeronaut. Res. Council, R & M No. 3252, London.

(45) Eichelbrenner, E.A. and Dumargue, P. (1962), "Le problème du jet parietal plan en régime turbulent pour un écoulement extérieur de vitesse U_e constant". J. Méchanique, Vol. 1, pp 109-134.

(46) Esquinazi, S. and Kruka, V. (1962), "Mixing of a Turbulent Wall-Jet into a Free Stream". Proc.Am.Soc. Civil Engrs., Vol. 88, EM2, pp 125-143.

(47) Gartshore, I.S. and Newman, B.G. (1969), "The Turbulent Wall-Jet in an Arbitrary Pressure Gradient". Aeronaut. Q., Vol. 20, pp 25-56.

(48) Glauert, M.B. (1956), "The Wall-Jet". J. Fluid Mech., Vol. 1, part 6, pp 625-643.

(49) Hari, V.M., (1973), "A Method to Analyse the Wall-Jet Flow". Aeronaut J., Vol. 77, pp 512-515.

(50) Kruka, V. and Eskinazi, Š. (1964), "The Wall-Jet in a Moving Stream". J. Fluid Mech., Vol. 20, part 4, pp 555-579.

(51) Narasimha, R., Narayan, K.Y., and Parthasarathy, S.P. (1973), "Parametric Analysis of Turbulent Wall-Jets in Still Air". Aeronaut. J., Vol. 77, pp 355-359.

(52) Newman, B.G. (1969), "The Prediction of Turbulent Jets and Wall-Jets". Can. Aeronaut. Space J., Vol. 15, pp 288-305.

(53) Patel, R.P. (1971), "Turbulent Jets and Wall-Jets in Uniform Streaming Flow". Aeronaut. Q., Vol. 22, pp 311-326.

(54) Rajaratnam, N. and Subramanya, K. (1967), "Plane Turbulent Free Jet and Wall-Jets". J.Roy.Aeronaut. Soc., Vol. 71, pp 585-587.

(55) Rajaratnam, N. and Subramanya, K. (1967), "An Annotated Bibliography on Wall-Jets". University of Alberta, Edmonton, (Canada).

(56) Schwarz, W.H. and Cosart, W.P. (1961), "The Two-Dimensional Turbulent Wall-Jet". J. Fluid Mech., Vol. 10, part 4, pp 481-495.

(57) Sigalla, A. (1958), "Measurements of Skin Friction in a Plane Turbulent Wall-Jet", J.Roy. Aeronaut., Vol. 62, pp 873-877.

(58) Sobey, R.J. (1973), "Flow Patterns in Lakes and Reservoirs". Ph.D. Thesis, University of London (Imperial College of Science & Technology).

OTHER REFERENCES

(61) Abou-Seida, M.M. (1963), "Wave Action Below Spillways". Proc.Am.Soc. Civil Engrs., Vol. 89, HY3, pp 133-152.

(62) Abu-Sayf, A. (1973), "Design of Expansions for Supercritical Flow". M.Sc. Thesis, University of London, (Imperial College of Science & Technology).

(63) Arumugan, K. (1955), "Surface Characteristics of Fast-Moving Water emerging from a Sluice". Ph.D. Thesis, University of London (Imperial College of Science & Technology).

(64) Crossley, H.E. and Harleman, D.R.F. (1952), "Studies on the Validity of the Hydraulic Analogy to Supersonic Flow", Part V. Techn. Rep. No. 11, Massachusetts Institute of Technology.

(65) Gill, M.A. (1970), "Bed Erosion Around Obstructions in Rivers". Ph.D. Thesis, University of London (Imperial College of Science and Technology).

(66) Herbich, J.H. and Walsh, P. (1972), "Supercritical Flow in Rectangular Expansions". Proc.Am.Soc. Civil Engrs., Vol. 98, HY 9, pp 1691-1700.

(67) Ippen, A.T. and Harleman, D.R.F. (1950), "Studies on the Validity of the Hydraulic Analogy to Supersonic Flow", Part I, II and III. Techn.Rep. No. 1 and 4, Massachusetts Institute of Technology.

(68) Krikorian, A.K. (1970), "Merging Flows in Channels". M.Sc. Thesis, University of London (Imperial College of Science and Technology).

(69) Law, S.W. and Reynolds, A.J. (1966), "Dividing Flow in an Open Channel". Proc.Am.Soc. Civil Engrs., Vol. 92, HY2, pp 207-231.

(70) Taylor, E.H. (1944), "Flow Characteristics at Rectangular Open-Channel Junctions". "Trans.Am.Soc. Civil Engrs, Vol. 109, pp 893-912.

(71) Webber, N.B. and Greated, C.A. (1966), "An Investigation of Flow Behaviour at the Junction of Rectangular Channels. Proc.Inst. Civil Engrs., Vol. 34, pp 321-334.